



Editor  
Nikos Mastorakis



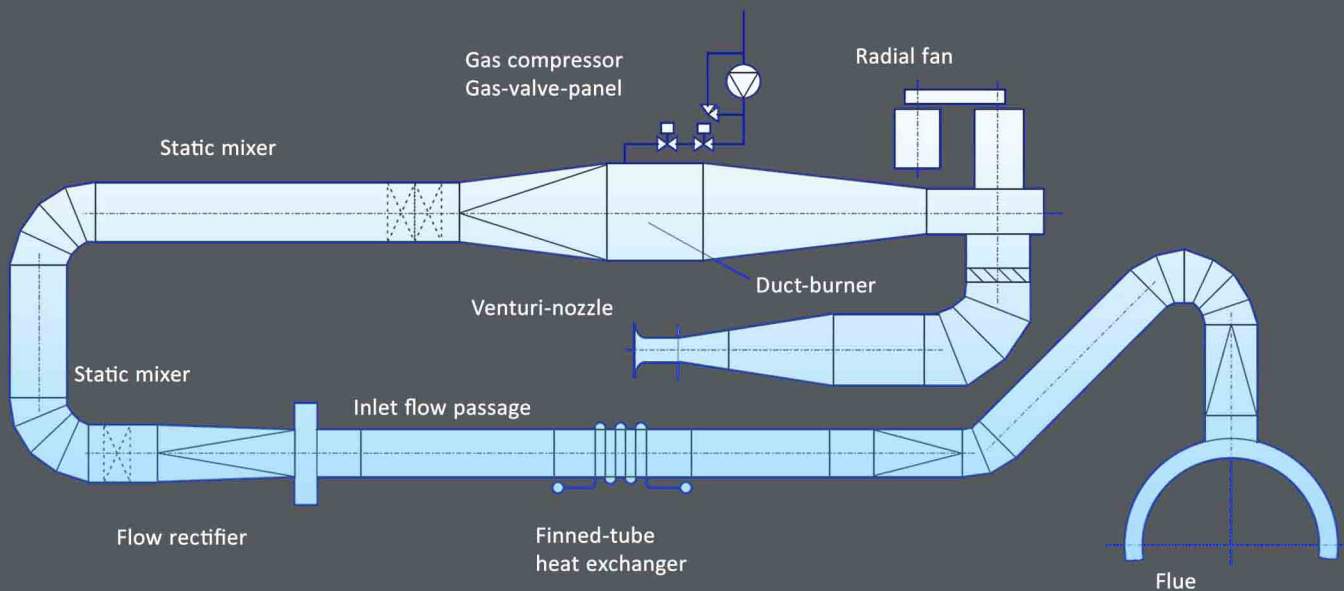
# Principles of Finned-Tube Heat Exchanger Design for Enhanced Heat Transfer - 2<sup>nd</sup> Edition

by  
**Dipl.-Ing. Dr. Friedrich Frass**

Translated and Edited by  
**Dipl.-Ing. Rene Hofmann**  
**Dipl.-Ing. Dr. Karl Ponweiser**

**Institute for Thermodynamics and Energy Conversion**  
**Vienna University of Technology**  
**Vienna, Austria**

Principles of Finned-Tube Heat Exchanger Design for Enhanced Heat Transfer - 2<sup>nd</sup> Edition







**Principles of Finned-Tube Heat Exchanger Design  
for Enhanced Heat Transfer - *2<sup>nd</sup> Edition***

**by**

**Dipl.-Ing. Dr. Friedrich Frass**

**Translated and Edited by  
Dipl.-Ing. Rene Hofmann  
Dipl.-Ing. Dr. Karl Ponweiser**

**Institute for Thermodynamics and Energy Conversion  
Vienna University of Technology  
Vienna, Austria**

# **Principles of Finned-Tube Heat Exchanger Design for Enhanced Heat Transfer - *2<sup>nd</sup> Edition***

Published by WSEAS Press

[www.wseas.org](http://www.wseas.org)

**Copyright © 2015, by WSEAS Press**

All the copyright of the present book belongs to the World Scientific and Engineering Academy and Society Press. All rights reserved. No part of this publication may be reproduced, stored in a retrieval system, or transmitted in any form or by any means, electronic, mechanical, photocopying, recording, or otherwise, without the prior written permission of the Editor of World Scientific and Engineering Academy and Society Press.

All papers of the present volume were peer reviewed by two independent reviewers. Acceptance was granted when both reviewers' recommendations were positive.  
See also: <http://www.worldses.org/review/index.html>

ISBN: 978-960-474-389-6



World Scientific and Engineering Academy and Society

## Preface

The present work was carried out at the Institute for Thermodynamics and Energy Conversion of the Vienna University of Technology in the course of several years during my activities as a scientific researcher. This work is based on measurements done on the experimental facility for heat transfer, described in the appendix, as well as on accompanying studies of the literature and reports about measurements taken using other methods.

My most grateful thanks go to o. Univ. Prof. Dr. W. Linzer for providing the impulse for this research and for the support during realization.

Many thanks to the Simmering Graz Pauker AG, as well as their successor company Austrian Energy and Environment, for allocating resources during the construction of the test facility and for providing, together with Energie und Verfahrenstechnik (EVT), the finned tubes.

Furthermore, I would like to thank our colleagues at the laboratory of the institute, M. Effenberg, H. Haidenwolf, W. Jandejsek, M. Schneider as well as R. Steininger, for the construction and assembly of the experimental facility in the lab and for altering the assembly many times in order to be able to examine other finned tube arrangements.

I also thank my colleagues at the Institute who gave me advice, particularly during the implementation of data collection and analysis.

The efforts of many individuals helped contribute to the development of this book. I would especially like to take this opportunity to thank Dipl.-Ing. Rene Hofmann whose encouragement and priceless assistance proved invaluable to the success of this work.

Finally I would like to thank Dr. Karl Ponweiser providing the impulse for doing further research on the experimental facility for optimization of heat transfer enhancement.

Dipl.-Ing. Dr. Friedrich Frass  
Institute for Thermodynamics and Energy Conversion  
Vienna University of Technology



# Table of Contents

<b>Preface</b>	<b>iii</b>
<b>List of Figures</b>	<b>vii</b>
<b>List of Tables</b>	<b>xiii</b>
<b>List of Symbols</b>	<b>xiv</b>
<b>Abstract</b>	<b>xvii</b>
<b>1 Introduction</b>	<b>1</b>
<b>2 Fundamentals of Heat Transfer</b>	<b>1</b>
2.1 Design of Finned Tubes	1
2.2 Fin Efficiency	3
2.2.1 Plain Geometry	4
2.2.2 Finned Tubes	7
2.3 Special Consideration in the Calculation of Heat Transfer	10
<b>3 Equations for the External Heat Transfer Coefficient</b>	<b>12</b>
3.1 Staggered Tube Arrangements	12
3.1.1 Overview of Equations	12
3.1.2 Equations for a Single Tube Row	20
3.1.3 Influence of Geometrical Dimensions of the Finned Tube and of Bundle Geometry	22
3.1.4 Evaluation of Different Calculation Formulas	30
3.2 In-line Tube Arrangements	37
3.2.1 Enumeration of Equations	37
3.2.2 Evaluation of the Influence of Fin Parameters with in-line Tube Arrangement	40
3.2.3 Proposal for an Enhanced Calculation Formula	47
3.3 Selection Method for Finned Tubes	48
3.4 Substitution of Fluid Properties	52
3.5 Heat Exchanger with a Small Number of Consecutive Tube Rows	54
3.5.1 Reduction Methods for Staggered Tube Arrangements as Presented in tables and Diagrams	54
3.5.2 Calculations According to Measurements on Staggered Finned Tube Bundles with less than 8 Tube Rows	55
3.5.3 Heat Exchanger with Small Number of Consecutive Tube Rows in in-line Arrangement	58
3.6 Serrated Fins	59
3.7 Geometrical Arrangement of Tubes in a Bundle	61
3.8 Summary of Heat Transfer	67
<b>4 Finned Tube Bundles with Continuous Fins</b>	<b>69</b>
4.1 Finned Tube Bundles with Continuous Smooth Fins and Circular Tubes	70
4.2 Finned Tube Bundles with Continuous Wavy Fins and Circular Tubes	72
4.3 Finned Tube Bundles with non-Circular Tubes and Continuous Smooth Fins	75
4.4 Finned Tube Bundles with Flat Tubes and Continuous Wavy Fins	80
<b>5 Pressure Drop</b>	<b>84</b>
5.1 Fundamentals for the Determination of Pressure Drop at Finned Tubes	84
5.2 Problems with Test Result Evaluation	84
5.3 Evaluation of Pressure Drop for Staggered Finned Tube Bundles	88
5.3.1 Equations for Pressure Drop in Staggered Finned Tube Bundles	89
5.3.2 Discussion of Cited Pressure Drop Equations	94
5.3.3 Recommendation for a Calculation to Predict Pressure Drop at Staggered Finned Tube Bundles in Cross-Flow	105
5.4 Calculation of Pressure Drop for Finned Tubes Arranged in Line	108
5.4.1 Presentation of Equations	108

5.4.2 Discussion of Pressure Drop Equations for in-line Tube Bundle Arrangements	112
<b>Conclusion and Recommendations</b>	121
<b>Appendix: Test Facility for Heat Transfer Measurements</b>	122
<b>Literature</b>	126

# List of Figures

1	Finned tube with annular fins . . . . .	3
2	Finned tube with spiral fins . . . . .	4
3	Finned tubes with spiral fins mounted by pressure . . . . .	4
4	Fins with t-shaped fin base . . . . .	5
5	Fins with l-shaped fin base . . . . .	6
6	Definition of fin efficiency . . . . .	7
7	Heat conduction through the finned tube . . . . .	13
8	Free-flow cross-section and free-flow cross-section within the out- line of the finned tube . . . . .	20
9	Influence of tube diameter on heat transfer with unmodified fin geometry and fin pitches . . . . .	24
10	Influence of tube diameter on heat transfer with unmodified fin geometry and adapted transverse pitch (staggered arrangement) .	26
11	Influence of tube diameter on heat transfer with unmodified fin geometry and transverse pitch (staggered arrangement) at constant Reynolds number . . . . .	26
12	Influence of tube diameter on heat transfer with unmodified Reynolds number and fin geometry and adapted transverse pitch (staggered arrangement) . . . . .	27
13	Influence of fin pitch on heat transfer (staggered arrangement) . .	27
14	Influence of fin height on heat transfer (staggered arrangement) .	28
15	Influence of fin height on heat transfer at adapted transverse pitch (staggered arrangement) . . . . .	29
16	Influence of fin thickness on heat transfer (staggered arrangement)	29
17	Influence of gas velocity on heat transfer (staggered arrangement)	30
18	Influence of transverse pitch on heat transfer (staggered arrange- ment) . . . . .	31
19	Influence of longitudinal pitch on heat transfer (staggered arrange- ment) . . . . .	32
20	Influence of triangular pitch on heat transfer . . . . .	32
21	Experimental results by Mirkovics showing the characteristic di- ameter $d_{Mi}$ . . . . .	33

22	Heat transfer measurements by Mirkovics and ITE on staggered finned tube arrangements evaluated with Mirkovics' formulas . . .	35
23	Heat transfer measurements by Mirkovics and ITE on staggered finned tube arrangements evaluated with formula (85) . . . . .	36
24	Heat transfer measurements by Mirkovics and ITE on staggered finned tube arrangements evaluated using formula (86) . . . . .	37
25	Heat transfer measurements by Mirkovics and ITE on staggered finned tube arrangements evaluated using formula (91) . . . . .	38
26	In-line finned tube arrangement . . . . .	40
27	Influence of tube diameter the heat transfer with constant Reynolds number (in-line arrangement) . . . . .	42
28	Influence of tube diameter on heat transfer at constant gas velocity (in-line arrangement) . . . . .	43
29	Influence of tube diameter on heat transfer at constant Reynolds number and with adapted tube pitches (in-line arrangement) . . .	43
30	Influence of tube diameter on heat transfer at constant gas velocity and with adapted tube pitches (in-line arrangement) . . . . .	44
31	Influence of fin pitch on heat transfer (in-line arrangement) . . . .	44
32	Influence of fin thickness on heat transfer (in-line arrangement) .	45
33	Optimum fin thickness with respect to heat transfer for St35.8 fins (in-line arrangement) . . . . .	46
34	Optimum fin thickness with respect to heat transfer for Austenite fins (in-line arrangement) . . . . .	46
35	Influence of fin height on heat transfer (in-line arrangement) . . .	47
36	Influence of fin height on heat transfer at adapted transverse pitch (in-line arrangement) . . . . .	48
37	Influence of fin height on heat transfer at adapted tube pitches (in-line arrangement) . . . . .	48
38	Influence of transverse pitch on heat transfer (in-line arrangement)	48
39	Influence of longitudinal pitch on heat transfer based on measurements by ITE (in-line arrangement) (tube diameter 38 mm, 150 fins per m, 16x1 mm, transverse pitch 80 mm) . . . . .	49
40	Influence of the Reynolds number on heat transfer at in-line arrangement . . . . .	50
41	Results of the proposed equation (100) in comparison with available equations for heat transfer at in-line finned tube bundles . .	50

42	Flow displacement in dependence of relative transverse pitch $a$ ( $a = (t_q - (d_A + 2h))/t_q$ ) . . . . .	54
43	Reduction coefficient for heat transfer with a small number of consecutive tube rows (staggered arrangement) . . . . .	55
44	Heat transfer with 8, 6, 4 and 2 consecutive tube rows with $d_{Ch}$ as characteristic dimension (staggered arrangement) . . . . .	56
45	Heat transfer with 8, 6, 4 and 2 consecutive tube rows with $d_A$ as characteristic dimension (staggered arrangement) . . . . .	58
46	Heat transfer with 8, 6, 4 and 2 consecutive tube rows with $d_{Mi}$ as characteristic dimension (staggered arrangement) . . . . .	58
47	Averages for heat transfer with 8, 6, 4 and 2 consecutive tube rows with $d_A$ as characteristic dimension (staggered arrangement) . . . . .	59
48	Reduction coefficient $K_z$ for heat transfer with 8, 4, 2 and 1 consecutive tube rows (staggered arrangement) . . . . .	60
49	Heat transfer with small number of consecutive tube rows and in-line arrangement . . . . .	60
50	Reduction coefficient for heat transfer with a small number of consecutive tube rows in in-line and staggered arrangement . . . . .	61
51	Sectional view of a finned tube with serrated fins . . . . .	62
52	Comparison of Nusselt numbers for finned tubes with serrated and annular fins . . . . .	62
53	Comparison of pressure drop coefficients for finned tubes with serrated and annular fins . . . . .	63
54	Staggered finned tube arrangement with semi-tubes on the channel wall . . . . .	64
55	Staggered finned tube arrangement . . . . .	65
56	Partly staggered finned tube arrangement . . . . .	65
57	Transition from an in-line to a staggered finned tube arrangement . . . . .	66
58	Heat transfer measurements of Stasiulevicius in dependence of the angle $\alpha$ according to figure (57) . . . . .	67
59	Heat transfer measurements by ITE in dependence of the angle $\alpha$ according to figure (57). Tube diameter 31.8 mm . . . . .	67
60	Heat transfer measurements by ITE in dependence of the angle $\alpha$ according to figure (57). Tube diameter 38 mm . . . . .	68
61	Heat transfer calculated according to ESCOA in dependence of the angle $\alpha$ according to figure (57) . . . . .	68

62	Schematic representation of the experimental setup by Stenin and Kunttysh [36] . . . . .	69
63	Experimental results of Stenin and Kunttysh [36] . . . . .	69
64	Circular tubes with continuous fins . . . . .	71
65	Wavy fins: corrugated or wavy formed . . . . .	74
66	Comparison of Nusselt numbers for circular tubes with continuous smooth or wavy fins . . . . .	75
67	Comparison of pressure drop coefficients at circular tubes with continuous smooth or wavy fins . . . . .	76
68	Comparison of performance numbers according to equation (132) for circular tubes with continuous smooth or wavy fins . . . . .	76
69	Flat tubes with continuous fins . . . . .	77
70	Flat tubes with differing profiles according to Geiser [30] . . . . .	81
71	Pressure drop coefficients of flat tubes with continuous fins . . . . .	84
72	Nusselt-numbers at flat tubes with continuous fins . . . . .	85
73	Performance numbers according to equation (132) for flat tubes with continuous fins . . . . .	85
74	Exponent n according to equation (138), tube diameter 38 mm, 150 fins per m (16 x 1 mm), $t_q=85\text{mm}$ . . . . .	88
75	Pressure drop measurements with and without heat transfer. Tube diameter 38 mm , fins 16 x 1 mm, $t_q=85$ mm. Eq.(7) in the figure is identical with equation (143) . . . . .	89
76	Correlation of pressure drop measurements at different gas temperatures. Tube diameter 31.8 mm, 200 fins per m, 15 x 1 mm. Eq.(7) in the figure is identical with equation (143) . . . . .	90
77	Pressure drop coefficient in dependence of fin height according to VDI 431 [38]. Tube diameter 38 mm, 150 fins per m, $t_q = 85$ mm, $t_l = 75$ mm, staggered arrangement . . . . .	95
78	Influence of tube diameter upon the pressure drop coefficient at constant velocity in the narrowest cross-section (staggered arrangement) . . . . .	97
79	Influence of tube diameter upon the pressure drop coefficient at constant Reynolds number (staggered arrangement) . . . . .	98
80	Influence of tube diameter upon the pressure drop coefficient at constant velocity in the narrowest cross-section and varied transverse pitch (staggered arrangement) . . . . .	99

81	Influence of tube diameter upon the pressure drop coefficient at constant Reynolds number and varied traverse pitch (staggered arrangement) . . . . .	99
82	Influence of fin thickness upon the pressure drop coefficient (staggered arrangement) . . . . .	100
83	Influence of fin thickness upon the pressure drop coefficient according to measurements by Mirkovics . . . . .	101
84	Influence of fin pitch upon the pressure drop coefficient (staggered arrangement) . . . . .	101
85	Influence of fin height upon the pressure drop coefficient (staggered arrangement) . . . . .	102
86	Influence of fin height and varied traverse pitch upon the pressure drop coefficient (staggered arrangement) . . . . .	103
87	Influence of transverse pitch upon the pressure drop coefficient (staggered arrangement) . . . . .	103
88	Influence of longitudinal pitch upon the pressure drop coefficient (staggered arrangement) . . . . .	104
89	Influence of magnitude of triangular pitch upon the pressure drop coefficient . . . . .	105
90	Influence of fin pitch upon the pressure drop coefficient: comparison of measured values and calculation. Tube diameter $d_A=38$ mm, fins $16 \times 1$ mm . . . . .	105
91	Influence of longitudinal pitch upon the pressure drop coefficient. Comparison of measured values and calculation for $d_A=31.8$ mm .	106
92	Influence of longitudinal pitch upon the pressure drop coefficient. Comparison of measured values and calculation for $d_A=38$ mm . .	107
93	Influence of the Reynolds number upon the pressure drop coefficient (staggered arrangement) . . . . .	108
94	Comparison of the pressure drop coefficient calculated according to equation (171) with the results of equations from the literature	110
95	Influence of tube diameter upon the pressure drop coefficient with constant velocity in the narrowest cross-section (in-line arrangement) . . . . .	113
96	Influence of tube diameter upon the pressure drop coefficient with constant Reynolds number (in-line arrangement) . . . . .	114

97	Influence of tube diameter upon the pressure drop coefficient with constant velocity in the narrowest cross-section and adapted transverse and longitudinal pitch (in-line arrangement) . . . . .	115
98	Influence of tube diameter upon the pressure drop coefficient with constant Reynolds number and at adapted transverse and longitudinal pitch (in-line arrangement) . . . . .	115
99	Influence of fin thickness upon the pressure drop coefficient (in-line arrangement) . . . . .	116
100	Influence of fin pitch upon the pressure drop coefficient (in-line arrangement) . . . . .	116
101	Influence of fin height upon the pressure drop coefficient (in-line arrangement) . . . . .	117
102	Influence of fin height upon the pressure drop coefficient at adapted transverse and longitudinal pitch (in-line arrangement) . . . . .	118
103	Influence of fin height upon the pressure drop coefficient with adapted transverse pitch (in-line arrangement) . . . . .	118
104	Influence of the Reynolds number upon the pressure drop coefficient (in-line arrangement) . . . . .	119
105	Influence of transverse pitch upon the pressure drop coefficient (in-line arrangement) . . . . .	119
106	Influence of longitudinal pitch upon the pressure drop coefficient (in-line arrangement) . . . . .	120
107	Influence of the number of consecutive tube rows upon the pressure drop coefficient (in-line arrangement) . . . . .	121
108	Constant of equation (191) calculated by measurement values of the pressure drop coefficient in dependence of the number of tube rows (in-line arrangement) . . . . .	122
109	Pressure drop coefficient values according to equation (191) in comparison with the values for in-line arrangements from the literature	122
110	Layout and design of the test facility . . . . .	126

## List of Tables

1	Constants in the formula of Brandt . . . . .	18
2	Function $E(n_R)$ . . . . .	57
3	$C_1$ and $C_2$ for few tube rows according to [19] . . . . .	74
4	Flat tubes with differing profiles according to Geiser [30] . . . . .	80
5	Circumference and surface of profile flat tubes . . . . .	82

## List of Symbols

Symbol	Unit	Physical dimension
$A$	$m^2$	surface area of the fin
$a$	m	small axis of the flat tube
$A_f$	-	fractional free flow cross-section with flat tubes
$A_{Ftot}$	$m^2$	total surface area with flat tubes
$a_{Ko}$	m	surface area of the fin top per m tube
$A_R$	m	surface area of the smooth tube
$A_{Ri}$	m	surface area of the fins per m tube
$a_{Ri}$	m	surface area of the fin side per m tube
$A_{Ro}$	m	surface area of the bare tube per m tube
$a_{Ro}$	m	surface area of the bare tube per m tube
$A_{tot}$	m	total surface area per m finned tube
$A_{0f}$	m	proportional free flow cross-section
$a_w$	m	shorter dimension of the rectangular fin
$b$	m	large axis of the flat tube
$b_w$	m	longer dimension of the rectangular fin
$C$	-	common constant
$C_1, C_2, \dots, C_7$	-	constant
$C1 \dots C6$	-	coefficient according to ESCOA
$D$	m	outside diameter of fins
$d_A$	m	outside diameter of tube
$d_E$	m	diameter equivalent to area
$d_e$	m	characteristic diameter according to HEDH
$d_i$	m	inside diameter of tube
$d_h$	m	hydraulic diameter
$d_q$	m	equivalent diameter according to FDBR
$d'$	m	equivalent diameter according to HEDH
$E1, E2, E3$	-	constant according to FDBR
$e_l$	-	dimensionless longitudinal pitch
$e_q$	-	dimensionless transverse pitch
$Eu$	-	Euler number
$f_f$	-	Fanning friction factor
$f_N$	-	factor according to Brandt to account for a small number of consecutive tube rows in cross-flow
$h$	m	fin height
$h'$	m	equivalent fin height
$h_{red}$	m	reduced fin height
$h_x$	m	fin height as a coordinate
$K_{An}$	-	arrangement factor according to Brandt

Symbol	Unit	Physical dimension
$Kf_t$	-	factor for bundle geometry
$Ku$	-	universal characteristic number for heat transfer
$K_z$	-	factor to account for a small number of consecutive tube rows in cross-flow
$l'$	m	characteristic dimension
$l_k$	m	characteristic dimension according to Mirkovics
$m$	$m^{-1}$	parameter for fin efficiency
$m^*$	$kg\ m^{-2}\ s^{-1}$	mass velocity
$n$	-	exponent
$n_A$	-	arrangement factor for smooth tube bundles
$n_R$	-	number of consecutive tube rows in cross-flow
$Nu$	-	Nusselt number
$Pr$	-	Prandtl number
$Pr_L$	-	Prandtl number of air
$R$	m	radius above fins
$r$	m	radius
$r_A$	m	radius of the basic tube
$R_b$	-	quotient according to Nir
$Re$	-	Reynolds number
$s$	m	half fin thickness as a function
$s_R$	m	fin thickness
$St$	-	Stanton number
$s_W$	m	head width of hexagonal fins
$s'_W$	m	smaller head width of hexagonal fins
$s''_W$	m	larger head width of hexagonal fins
$t_d$	m	diagonal pitch
$t_l$	m	longitudinal pitch
$t_q$	m	transverse pitch
$t_R$	m	fin pitch
$U$	m	circumference
$V$	$m^3$	volume
$W$	-	$A_{tot}/A_{0f}$
$w_E$	$m\ s^{-1}$	gas velocity in the narrowest cross-section
$w_m$	$m\ s^{-1}$	mean gas velocity
$w_R$	$m\ s^{-1}$	effective gas velocity
$w_0$	$m\ s^{-1}$	gas velocity in the empty channel
$y'$	-	variable
$z$	-	variable
$z_q$	-	factor for transverse pitch according to Wehle
$\alpha$	$W\ m^{-2}\ K^{-1}$	heat transfer coefficient

Symbol	Unit	Physical dimension
$\alpha_i$	$\text{W m}^{-2} \text{K}^{-1}$	inside heat transfer coefficient of the bare tube
$\alpha_0$	$\text{W m}^{-2} \text{K}^{-1}$	real heat transfer coefficient
$\Delta p$	$\text{N m}^{-2}$	pressure drop
$\eta$	$\text{kg m}^{-1} \text{s}^{-1}$	dynamic viscosity
$\vartheta$	$^{\circ}\text{C}$	temperature
$\lambda$	$\text{W m}^{-1} \text{K}^{-1}$	thermal conductivity
$\nu$	$\text{m}^2 \text{s}^{-1}$	kinematic viscosity
$\xi$	-	pressure drop coefficient
$\rho$	$\text{kg m}^{-3}$	density
$\varphi$	-	factor
$\psi$	-	porosity

Index	Denoation
$Bm$	mean boundary layer
$F$	fluid
$gm$	gas mean
$g1$	gas inlet
$g2$	gas outlet
$m$	mean
$RF$	fin base
$Ri$	fin
$Ro$	tube
$Wa$	wall
$wm$	water mean

Abbreviation	Denoation
<i>ESCOA</i>	Extended Surface Corporation of America
<i>HEDH</i>	Heat Exchanger Design Handbook
<i>FDBR</i>	Fachverband Dampfkessel-, Behaelter- und Rohrleitungsbau

## Abstract

In designing and constructing heat exchangers with transverse finned tubes in cross-flow, it is necessary to know correlations for calculating heat transfer and pressure drop. In addition to the common use of the Reynolds and Nusselt groups of dimensionless numbers, heat conduction in the fins also has to be accounted for in calculating heat transfer. A reduction coefficient termed “fin efficiency” is therefore introduced, by which the actual heat transfer coefficient is multiplied in order to get the apparent heat transfer coefficient. “Fin efficiency” is computed according to the laws of heat conduction under the assumption that the actual heat transfer coefficient is uniformly distributed across the fin surface.

Introducing geometrical constants for the fins, that is fin height, fin pitch, and fin thickness, into the equations for heat transfer and pressure drop makes these equations more bulky than the one for bare tube heat exchangers. Moreover, there is no self-evident characteristic dimension for a finned tube, as is the case with tube diameter for bare tubes, therefore many different proposals for the characteristic dimensions exist, which are in turn needed for setting the Reynolds and Nusselt dimensionless number groups. Some authors even use different characteristic dimensions for the Reynolds number and for the calculation of heat transfer and pressure loss.

Due to the complex geometry of finned tube designs, equations for heat transfer and pressure loss are derived mostly from experiments. When using for design purposes the equations obtained, a thorough knowledge of the condition of the tested finned tubes is necessary, i.e. of the materials and shape of fins, tubes and mode of attachment. For steam boilers and high pressure heat exchangers in the process industry, spiral finned tubes are commonly used today; here a ribbon of steel is wound spirally around a boiler tube and welded to it. For these finned tubes, coefficients of heat transfer and pressure loss are higher than for tubes with circumferential fins. Finned tubes are mostly arranged in bundles, which may be arranged staggered or in line. The later coefficients of heat transfer are in fact approximately only two thirds compared to staggered arrays. Therefore, many more staggered finned tube bundles have been tested. The equations for heat transfer in finned tube bundles give the results for a certain number of rows in longitudinal direction. For a smaller number of rows in staggered bundles, heat transfer is lower, while for in-line bundles it is higher.

With air coolers and heaters, tube bundles often have continuous fins, which may be easier to manufacture as long as fin pitch and the tube diameter are small. The equations for heat transfer and pressure loss are somewhat different for such tube bundles with continuous fins as compared to serrated finned tubes. In order to achieve a very small air-side pressure loss, extended tubes of various shapes may be used in the place of circular tubes, when fluid pressure in the tubes permits non-circular tubes. In some cases, corrugated or wavy fins are used, whereas corrugated fins increase heat transfer and wavy fins have a better ratio of heat transfer to pressure loss.



# 1 Introduction

Heat exchangers with extended surfaces are widely used whenever heat is to be exchanged between a medium that transports heat well (e.g. liquid, liquid with phase transition) and one that does not (e.g. gas with small density). On the side of the medium transporting heat poorly, the heat-transferring surface is enlarged by an arrangement of fins or other elements such as pins or needles. These elements for enlarging the surface can be attached up to a relatively great height to the surface, or they can be small and formed from the tube material itself. Fins can be arranged in tubes on both the outside and the inside and mainly transversely or along the sleeve shaft axis. From among the great abundance of possible arrangements, only tubes with outside fins, arranged in an approximately orthogonal direction to the sleeve shaft, will be considered here.

## 2 Fundamentals of heat transfer

### 2.1 Design of finned tubes

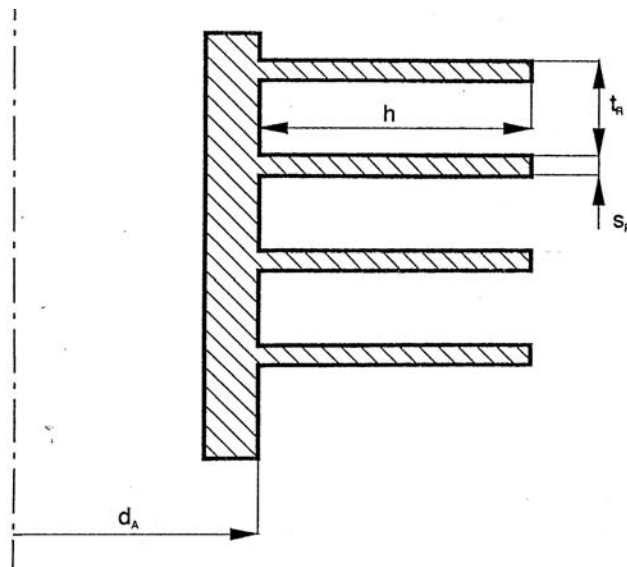


Figure 1: Finned tube with annular fins

Depending on their intended purpose, finned tubes are manufactured in numerous designs from many materials or fin/tube material combinations. As an initial design, cast finned tubes for economizers were used. Only a small number of finned tubes were manufactured from solid materials for testing purposes. Both were made with annular fins (figure (1)).

Today, spiral tubes in chemical engineering installations and steam boilers prevail. Fins in the form of steel strips are wound around a boiler tube and affixed to the core tube either by means of resistance or by laser welding (figure (2)).

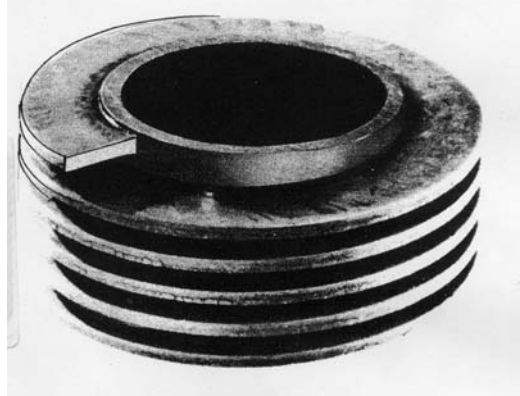


Figure 2: **Finned tube with spiral fins**

In cases of reduced requirements upon heat transfer and not too high gas temperatures, finned tubes with fins wound around the tube only by pressure are also used (figure (3)). These fins are often zinc-plated after production to be more resistant against corrosion. This additionally results in a tighter connection between fin and tube that conducts heat better.

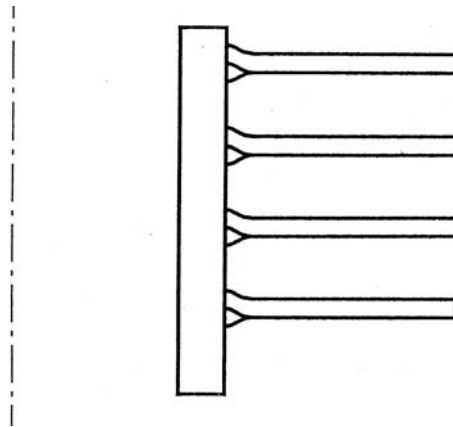


Figure 3: **Finned tubes with spiral fins mounted by pressure**

In ventilation and air conditioning (HVAC) engineering, finned tubes with mounted fins are also used; these are either copper (Cu) tubes with Cu or aluminium fins or steel tubes with steel fins. Fins can also be soldered to the tube (Cu tube with Cu fins) or zinc-plated (steel tube with steel fins).

For improved conduction at the tube base, mounted fins which are often only wound by pressure around the tube are fitted with a T-shaped (figure (4)) or

L-shaped base (figure (5)). Coiled fins can also have an L-shaped base.

Mounted fins can also be attached to tubes with a non-circular cross-section, for example oval or flat tubes; the latter are used to reduce gas-side pressure drop. In HVAC as well as refrigeration engineering, fins which pass through several tubes are also used. Mounted fins also can have wavy form orthogonal to the direction of the flow to improve heat transfer.

## 2.2 Fin efficiency

For heat exchange between a medium transporting heat well (e.g. liquid, liquid with phase transition) and a medium transporting heat poorly (e.g. gas with a low density), finned tube heat exchangers are often used. The heat-exchanging surface on the side of the medium transporting heat poorly is enlarged by an arrangement of fins. The external surface per m tube is increased by up to 15 times by the fin arrangement, the transferable amount of heat does not, however, increase to the same extent. This is due to heat conduction through the fins, whereby the external fin sections reach a different temperature from the tube base, i.e. one that is closer to the gas temperature, and therefore the effective temperature difference of the heat transfer is reduced.

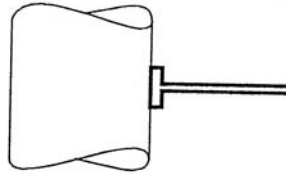
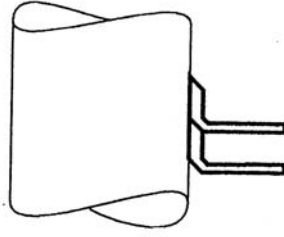


Figure 4: **Fins with t-shaped fin base**

The amount of heat conduction through simply shaped fins, e.g. fins on a flat plate or annular fins of constant thickness around a core tube, may be calculated strictly by mathematical means.

It is common practice to consider heat conduction through the fin in terms of the so-called fin efficiency, which results from the following consideration: the heat transferred at the surface element is proportional to the difference in each case between the fin temperature and the gas temperature integrated over the fin surface. It equals the temperature difference between the gas and the core tube multiplied by the fin efficiency.

The heat transfer of a tube with an enlarged surface would be calculated in the same way as for a normal tube if the fins or pins, which are arranged for enlargement of the surface, display an infinitely high amount of thermal conductivity. Since this is not the case, the finite conduction through the fin element causes

Figure 5: **Fins with l-shaped fin base**

an approximation of the temperature to that of the heat-transferring medium. The effective temperature difference for the heat transfer between the fin surface and the ambient medium is thus lowered and reduces in this way the amount of heat transferred. This process is taken into consideration by the introduction of the concept of fin efficiency, which represents neither a quality criterion nor one of economic efficiency. Heat exchangers with low fin efficiency can be technically and economically comparable to those with high fin efficiency.

$$Q = \frac{A_{Ro} + A_{Ri}\eta_R}{A_{tot}} \quad (1)$$

Fin efficiency is of course only applied to those parts of the entire surface which are in contact with elements for enlarging the surface or with the fin.

### 2.2.1 Plain geometry

The differential equation for the temperature change in the straight and flat fin with a constant cross-section is given here in order to derive relationships for fin efficiency.

$$\frac{d^2\vartheta}{dx^2} - \frac{2\alpha}{\lambda_{Ri}s_R}\vartheta = 0 \quad (2)$$

The heat transfer coefficient  $\alpha$  is assumed in this case as constant and independent of location. From equation (2) the temperature change in the fin can be calculated; this is dependent on the parameter

$$m = \sqrt{\frac{2\alpha}{\lambda_{Ri}s_R}}. \quad (3)$$

When considering boundary conditions, and depending on the distance  $x$  from the fin base  $\vartheta(x)$ , the temperature is given by:

$$\vartheta = \vartheta_{RF} \frac{\cosh(m(h-x))}{\cosh(mh)} \quad (4)$$

The fin efficiency is the ratio of the effective heat flow emitted by the fin to the heat flow the fin would emit if it had the same temperature overall as the fin base  $\vartheta_{RF}$  instead of the lower average temperature  $\vartheta_{Ri}$ , (figure (6)).

$$\eta_R = \frac{A \alpha (\vartheta_{Ri} - \vartheta_F)}{A \alpha (\vartheta_{RF} - \vartheta_F)} = \frac{(\vartheta_{Ri} - \vartheta_F)}{(\vartheta_{RF} - \vartheta_F)} \quad (5)$$

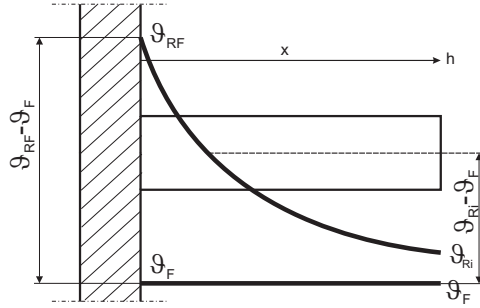


Figure 6: **Definition of fin efficiency**

In this case  $\vartheta_F$  is the constant temperature of the fluid surrounding the fin. The effective heat flow emitted by the fin equals the heat flow which is achieved by conduction from the fin base into the fin and can be calculated by:

$$Q_R = -\lambda_{Ri} b s_R \frac{d\vartheta}{dx} \Big|_{x=0} \quad (6)$$

This leads to the known equation for the fin efficiency of flat fins of constant cross-section.

$$\eta_R = \frac{\tanh(mh)}{mh} \quad (7)$$

Fins do not however necessarily have a constant cross-section (rectangular profile). For example, a parabolic profile with a spike at the end results from the heat conduction-equation for a fin with the lowest weight at a certain thermal output. A triangular profile, or because of easier manufacturing and handling, a trapezoidal profile best represents this solution. A closed solution for the triangular profile exists, however only by using Bessel functions.

$$\eta_R = \frac{1}{mh} \frac{I_1(2mh)}{I_0(2mh)} \quad (8)$$

A calculation with Bessel functions can be avoided by means of an approximation. In this case the formula (7) is used, however  $\phi m h$  is inserted in place of  $m h$ . According to [34] the following formula is should be used for  $\phi$ , which yields a approximation for  $\eta_R$  with an accuracy of 0.1%.

$$\phi = 0.99101 + 0.31484 \frac{\tanh(0.74485 m h)}{m h} \quad (9)$$

In most cases, a much rougher approximation is sufficient for the calculation of a triangular fin. With this method a corrected fin thickness is used in the equation for a rectangular fin (7):

$$s_R = \frac{3}{4} s'_R \quad (10)$$

In this case the thickness of the triangular fin at the base is  $s'_R$ . For this formula a generalization exists, whereby the triangular fin is considered as a special case of the trapezoidal fin; for the latter one

$$s_R = \frac{3}{4} s'_R + \frac{1}{4} s''_R \quad (11)$$

is valid, where  $s''_R$  is the thickness of the trapezoidal fin at the top. To simplify more complex fin cross-sections,  $\frac{s_R}{2}$  can be replaced by  $\frac{A}{U}$  in equation (3). Here  $A$  is the mean heat-conducting cross-section of the fin and  $U$  the mean circumference at which heat is transferred. Thus:

$$m^* = \sqrt{\frac{\alpha U}{\lambda_{Ri} A}} \quad (12)$$

Closed solutions exist for the calculation of fin efficiency of flat fins. In this case the relation

$$s = \frac{s'_R}{2} \left(1 - \frac{h_x}{h}\right)^{\frac{1}{2}}, \quad (13)$$

for the fin profile of fins with parabolic cross-section results in an efficiency value as follows:

$$\eta_R = \frac{1}{m h} \frac{I_{\frac{2}{3}}(4/3 m h)}{I_{-\frac{1}{3}}(4/3 m h)}. \quad (14)$$

This fin geometry is hardly used because it does not offer any thermal advantages in comparison with others. An existing closed solution for fin efficiency  $\eta_R$  is not

a sufficient reason for an application. The other kind of parabolic fin, with the vertex of the parabola at the fin top, results in a fin with a sharp spike at the top which is a disadvantage for production and handling. This profile is, according to Th. E. Schmidt [1], the one with the smallest volume and weight for a given transferable amount of heat. The fin profile is given by:

$$s = \frac{s'_R}{2} \left(1 - \frac{h_x}{h}\right)^2 \quad (15)$$

In this way fin efficiency is calculated as:

$$\eta_R = \frac{2}{\sqrt{(2mh)^2 + 1} + 1} \quad (16)$$

Needles or pins can also be attached to enlarge the surface. Needle fins with cylindrical cross-section are commonly used. Fin efficiency here can be calculated as

$$\eta_R = \frac{\tanh(\sqrt{2}mh)}{\sqrt{2}mh} \quad (17)$$

where  $m$  is derived from the diameter of the needles. This relationship is identical to equation (7) if the equivalent fin thickness is half the diameter of the needle fin.

### 2.2.2 Finned tubes

Fins are used to enlarge the flat surfaces of any kind of tube. The basic considerations about fin efficiency are also valid for cylindrical geometry. Solutions of the differential equation in cylindrical polar coordinates are of a different nature than solutions in Cartesian coordinates.

$$s(r) \frac{d^2\theta}{dr^2} + \left( \frac{s(r)}{r} + \frac{ds(r)}{dr} \right) \frac{d\theta}{dr} - \frac{\alpha}{\lambda_{Ri}} \theta = 0 \quad (18)$$

$s(r)$  in this case is one-half the fin thickness depending on the radius  $r$ . The solution has to satisfy the boundary conditions at the fin base

$$r = r_0 \quad \theta = \theta_0 \quad (19)$$

and at the fin top

$$r = r_0 + h \quad \frac{d\theta}{dr} = 0. \quad (20)$$

As is to be expected for the differential equation in cylindrical polar coordinates above, an expression with modified Bessel functions results for fin efficiency.

$$\eta_R = \frac{2}{mh\left(\frac{R}{r_A} + 1\right)} \left[ \frac{I_1(mr_A)K_1(mR) - I_1(mR)K_1(mr_A)}{I_0(mr_A)K_1(mR) + I_1(mR)K_0(mr_A)} \right] \quad (21)$$

$r_A$  in this case is the radius of the core tube,  $R$  the radius above the fins.

Not long ago the detection and interpolation of Bessel functions in mathematical tables was still arduous and laborious. Thus approximations were introduced to replace this activity. The approximation by Brandt [9] is the most precise equation.

$$\eta_R = \frac{2r_A \tanh mh}{(2r_A + h)mh} \left[ 1 + \frac{\tanh mh}{2mr_A} - 0.71882 \frac{[\tanh mh]^{3.7482}}{[mh]^{1.481}} \right] \quad (22)$$

Much simpler, yet still precise enough, is the approximation equation by Th. E. Schmidt [1]. The maximum error for  $\eta_R > 0.5$  is approx. 1%.

$$\eta_R = \frac{\tanh (mh\varphi)}{mh\varphi} \quad (23)$$

$$\varphi = 1 + 0.35 \ln \left( 1 + \frac{h}{r_A} \right) \quad (24)$$

With annular fins, only a closed solution exists for rectangular fins and hyperbolic fins with the profile  $s = s'' \frac{r_A}{2r}$  [11]. Finned tubes with triangular or trapezoidal fins are calculated with a corrected fin thickness. This is the arithmetic mean of fin thickness at the fin base and at the fin top.

The heat transfer at the fin top is not considered in the mathematical solutions for heat conduction in annular fins shown above. To take this into account, according to Th. E. Schmidt [1] the fin height should be increased by one-half the fin thickness at the fin top:

$$h' = h + \frac{sR}{2} \quad (25)$$

Equation (23) thus becomes:

$$\eta_R = \frac{\tanh (mh'\varphi)}{mh'\varphi} \quad (26)$$

Tubes with mounted rectangular fins are frequently used. Rectangular or hexagonal fin forms result in particular when fins are made to pass over several tubes. Whether fins are calculated as square, rectangular or hexagonal only depends on the arrangement of tubes as well as the transverse and longitudinal pitch. The fins of tubes arranged in line should be considered rectangular while those of tubes in staggered arrangement as hexagonal. The equivalent fin height for rectangular fins can be calculated according to the following equation:

$$h = 0.565 b_w \sqrt{\frac{a_w}{b_w} - r_A} \quad (27)$$

$b_w$  in this case represents the longer side of the rectangle,  $a_w$  the shorter one. According to [15] a similar formula which provides more precise results is valid:

$$h = 0.64 b_w \sqrt{\frac{a_w}{b_w} - 0.2 - r_A} \quad (28)$$

The difference between the simple formula and the more precise one is particularly important in the case of smaller aspect ratios  $\frac{a_w}{b_w}$ . According to the VDI Waermeatlas [15], equation (7) is to be written as:

$$\eta_R = \frac{\tanh(\varphi_A \frac{d_A}{2} m)}{\varphi_A \frac{d_A}{2} m} \quad (29)$$

$h$  is thus related to the tube radius  $d_A/2 = r_A$  using a shape factor  $\varphi_A$ :  $h = \varphi_A d_A/2$ . If fins are attached to separately the each individual tube, the reduced fin height  $h'$  of rectangular fins is determined according to equation (25) to take into account heat transfer at the fin top. This is more vividly demonstrated by using this notation than that used in VDI Waermeatlas [15]. If fins pass over several tubes, the heat transfer at the fin top is taken into account less or dropped completely. For a fin with a regular hexagon, the equivalent fin height becomes:

$$h = 0.551 s_W - r_A \quad (30)$$

$s_W$  in this case is the width across flats of the hexagon. The fin height  $h$  for an irregular hexagon is calculated as:

$$h = 0.635 s'_W \sqrt{\frac{s''_W}{s'_W} - 0.3 - r_A} \quad (31)$$

In this case  $s''_W$  is the larger width across flats, which is obtained by  $s''_W = \sqrt{t_l^2 + t_q^2/4}$ .  $s'_W$  becomes  $s'_W = t_q$  if  $t_l \geq t_q/2$ . If  $t_l < t_q/2$  then  $s'_W = 2 t_l$ .

A short remark should be made here concerning the selection of fin height and fin thickness in dependence of the thermal conductivity of the material of the fin and the heat transfer number.

According to [34], for flat fins with a height  $h$  and a thickness  $s_R$  a condition for the maximum of transferred heat results from:

$$m \cdot h = \sqrt{\frac{2\alpha}{\lambda_{Ri} s_R}} h = 1.4192 \quad (32)$$

Hence a dependency results between the fin height, on the one hand, and the square root of the fin thickness as well as the square root of the heat conduction coefficient and, reciprocally, the square root of the heat transfer number on the other. Thus, in those few cases when one is free in the choice of fin dimensions, it is possible to get a reasonable specification using the simple equation showed above.

### 2.3 Special consideration in the calculation of heat transfer

The external surface per m tube is enlarged by up to 15 times through the fin arrangements. The transferable amount of heat does not increase to the same extent, however. The reason for this is the conduction through the fins, which results in the external fin sections adopting a different temperature from the core tube, one that is closer to the gas temperature, thus reducing the effective temperature difference of the heat transfer.

With the aid of fin efficiency, the apparent heat transfer coefficient  $\alpha$  is calculated from the actual or real heat transfer coefficient  $\alpha_0$  (occurring at the surface) using the equation:

$$\alpha = \alpha_0 \frac{A_{Ri} \eta_R + A_{Ro}}{A_{Ri} + A_{Ro}} \quad (33)$$

For a further calculation of a overall heat transfer coefficient for finned tube bundles, one has to take into account in particular the different surfaces on the gas side (fins) and on the liquid side (internal tube surface). It is for example possible to calculate this using the well known equation:

$$k = \frac{1}{\frac{1}{\alpha} + \frac{A_{tot}}{A_R} \left( \frac{d_A}{2\lambda_{Ro}} \ln \frac{d_A}{d_i} + \frac{d_A}{d_i \alpha_i} \right)} \quad (34)$$

$\alpha_i$  is the heat transfer coefficient for the tube medium while the preceding expression  $\frac{d_A}{2\lambda_{Ro}} \ln \frac{d_A}{d_i}$  accounts for conduction through the tube wall. The quotient  $\frac{A_{tot}}{A_R}$  represents the different surfaces which are available on the gas side and on the tube side for heat transfer to the tube interior.  $A_R$  in this case is the entire external surface of the plain tube per m tube, that is  $A_R = d_A\pi$  (figure (7)).

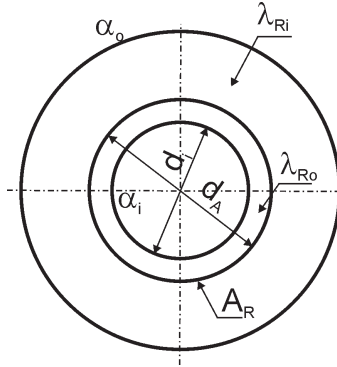


Figure 7: **Heat conduction through the finned tube**

The thermal conductivity  $\lambda_{Ro}$  of the tube material is not in general the same as for the fin material  $\lambda_{Ri}$ ; thus, both thermal properties have to be known and inserted at the correct place in each case.

### 3 Equations for the external heat transfer coefficient

The external heat transfer coefficient  $\alpha_0$  is calculated from the common dimensionless numbers for heat transfer,  $Re$  and  $Pr$ , as a dimensionless groups for heat transfer  $Nu$ . In this case the resulting dimensionless number  $Nu_0$  is set in the formulas in place of  $\alpha_0$ .

$$Nu_0 = \frac{\alpha_0 l'}{\lambda_G} \quad (35)$$

Selection of the characteristic dimension  $l'$  for finned tubes in the dimensionless numbers  $Nu$  and  $Re$  poses a problem; unlike the internal diameter  $d_i$  (for the heat transfer in a tube) or the outer tube diameter  $d_A$  (in the case of the heat transfer upon smooth tubes in cross-flow) an obvious choice for a characteristic length is missing in this case. According to the calculation method of Th. E. Schmidt [1], Stasiulevicius et al. [3] and other authors, the diameter of the core tube  $d_A$  is used for  $l'$ . Yet the choice of  $d_A = l'$  does not exactly describe the physical processes of heat transfer at finned tubes, hence additional parameters are adopted.

#### 3.1 Staggered tube arrangements

##### 3.1.1 Overview of equations

1. Calculation according to Th. E. Schmidt (abbr.: MM)

For the evaluation of heat transfer in finned tubes, measurements were performed by Th. E. Schmidt[1] on behalf of the tube manufacturer Mannesmann. From these measurements equations have been developed which are associated with his name. According to Th. E. Schmidt, adoption of the bare tube diameter in terms of significance as a variable for determining heat transfer at finned tubes is compensated by the addition of the area ratio  $A_{tot}/A_R$ .

$$Nu_0 = C Re^{0.625} Pr^{1/3} \left(\frac{A_{tot}}{A_R}\right)^{-0.375} \quad (36)$$

This equation can also be expressed as:

$$Nu_0 = C \left(\frac{Re A_{tot}}{A_R}\right)^{0.625} \frac{A_{tot}}{A_R} Pr^{\frac{1}{3}} \quad (37)$$

The expression within the brackets can also be seen as Reynolds number, calculated with a characteristic length  $l'$ :

$$l' = d_A \frac{A_{tot}}{A_R} \quad (38)$$

In this case  $A_{tot}$  is the entire gas-side heating surface per m tube and  $A_R$  is the heating surface of the smooth bare tube per m. The constant  $C$ , according to Th. E. Schmidt, is  $C = 0.45$  for staggered tube arrangements and  $C = 0.30$  for in-line arrangements. Schmidt does not mention this to dependent on the tube pitch in the tube bundles. The values of the constants are average values resulting from many test cases, mostly with annularly fins, which offer lower heat transfer coefficients than spiral fins. For the latter, the constants might be increased around approx. 10%.

## 2. Calculation according to Mannesmann-Carnoy (MC)

The fact that heat transfer for welded spiral finned tubes is a little higher than for annular finned tubes is taken in account by replacing the constant of 0.45 in the formula of Th. E. Schmidt by an expression depending on the fin pitch.

$$Nu_0 = (0.491 + 6.10^{-4}n_R - 4.10^{-7}n_R^2) Re^{0.625} Pr^{1/3} \left(\frac{A_{tot}}{A_R}\right)^{-0.375} \quad (39)$$

$n_R$  in this case is the number of fins per m tube and thus  $n_R = \frac{1}{t_R}$ . This formula was not published officially but rather developed by users according to the specifications of the manufacturer Mannesmann-Carnoy.

## 3. Calculation according to Stasiulevicius et al. and HEDH (HE)

According to Stasiulevicius et al.[3] and HEDH [2], other geometrical parameters of finned tube are taken into account with the help of additional terms, e.g. fin height, fin thickness, fin pitch. Since finned tubes are mostly used in form of tube bundles, certain parameters have to be added, such as the transverse pitch and the longitudinal pitch as well as the specification of tube arrangement, i.e. staggered or in-line. The common equation for the heat transfer on the air side of finned tube bundles is basically:

$$Nu_0 = C Re^{C_1} Pr^{C_2} \left(\frac{h}{d_A}\right)^{C_3} \left(\frac{t_R}{d_A}\right)^{C_4} \left(\frac{s_R}{d_A}\right)^{C_5} \left(\frac{t_q}{d_A}\right)^{C_6} \left(\frac{t_l}{d_A}\right)^{C_7} \quad (40)$$

In the calculation formula for  $Nu_0$ , it is necessary to separate the parameters related to the finned tube from those for the tube bundle; the influence of  $h, t_R, s_R$  is represented by additional terms or by the characteristic length  $l'$ .

The additional factors of  $t_q/d_A$  and  $t_l/d_A$  are introduced for the transversal and the longitudinal pitch.

The specific form of the equation, which was discovered by [3] and then taken over by HEDH [2], is as follows for a staggered tube arrangement:

$$Nu_0 = C Re^{C_1} Pr^{1/3} \left(\frac{t_q}{t_l}\right)^{0.2} \left(\frac{t_R - s_R}{d_A}\right)^{0.18} \left(\frac{h}{d_A}\right)^{-0.14} \quad (41)$$

For the constant  $C$  and the exponent  $C_1$  of  $Re$  the following holds:

$$\begin{aligned} 10^2 < Re < 2 \cdot 10^4 & C = 0.19 & C_1 = 0.65 \\ 2 \cdot 10^4 < Re < 2 \cdot 10^5 & C = 0.05 & C_1 = 0.80 \\ 2 \cdot 10^5 < Re < & C = 0.008 & C_1 = 0.95 \end{aligned}$$

The slope of the function for the Nusselt number increases with the Reynolds number.

#### 4. Mirkovics' equation (MI)

Mirkovics [5] also suggests a similar equation which uses a characteristic length  $l'$  in the place of  $d_A$  for the calculation of heat transfer. The remaining parameters are similar to [3] and [2].

$$l' = \frac{2A_{tot}}{\pi l_k} \quad (42)$$

The length  $l_k$  is expressed as follows

$$l_k = \frac{2h + t_R}{t_R} \quad (43)$$

as one-half the circumference of the flow channel.

$$Nu_0 = 0.224 \left(\frac{t_q - d_A}{d_A}\right)^{0.1} \left(\frac{t_l - d_A}{d_A}\right)^{-0.15} \left(\frac{t_R - s_R}{h}\right)^{0.25} Re^{0.662} Pr^{0.33} \quad (44)$$

The velocity, which influences the dimensionless number  $Re$ , is generally the velocity at the narrowest cross-section. In staggered tube arrangements, this does not necessarily have to be arranged absolutely orthogonal to the flow direction.

#### 5. Brandts equation (BA)

Pursuing another course, Brandt [9] uses as a characteristic length

$$l' = \frac{\pi}{2} \sqrt{d_A^2 + h^2} \quad (45)$$

In addition to this, termed flooding length, an arrangement factor has to be calculated, which is determined by the remaining geometrical data.

Brandt[9] calculates  $Nu_0$  according to the equations of Gnielinski [23]:

$$Nu_0 = 0.3 + \sqrt{(Nu_{lam})^2 + (K Nu_{turb})^2} \quad (46)$$

$Nu_{lam}$  in this case is:

$$Nu_{lam} = 0.664 \sqrt{Re_l} Pr^{1/3} \quad (47)$$

and for  $Nu_{turb}$  follows:

$$Nu_{turb} = \frac{0.037 Re_l^{0.8} Pr}{1 + 2.443 Re_l^{-0.1} (Pr^{2/3} - 1)} \quad (48)$$

The turbulent Nusselt number is multiplied by the factor K, which is derived from the fin height and the tube diameter.

$$K = 1 - 0.15 e^{-10 \frac{h}{d_A}} \quad (49)$$

The factor K includes the fin height with the term  $h/d_A$ . Yet, another arrangement factor  $K_{An}$  exists which considers all geometrical data of the finned tube bundle. A selection of the constants for the calculation of  $K_{An}$  also takes into account the staggered or in-line arrangement of finned tube bundles. The longitudinal pitch  $t_l$  is used, it hardly has any influence, however. The factor K is used in the formula above because Brandt [9] tried to develop a generally valid equation which takes into account all conceivable variants of finned tubes with fin height "zero", that is a bundle of smooth tubes in cross-flow up to a tube diameter of "zero" or a group of plates in longitudinal flow.

The arrangement factor  $K_{An}$  for the finned tube bundle is supposed to satisfy the boundary conditions for  $d_A = 0$  and for  $h = 0$ .

$$K_{An} = (A + (1 - A)x^m + (n_A - A)(\exp(-E x) - \exp(-E)x)) f_N \quad (50)$$

In this case  $n_A$  is the arrangement factor for a smooth tube bundle, whereas  $x = 2h/D$  is the related fin height as well as the following factors are related to the diameter above the fins  $D = d_A + 2h$ .

$$\begin{aligned} x_s &= s_R/D \\ x_a &= (t_R - s_R)/D \\ x_q &= t_q/D \end{aligned}$$

Table 1: Constants in the formula of Brandt

-	staggered	in-line
$A_1$	-8.584	-6.863
$A_2$	0.4177	7.473
$m_a$	0.832	0.0393
$m_s$	-1.030	-0.0233
$m$	1.112	1.1785
$E$	0.0127	13.75
$f_{n1}$	0.87	0.951
$z_1$		0.0465
$z_2$		2.22
$z_3$		1.6
$z_4$		0.13
$z_5$		5.346

$E$  and  $m$  are constant values and/or exponents depending on in-line or staggered tube arrangement.  $f_N$  is a factor for less than 8 tube rows. Brandt [9] assumes that only the first tube row of a bundle shows a differing amount of heat transfer with the factor  $f_{n1}$ . Under this assumption the reduction coefficient for a few tube rows is:

$$f_N = (f_{n1} + (n_R - 1))/n_R. \quad (51)$$

The variable  $A$ , furthermore, is:

$$A = (A_1 + A_2 x_a^{m_a} x_s^{m_s}) z_q \quad (52)$$

$m_a$  and  $m_s$  depend on the tube arrangement;  $z_q$  is a factor developed by Wehle [40] which takes into account the transverse pitch.

$$z_q = 1 + z_1(\tanh(z_2(x_q - z_3)) + 1) + z_4 \exp(-z_5(x_q - z_3)^2) \quad (53)$$

The factors  $z_1$  to  $z_5$  are constant. All factors are listed in table 1, which is taken from a summary in 1998 by Brandt and not from [9].

Finally, the arrangement factor for the smooth tube bundles has to be defined; this of course depends on the tube arrangement. For in-line tube arrangement the distinction is made whether  $e_l = t_l/d_A > 1.25$ , in which case the following holds:

$$n_A = 1 + 0.2369 \exp(-0.1(\ln(z) + 0.6)^2) \quad (54)$$

In the other case, when  $e_l$  is  $< 1.25$ , this holds:

$$n_A = 0.5 + 0.4 \exp(-0.42 (\ln(z) + 0.6)^2) \quad (55)$$

The parameter  $z$  depends on the derived transverse and longitudinal pitch; the former is  $e_q = t_q/d_A$

$$z = \frac{4}{\pi} e_q - \frac{1}{e_l} \quad (56)$$

The following equation is to be used for a staggered tube arrangement:

$$n_A = (1 + 0.2973 \exp(-0.05 (\ln(z) + 0.6)^2))zv \quad (57)$$

and for the factor  $zv$  it follows that

$$zv = 1 + dv \exp(-2.422 (\log(x) - 0.5)^2) \quad (58)$$

The factor  $dv$  is  $dv = 0.1685$  for  $e_l > 1$ , otherwise  $dv = 0.0562$ .

#### 6. Equation of FDBR (FD)

FDBR [10] selects for the characteristic length the equivalent in area diameter according to Schmidt [1].

$$l' = \frac{A_{tot}}{\pi} \quad (59)$$

The equation of FDBR [10] seems to be different from Th. E. Schmidt's [1], but a closer comparison with [1] reveals that FDBR just uses another notation.

#### 7. Biery's equation (BI)

Among calculations of heat transfer, Biery's equation [7] is a special case, as it reduces every finned tube bundle to a smooth tube bundle in equilateral triangular pitch.

#### 8. Equation of ESCOA (EG)

Further equations for external heat transfer at finned tubes are defined by ESCOA (Extended Surface Corporation of America) [12] as well as Mannesmann, a finned tube manufacturer.

ESCOA's equation for staggered arrangements of tubes with smooth fins is given, after transformation from American notation, by:

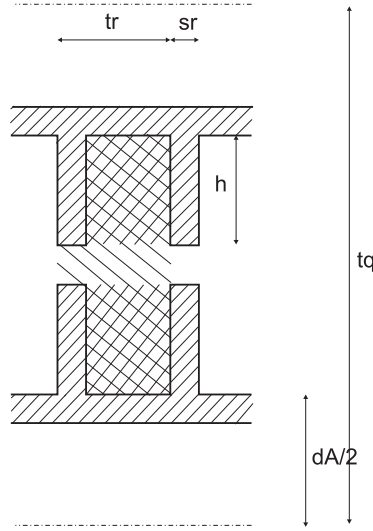


Figure 8: **Free-flow cross-section and free-flow cross-section within the outline of the finned tube**

$$Nu = 0.25 Re^{0.65} Pr^{1/3} \left( \frac{\vartheta_{gm} + 273.2}{\vartheta_{rm} + 273.2} \right)^{1/4} \left( \frac{D}{d_A} \right)^{0.5} C_3 C_5 \quad (60)$$

In this case  $\vartheta_{gm}$  is the mean gas temperature,  $\vartheta_{rm}$  is the mean fin temperature,  $D$  the diameter above the fins, i.e.  $D = d_A + 2h$  and  $C_3$  is a factor which specifies the influence of the fin height and the fin distance:

$$C_3 = 0.35 + 0.65 \exp(-0.25 h / (t_R - s_R)) \quad (61)$$

$C_5$  accounts for the influence of the transversal and the longitudinal pitch in the fin bundle as well as the number of consecutive tubes in cross-flow.

$$C_5 = 0.7 + (0.7 - 0.8 \exp(-0.15 n_R^2)) \exp(-t_l / t_q) \quad (62)$$

ESCOA also defines an equation for finned tubes with serrated fins [17]: (abbr.: ES). The formula for  $Nu$  in this case is identical with equation (60) and the coefficient  $C_5$  also remains constant. The following holds only for the coefficient  $C_3$  with serrated fins:

$$C_3 = 0.55 + 0.45 \exp(-0.35 h / (t_R - s_R)) \quad (63)$$

#### 9. Equation of the VDI Waermeatlas, 7th edition (WA)

A further equation for heat transfer at staggered finned tube bundles is specified in the VDI Waermeatlas, 7th edition, pages Mb1-Mb4 [15]. This

equation is very similar to Schmidt's but uses other coefficients and exponents;  $d_A$  is also used as the characteristic length.

$$Nu = 0.38 Re^{0.6} Pr^{1/3} \left( \frac{A_{tot}}{A_R} \right)^{-0.15} \quad (64)$$

This equation is valid for 4 or more consecutive tube rows. The constant is 0.36 for 3 tube rows and 0.33 for 2 tube rows.

#### 10. Nir's equation (NI)

Nir's approach [18] uses the hydraulic diameter, which is determined with the help of the flow cross-section at the profile of the finned tube as related to the heating surface and the diameter above the fins.

$$d_h = 4 d_F / W \quad (65)$$

The quotient  $W = A_{tot}/A_{of}$  is be found once again in the equation for  $Nu$ .

$$Nu = 1.745 Re(d_h)^{0.60} Pr^{1/3} W^{-2/3} R_b^{-0.40} K_z \quad (66)$$

The related free-flow cross-section  $A_{of}$  can be written in this way:

$$A_{of} = t_q - d_A - 2 h \frac{s_R}{t_R} \quad (67)$$

$R_b$  is the quotient of the total free-flow cross-section (\\\\) divided by the free-flow cross-section within the perimeter of the tube (///), as shown in figure (8), and thus can be expressed as:

$$R_b = \frac{t_q - d_A - 2 h \frac{s_R}{t_R}}{2 h \left( 1 - \frac{s_R}{t_R} \right)} \quad (68)$$

$K_z$  is a reduction factor for less than 4 consecutive tubes in cross-flow.

#### 11. Vampola's equation (VA)

The J. Vampola's equation [14] for staggered finned tube bundles is not well known in this country. The original work, written in Czech, uses a characteristic length which is derived from the tube diameter  $d_A$  and an equivalent fin diameter  $\sqrt{A_{Ripp} t_R} 1/2$  with a weighted average value for the bare tube surface and the fin surface.

$$d_h = \frac{A_{Rohr} d_A + A_{Ripp} \sqrt{A_{Ripp} t_R} 1/2}{A_{Rohr} + A_{Ripp}} \quad (69)$$

During calculation of heat transfer, a distinction is made between whether the diagonal pitch  $t_d$  is greater or smaller than the transverse pitch.

$$t_d = \sqrt{\left(\frac{t_q}{2}\right)^2 + t_t^2} \quad (70)$$

If it is smaller, i.e.  $t_d < t_q$ , the following holds:

$$Nu = 0.251 Re_{dh}^{0.67} \left(\frac{t_q - d_A}{d_A}\right)^{-0.2} \left(\frac{t_q - d_A}{t_R - s_R} + 1\right)^{-0.2} \left(\frac{t_q - d_A}{t_d - d_A}\right)^{0.4} \quad (71)$$

Otherwise, i.e.  $t_d > t_q$ , the following holds:

$$Nu = 0.251 Re_{dh}^{0.67} \left(\frac{t_q - d_A}{d_A}\right)^{-0.2} \left(\frac{t_q - d_A}{t_R - s_R} + 1\right)^{-0.2} \quad (72)$$

For  $t_d = t_q$  the last term in equation (71) becomes 1. In this case the two formulas for  $t_d = t_q$  result in identical values. The formula specified above is valid for smooth fins. Vampola also defines formulas for wavy fins and for pin fins. In his equations for heat transfer, Vampola does not include the term with the Prandtl number. The formulas are valid for air as the flow gas because, as Vampola mentions, the test cases were carried out with air.

If the Prandtl number differs considerably from the value for air, the formula has to be multiplied by  $(Pr/Pr_L)^{1/3}$ .

### 3.1.2 Equations for a single tube row

The equations mentioned above are valid in general for several consecutive tube rows in cross-flow. Yet there is no agreement between individual authors on the tube row number at which the heat transfer coefficient remains constant. Equations for one tube row are required, since two or even only one tube row occur sometimes in heat recovery boilers.

1. Equation for one tube row according to VDI Waermeatlas 4th edition (1R)

There is no specification in [15] for only one tube row, however in the older 4th edition (1984) of VDI Waermeatlas [4] instructions can be found for calculating only one finned tube row. (On the other hand, this suggestion for calculation of heat transfer at finned tube bundles cannot be recommended). The calculation of heat transfer at only one finned tube row in [4] is based on the calculation of heat transfer at the body surrounded by the flow and is similar to Brandt [9] and draws on Gnielinski [23]. The

flooding length  $l$  is used in this case as the characteristic length. For finned tubes this is determined as:

$$l = \frac{\pi}{2} \sqrt{d_A^2 + h^2} \quad (73)$$

For the calculation of the Reynolds number, the average velocity in the tube bundles has to be used as the standard velocity  $w_R$  in the case of the following calculation method:

$$w_R = w_m = \frac{1}{2}(w_0 + w_E) \quad (74)$$

This holds if the fin edges almost touch each other. This is the case when  $(t_q - d_A - 2h)/t_q < 0.1$  is valid. On the other hand, if  $(t_q - d_A - 2h)/t_q > 0.2$ , then  $w_R$  is calculated according to the following equation:

$$w_R'' = w_m \frac{1 - (0.31Re^{-0.04} [h/(t_R - s_R)]^{0.5} (d_A/h)^{0.25}}{1 - s_R/t_R} \quad (75)$$

If the distance between the fin edges lies between the two criteria, linear interpolation must be done; in this case  $a_q = (t_q - d_A - 2h)/t_q$ .

$$w_R' = \frac{a_q - 0.1}{0.1} w_R'' + \frac{0.2 - a_q}{0.1} w_m \quad (76)$$

Once  $Re$  is ascertained using  $l$  and  $w_R$  and/or  $w_R'$ , calculation continues according to the formulas for tubes given in the Waermeatlas [15], page Ge 1.

According to Gnielinski [23], the following holds:

$$Nu_0 = 0.3 + \sqrt{(Nu_{lam})^2 + (Nu_{turb})^2} \quad (77)$$

The laminar Nusselt number  $Nu_{lam}$  in this case is

$$Nu_{lam} = 0.664 \sqrt{Re_l} Pr^{1/3} \quad (78)$$

while the turbulent Nusselt number  $Nu_{turb}$  is:

$$Nu_{turb} = \frac{0.037 Re_l^{0.8} Pr}{1 + 2.443 Re_l^{-0.1} (Pr^{2/3} - 1)} \quad (79)$$

## 2. ESCOA Equations

According to the ESCOA equation, heat transfer may be calculated even for one tube row, for both staggered tube arrangements (using the relation stated above) and for in-line tube arrangements (according to the method described below). Since it makes no sense to specify staggered or in-line arrangement for one tube row, both relations have to show the same result for  $n_R = 1$ . Verification shows that this indeed holds for large values for  $h/(t_R - s_R)$ , while for small values for  $h/(t_R - s_R)$  the formula for in-line arrangement results in as much as 15% higher heat transfer values compared with the formula for staggered arrangement.

Test cases with only one tube row, as well as with a second row in both in-line and staggered arrangement, are found in the work of Kearney and Jacobi [22]. In this publication, the geometrical data of finned tubes as well as pitches were unfortunately not varied. The pitches are chosen in such a way that in both arrangements (in-line and staggered) the fin edges touch each other. The data presented may therefore be used only as measurement values. At the ITE it was only possible to carry out one series of measurements with a one-tube row arrangement. For more information refer to section 3.5.2.

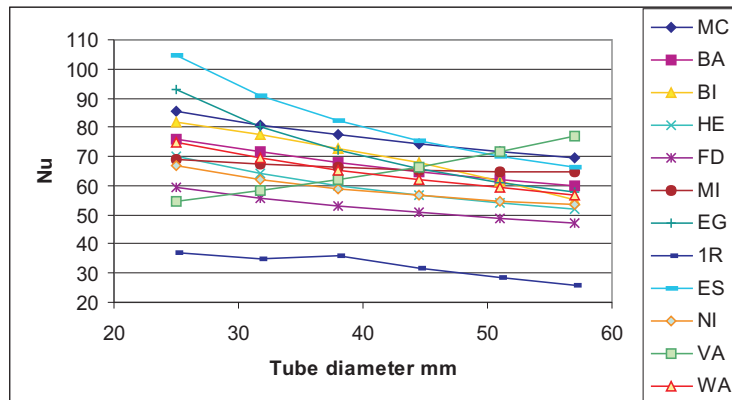


Figure 9: Influence of tube diameter on heat transfer with unmodified fin geometry and fin pitches

### 3.1.3 Influence of geometrical dimensions of the finned tube and of bundle geometry

The influence of the geometrical dimensions of a single finned tube is first to be considered without the factors which characterize the finned tube bundle. For comparison, the dimensional heat transfer coefficient  $\alpha$  can be used; the

dimensionless Nusselt number provides no useful basis of comparison since the characteristic lengths are defined differently, i.e. as hydraulic diameters. Alternatively, the Nusselt numbers derived from differing characteristic lengths can be converted to one characteristic length, which in our case would be the tube diameter  $d_A$ . The comparable calculations are performed for a finned tube with a basic configuration as follows: a diameter of 38 mm and a fin height of 16 mm, fin thickness of 1 mm and a fin pitch of 6.67 mm (150 fins per m tube). For the finned tube bundle, assumptions are made as follows: a transverse pitch of 85 mm and a longitudinal pitch of 75 mm for 8 consecutive tube rows in staggered arrangement.

**Tube diameter:** All equations for the calculation of the heat transfer coefficient show that the heat transfer coefficient  $\alpha$  declines with an increase in tube diameter; only the magnitude varies. The decline is smallest with BA and MI and still small with FD, 1 R and MC, and even with NI, somewhat greater with WA and HE, and the greatest with EG, ES and BI, as seen in figure (9).

The characterization stated above is only valid for variations in tube diameter with constant fin geometry and fixed transverse and longitudinal pitch. These pitches have to be designed with consideration to the largest tube diameter and are therefore, with respect to space requirements and heat transfer, unfavorable for smaller tube diameters. Factors affecting variation of the tube diameter with unchanged fin geometry and adapted transverse pitch were also examined. Modification was done in such a way that the transverse distance between the fin edges remained constant and the longitudinal pitch was not changed.

The lowest variation of heat transfer results at 1 R, the highest at ES, whereas, similar to a constant transverse pitch, the heat transfer coefficient declines with an increasing tube diameter. The only exception is the VA equation, which results in a heat transfer coefficient that even rises a little with tube diameter; refer to figure (10).

All statements made above are valid for the case that the velocity in the narrowest cross-section remains constant ( $w_E = const.$ ). In this case the Reynolds number rises with the tube diameter. If the Reynolds number  $Re$ , and not the velocity  $w_E$ , is kept constant, figure (11) is the result for an identical transverse pitch. The Nusselt number declines consistently with increasing diameter. Only equation 1R results in an initial decline and a subsequent rise in the middle range from 38 mm to 44.5 mm.

When varying the transverse pitch with the tube diameter, figure (12) results for a constant Reynolds number. In this figure, without exception all Nusselt numbers decline consistently with an increasing tube diameter.

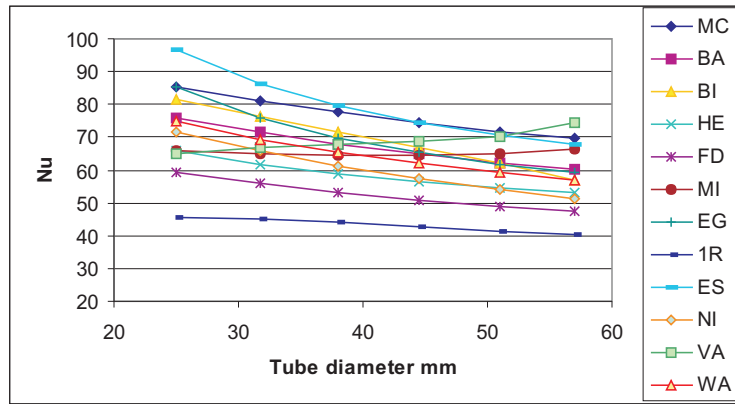


Figure 10: Influence of tube diameter on heat transfer with unmodified fin geometry and adapted transverse pitch (staggered arrangement)

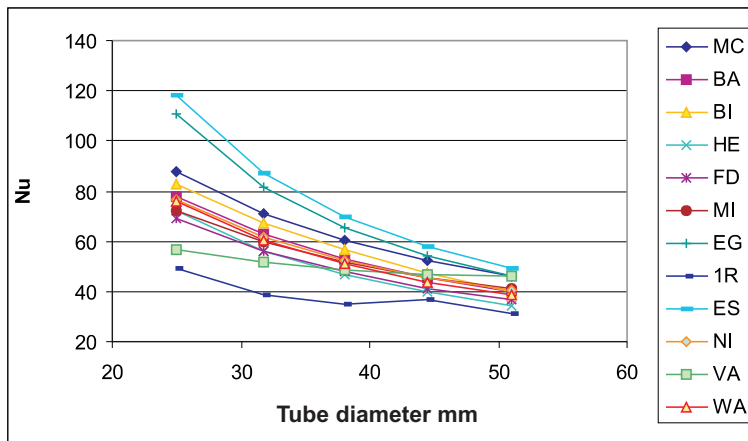


Figure 11: Influence of tube diameter on heat transfer with unmodified fin geometry and transverse pitch (staggered arrangement) at constant Reynolds number

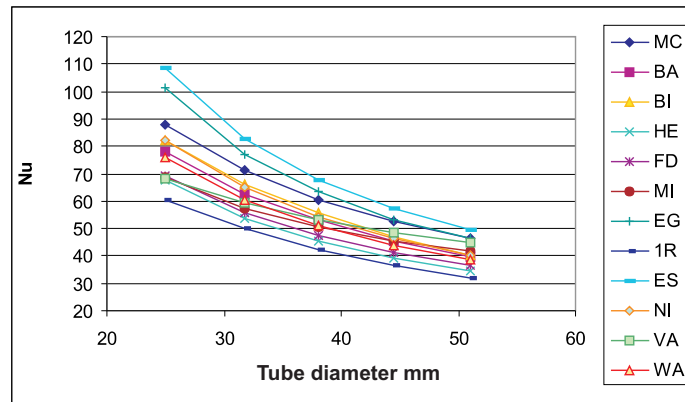


Figure 12: Influence of tube diameter on heat transfer with unmodified Reynolds number and fin geometry and adapted transverse pitch (staggered arrangement)

**Fin pitch:** With an increasing fin pitch, the heat transfer coefficient  $\alpha_0$  also increases, yet not proportionally, so that the decreasing heating surface per m tube is not completely compensated. As narrow a fin pitch as possible is still advantageous for a compact heat exchanger design if dirt deposits are not a great problem. Except for BA, all relations show an unequivocal tendency. The heat transfer coefficient  $\alpha_0$  increases more strongly with smaller pitches, with greater pitches, on the other hand, it increases only weakly, as follows from figure (13).

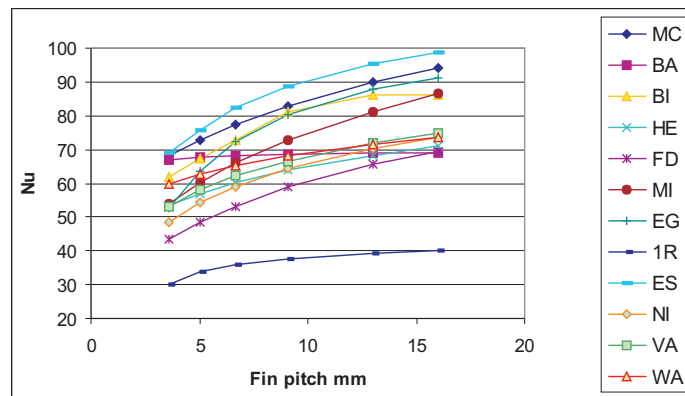


Figure 13: Influence of fin pitch on heat transfer (staggered arrangement)

**Fin height:** First of all, it was examined what effect a variation of the fin height with constant transverse pitch has, whereas the pitch had to be determined

at the greatest fin height. As expected, the heat transfer coefficient declines with increasing fin height, however only weakly. There is a gain from the heating surface, which increases with  $h$ . This observation was made without considering conduction in the fin. Since fin efficiency is not considered here, only  $\alpha_0$  (or  $Nu_0$ ), i.e. heat transfer with infinite thermal conductivity of the fin, is discussed. Heat transfer declines somewhat with ES and EG. In contrast to this, with 1 R heat transfer declines a little at first, then, from a fin height of 16 mm to 19 mm, a small increase takes place, and after that another decline is found (this is valid for a tube diameter of 38 mm). A maximum fin height results furthermore from limitations placed by finned tube production, i.e. by manufacturing methods as well as by the need to avoid fouling. There is, however, another exception among these equations: the NI calculation predicts at first a very small increase for small fin heights, then however a very small decrease of  $\alpha_0$  with the fin height. This leads to the result that the heat transfer coefficient does not depend on fin height. There are further differences in the curves for the remaining equations. The functions show linear dependence as well as progressive and digressive characteristics, as seen in figure (14).

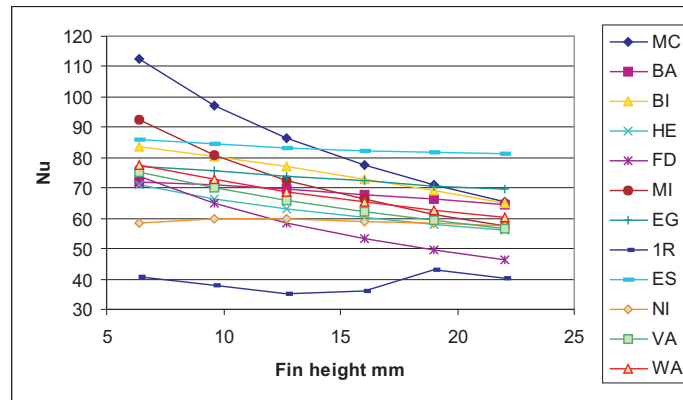


Figure 14: **Influence of fin height on heat transfer (staggered arrangement)**

Afterwards, it was examined what effect occurs as a result of a variation of the fin height with a simultaneous variation of the transverse pitch. In this case the transverse pitch was adapted in such a way that the distance between the fin edges remains constant at 5 mm for a tube diameter of 38 mm. In figure (15) the decline of the heat transfer resulting from increasing fin height is shown. This decline is above average with MC, however only in comparison with other equations. The curve of the heat transfer coefficient is identical with the previous one in figure (14), since transverse pitch does not occur in the MC equation at all. A similarly strong decline is observed

with VA, whereas with EG and ES an insignificant increase occurs. With 1 R an insignificant increase can be seen for fin heights less than 10 mm; the same decline can be seen for fin heights greater than 15 mm.

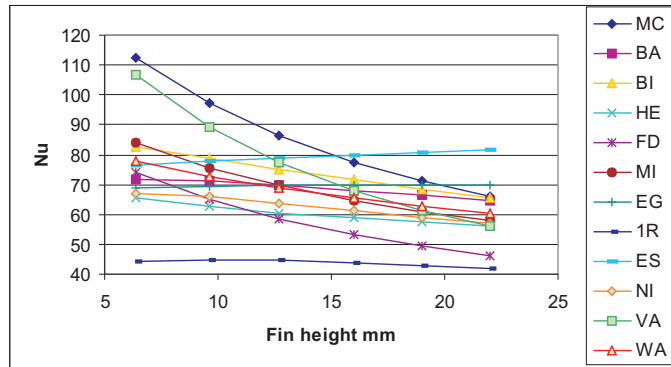


Figure 15: Influence of fin height on heat transfer at adapted transverse pitch (staggered arrangement)

**Fin thickness:** Fin thickness  $s_R$  hardly influences the heat transfer coefficient at all; its influence becomes noticeable in the case of fin efficiency. With increasing fin thickness, an insignificant decline in  $\alpha_0$  is detectable with the equations EG, ES and VA. With the equations MC, BA, HE and 1 R, a small increase is seen, while with one (FD) no influence at all is observed; figure (16).

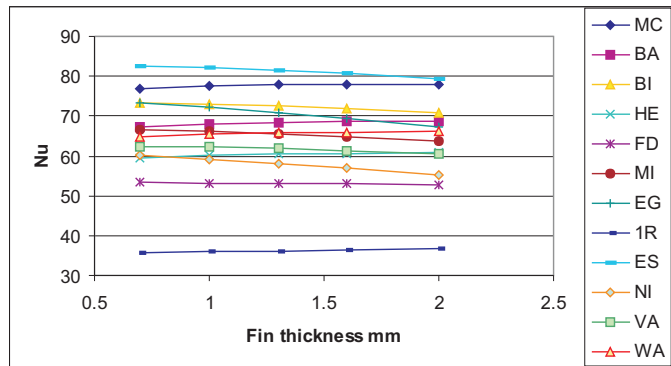


Figure 16: Influence of fin thickness on heat transfer (staggered arrangement)

**Gas velocity:** The influence of gas velocity is represented by the Reynolds number; yet the characteristic length is variously defined in the different for-

mulas, making an immediate comparison impossible. The resulting Nusselt and Reynolds numbers are standardized with the tube diameter  $d_A$  for all equations. The velocity in the narrowest cross-section is regarded as the standard gas velocity.

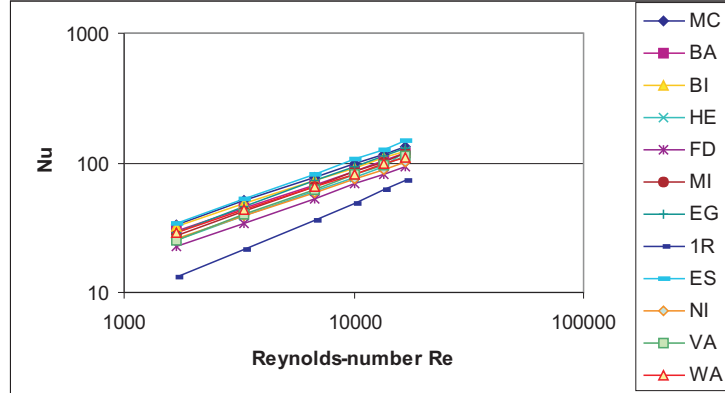


Figure 17: **Influence of gas velocity on heat transfer (staggered arrangement)**

The influence is basically represented by the exponent of  $Re$ . Deviations from this are only insignificant: in 1R,  $Nu$  is estimated as the square root of the sum of  $Nu_{lam}$  squared and  $Nu_{turb}$  squared. In a double-logarithmic diagram, a curve that more strongly rises with  $w_E$  results for  $\alpha_0$  instead of a straight line; see figure (17). With HE, three different exponents for  $Re$  are given for three different ranges of Reynolds numbers, whereas larger exponents are valid for higher Reynolds numbers; refer to the HE formulas of [2].

Influence of bundle geometry:

The influence of the geometry of the finned tube bundle with a completely staggered tube arrangement is presented in this section. The tubes in a single row in direction of flow are arranged in the middle between the positions of the tubes of the preceding tube row. The equations MC, WA and FD consider neither any influence of transverse pitch nor of longitudinal pitch. The formulas BA and NI do not recognize any influence of longitudinal pitch. Several equations do not consider the influence of the number of the tube rows consecutively arranged in direction of flow; this is treated in a separate section.

**Transverse pitch:** The influence of transverse pitch on the heat transfer coefficient is evaluated to various degrees. Several relations result in a moderate increase in the heat transfer coefficient with transverse pitch; see figure (18). This increase is somewhat greater with EG and ES, and somewhat smaller

with MI and HE. According to BI, heat transfer increases in the case of small transverse pitches then, however, reaches a final value. A decrease of  $\alpha_0$  with the transverse pitch is found by NI, and even a strong decrease is found with VA. 1 R indicates an initial increase, in cases of smaller transverse pitches up to  $t_q = 78$  mm, but then a moderate decrease, and a very small increase from  $t_q = 90$  mm on. All of these results were obtained with the standard geometry defined above. In the relations MM, MC, FD and WA, transverse pitch does not occur.

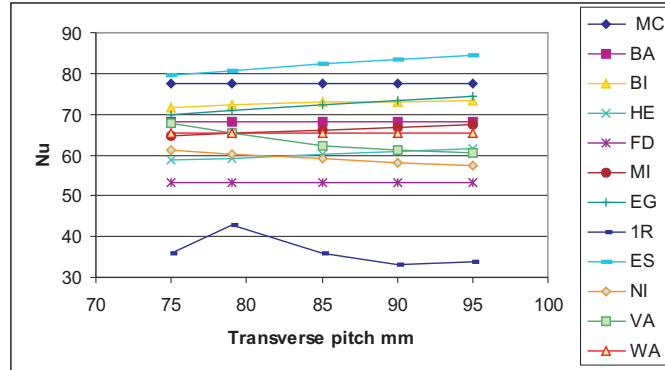


Figure 18: Influence of transverse pitch on heat transfer (staggered arrangement)

**Longitudinal pitch:** The majority of the equations ascertain a decrease in the heat transfer coefficient with a rising longitudinal pitch. With MI, ES and EG the decrease is greatest, with HE it is quite small and with VA large for small longitudinal pitches up to 75 mm. Heat transfer does not vary after that for greater longitudinal pitches. This is only valid for the underlying example. BI represents an exception, predicting an increase in  $\alpha_0$  for small longitudinal pitches. In the equations MM, MC, WA, NI and FD, longitudinal pitch does not occur. With BA it does not show any noticeable influence; see figure (19).

**Triangular pitch:** For staggered tube arrangements, a so-called triangular pitch is frequently chosen. In this case three tubes are arranged in an equilateral triangle. This is the arrangement with the best use of space, in which the greatest heating surface per volume unit is achieved for a specified distance between the finned tubes. If one examines the different relations with respect to the influence of the size of the triangular pitch on heat transfer, one ascertains that many equations do not take into account such an influence. Among these are also equations which explicitly consider the influence of

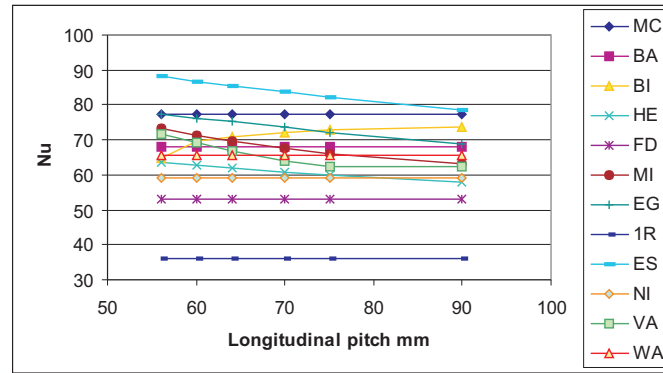


Figure 19: **Influence of longitudinal pitch on heat transfer (staggered arrangement)**

transverse and longitudinal pitch, as can be seen in figure (20). An example of this is the HE equation, in which this influence results from the quotient of the transverse and longitudinal pitch,  $t_q/t_l$ , which is independent of the size of the triangular pitch. Among the exceptions is the BI equation, which results in an increase in heat transfer with the pitch, as well as the relations MI, with an almost imperceptible decline, NI with insignificant and VA with a noticeable decline with increasing pitch.

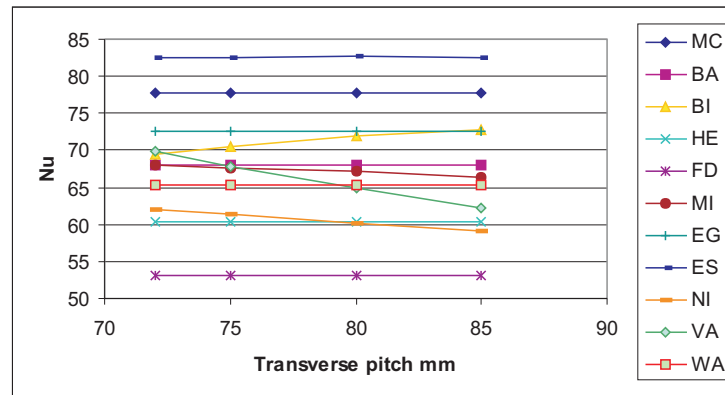


Figure 20: **Influence of triangular pitch on heat transfer**

### 3.1.4 Evaluation of different calculation formulas

If one considers only the range of application in industrial use, one will (in European countries) use either the Schmidt's formula [1] or the FDBR [10] or HEDH formula [2]; see figure (6). The equations proposed by ESCOA [12] are also very

suitable. These are, however, mostly used in the United States. Referring to the formula of Schmidt by way of example, a weakness will be pointed out, without wishing to detract from the achievements of this scientific work.

Formula (36) is very useful if it is applied to those tubes it was created for, i.e. welded spiral finned tubes for steam generators and cast finned tubes for economizers. Yet limitations to the validity of this formula may be seen in the case of a fictitious finned tube with the same ratio of  $A_{tot}/A_R$ , yet with fins having twice as large a surface and double the fin pitch. The equation predicts two equal heat transfer coefficients for these two different finned tube geometries with the same heating surface per meter; this does not correspond with the facts, as later measurements reveal.

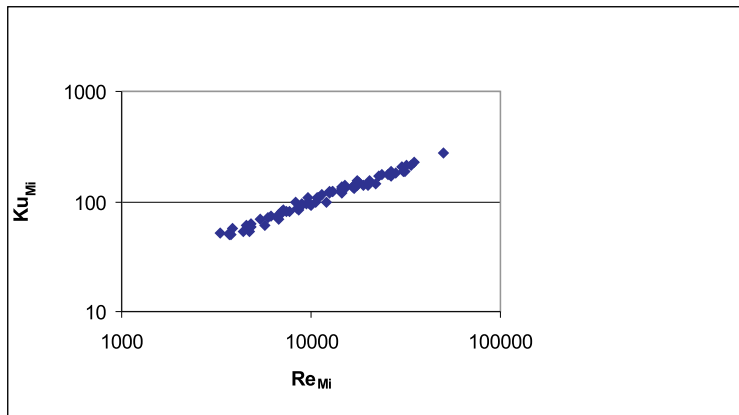


Figure 21: **Experimental results by Mirkovics showing the characteristic diameter  $d_{Mi}$**

For the calculation of heat transfer at finned tube bundles, various formulas are presented above whose range of validity is mostly not indicated or somewhat diffuse. The achievable results are therefore not of the required accuracy, not least due to the complex geometry; this holds in particular when considering the construction design of finned tubes, i.e. annular fins, spiral finned tubes or others. This section intends to develop a calculation equation for spiral finned tubes by using our own and other published measurements. The most important decision in this case is the characteristic length of the single finned tube. On the one hand, there is the diameter of the bare tube, for example in the equations of Mannesmann (established by Schmidt [1]) and HEDH (established by Zukauskas et al. [3]), as well as the equations by ESCOA [12] with the disadvantages and advantages already discussed above. On the other hand, custom-made characteristic diameters are used, as in the case of Mirkovics [5] or Brandt [9]. The system of equations by Mirkovics describes our own measurements very well, as seen in figure (21). Yet, in our view, the characteristic diameter used is hardly evident.

For this reason, improvements are to be developed in two directions:

Firstly: by supplementing the Mannesmann equations with expressions that account for the dependence of the heat transfer coefficient on the geometry of the tube bundles.

Secondly: by considering the flow between the fins as a channel flow and determining a hydraulic diameter on this basis.

Test runs carried out by Mirkovics are used for the first point to investigate the dependence of the heat transfer on transverse and longitudinal pitch, while the remaining parameters, in particular the tube diameter, are left unchanged. The dimensionless parameter  $\frac{t_q - d_A}{2h}$ , through which the distance between two tubes is put in relation to the double fin height, is used for the investigation of the influence of the transverse pitch. Mirkovics uses the parameter  $\frac{t_q - d_A}{d_A}$ . The same method follows for the longitudinal pitch, in which case a dimensionless parameter  $\frac{t_l}{t_q}$  is used. Here Mirkovics uses the expression  $\frac{t_l - d_A}{d_A}$ .

The factor  $Kf_t$  thus indicates the influence of bundle geometry on heat transfer as:

$$Kf_t = \left(\frac{t_q - d_A}{2h}\right)^{-0.21} \left(\frac{t_l}{t_q}\right)^{0.239} \quad (80)$$

The exponents for  $\frac{t_q - d_A}{2h}$  and  $\frac{t_l}{t_q}$  were determined using the experimental results of Mirkovics. The Mannesmann formula could be supplemented with the factor  $Kf_t$  to indicate an influence of transverse pitch and longitudinal pitch. With a further additional factor  $C_z(n_R)$ , for a smaller number of tube rows than 8, the formula appears as follows:

$$Nu_0 = CRe^{0.625} Pr^{(1/3)} \left(\frac{A_{tot}}{A_R}\right)^{-0.375} Kf_t C_z \quad (81)$$

The exponent of the Reynolds number is approx. 0.67, instead of 0.625 as with Mannesmann, based on measurements in the range of Reynolds numbers from 4000 to 32000 carried out by the ITE on spiral finned tubes. The complete formula for spiral finned tubes is therefore:

$$Nu_0 = 0.338 Re^{0.67} Pr^{(1/3)} \left(\frac{A_{tot}}{A_R}\right)^{-0.375} Kf_t C_z \quad (82)$$

The expression  $A_{tot}/A_R$  may, however, be replaced by the simpler expression  $h/(t_R - s_R)$ , which is not less accurate. Then the equation becomes:

$$Nu_0 = 0.22 Re^{0.67} Pr^{(1/3)} \left(\frac{h}{t_R - s_R}\right)^{-0.35} Kf_t C_z \quad (83)$$

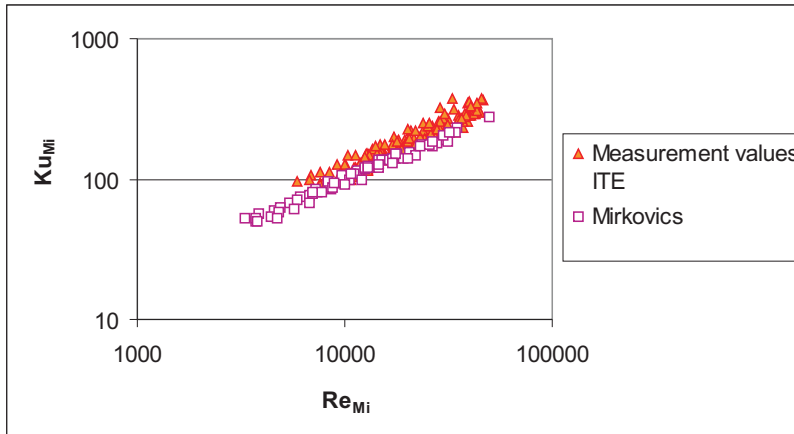


Figure 22: **Heat transfer measurements by Mirkovics and ITE on staggered finned tube arrangements evaluated with Mirkovics' formulas**

A comparison between the measurements of Mirkovics and the test cases of the ITE is also of interest. The experimental facilities are comparable in their fundamental design and both use spiral finned tubes in staggered arrangement.

The direction of the heat transfer corresponds too. In both experimental facilities the direction of heat transfer is from the hot gas to the finned tubes. Yet Mirkovics heats the air by means of a heat exchanger, supplied by steam, up to temperatures of 130°C. At the test facility of the ITE, air is heated up to a temperature of maximum 400 °C by means of combustion of natural gas in a duct burner and the flue gases are then conducted through the finned tube heater exchanger.

Like the ITE measurement series, Mirkovics uses 8 consecutive tube rows, but only 5 or 6 parallel tube rows. In every second tube row a semi-tube is mounted on the channel wall. The publication does not, however, specify whether these semi-tubes are cooled or not. At the experimental facility of the ITE, 10, 11 or 12 tube rows are arranged in parallel, according to their diameter. A semi-tube assembly was rejected, however, because of the difficulties in producing cooled semi-tubes and their differing water-side flow characteristics and heat transfer properties. Hence the semi-tubes were simply left out. Instead of this, cooling water temperatures are measured at the inlet and the outlet of every single tube row. It is thus possible to exclude the tube row on the channel wall during calculation, so that the influence of the wall and of the missing semi-tubes can be eliminated. At the ITE test facility, a cross counter-flow heat exchanger is used, whereas Mirkovics used a two-row cross counter-flow heat exchanger, in which case cooling water temperatures were only measured in the header.

A comparison of the results of measurements was carried out for different systems

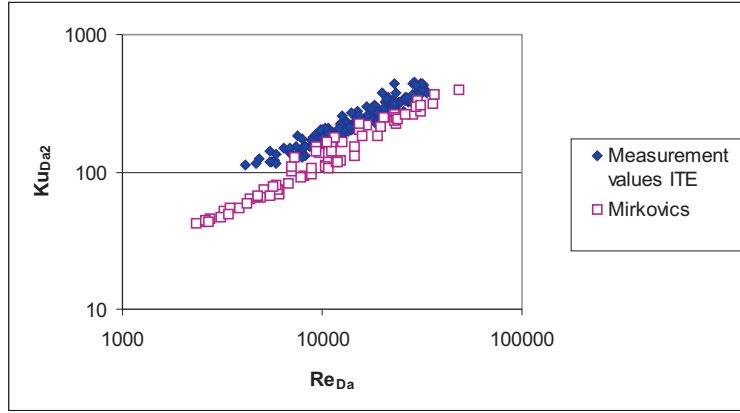


Figure 23: **Heat transfer measurements by Mirkovics and ITE on staggered finned tube arrangements evaluated with formula (85)**

of formulas during evaluation. Since neither the dimensions of the finned tubes nor the pitches agree exactly, a comparison was carried out by means of a "universal" dimensionless number. Test cases with different finned tubes in different arrangements can also be compared by using this dimensionless number. For the evaluation according to Mirkovics, this universal dimensionless number is:

$$Ku_{Mi} = Nu_{Mi} Pr^{(-1/3)} \left( \frac{t_q - d_A}{d_A} \right)^{-0.1} \left( \frac{t_l - d_A}{d_A} \right)^{0.15} \left( \frac{t_R - s_R}{h} \right)^{0.25} \quad (84)$$

This number is calculated depending on the Reynolds number  $Re_{Mi}$  (derived using the characteristic diameter according to Mirkovics) and represented in a double-logarithmic diagram. In figure (22), the evaluation, according to the Mirkovics method, of the test cases by Mirkovics and by ITE can be seen.

In each case a set of points result which are gathered approximately around a straight line. The results obtained through evaluation using the Mirkovics method, of the test cases by ITE, are approx. 21 % higher than the results of Mirkovics. This is a relatively large difference which demands an explanation. Before that, however, comparison is to be made according to other evaluation formulas, equation (82) or equation (83) for example. The universal dimensionless number obtained through evaluation according to the former formula is:

$$Ku_{Da2} = Nu_{Da2} Pr^{(-1/3)} \left( \frac{A_{tot}}{A_R} \right)^{0.375} K f_t^{-1} \quad (85)$$

A comparison of the measurements by Mirkovics with those of ITE using equation (85) results in higher values for the measurements made by ITE. Especially the values for  $Ku_{Da2}$  higher, by approx. 57% at  $Re_{Da} = 4000$  are approx. 28% at  $Re_{Da} = 40000$ . An evaluation according to equation (85) shows that the exponent

of  $Re$  is noticeably higher at 0.75 in the case of Mirkovics than in the case of ITE at 0.67, while it is almost identical to an evaluation according to Mirkovics; see figure (23).

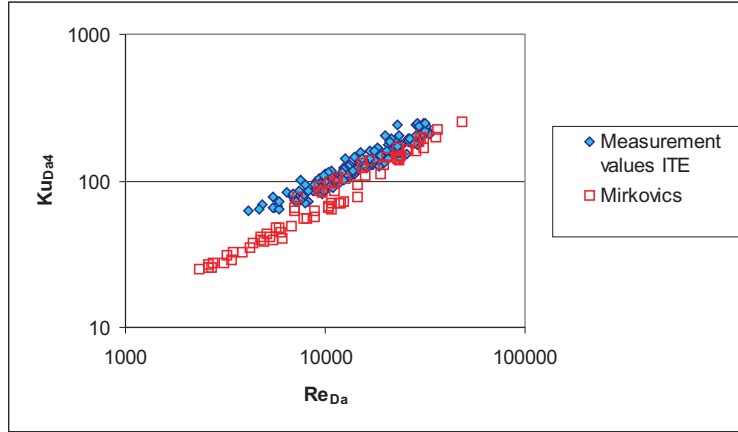


Figure 24: **Heat transfer measurements by Mirkovics and ITE on staggered finned tube arrangements evaluated using formula (86)**

A comparison of the measurements by Mirkovics with those of ITE using equation (83) yields the following universal dimensionless number where the tube row number is greater than or equal to 8, as in the previous comparisons, and thus  $K_z$  is 1.

$$Ku_{Da4} = Nu_{Da4} Pr^{(-1/3)} \left( \frac{h}{t_R - s_R} \right)^{0.35} K f_t^{-1} \quad (86)$$

A similar figure to that of the preceding equation results. The ITE measurement values are approx. 51% higher at  $Re_{Da} = 4000$  than those of Mirkovics and approx. 21% higher at  $Re_{Da} = 40000$ ; refer to figure (24).

Lastly, a comparison should be done according to a completely different equation. Here the finned tube bundle is regarded as a sequence of flow channels between the fins with a width of  $(t_R - s_R)$  and a height of  $(t_q - d_A)$ . Because of the circular outline of the channel walls the hydraulic diameter is derived based on the general formula

$$d_{ch} = 4 \frac{V}{O}, \quad (87)$$

in which  $V$  is the volume of the flow channel and  $O$  its heat transferring surface. Both are defined per length unit of finned tube.

$$V = ((d_A + 2h)^2 - d_A^2) \frac{\pi}{4} (t_R - s_R) \quad (88)$$

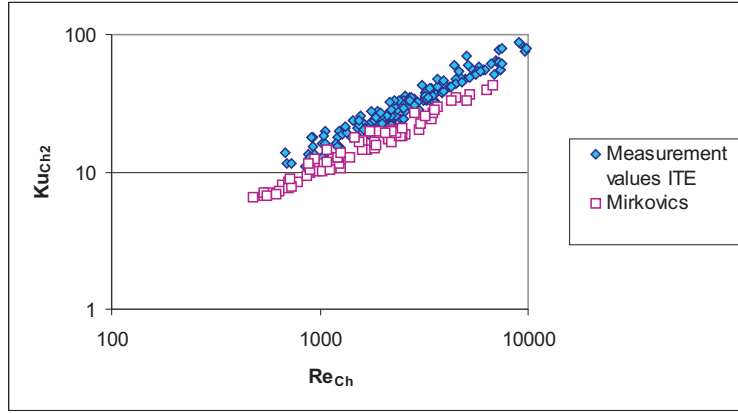


Figure 25:

**Heat transfer measurements by Mirkovics and ITE on staggered finned tube arrangements evaluated using formula (91)**

$$O = 2((d_A + 2h)^2 - d_A^2) \frac{\pi}{4} + d_A \pi(t_R - s_R) + (d_A + 2h)\pi s_R \quad (89)$$

Since another characteristic length for a different geometrical finned tube requires a conversion of the Nusselt numbers and the Reynolds numbers, the terms for the determination for the influence of the geometrical data of the finned tubes now have to be specified anew.

Particularly the exponents for a determination of the influence of  $\frac{t_R - s_R}{h}$  need to be specified again. In the case of equations (85) and (86) the diameter  $d_A$  is the same for all finned tubes examined, not however the characteristic diameter  $d_{Mi}$  used by Mirkovics. The characteristic diameters  $d_{ch}$  are different for every finned tube, and therefore the exponent has to be determined again.

In the case of measurements for the determination of any dependence from characteristic sizes  $t_q$  and  $t_l$  of the finned tube bundle, identical finned tubes were used. Thus, no new determination of the exponents was necessary. For identical finned tubes all characteristic lengths are the same as long as  $t_q$  and  $t_l$  do not occur, which is the case here. In the case of the conversion stated above, one has to pay attention to the determination of the exponent of  $\frac{t_R - s_R}{h}$ , which according to Mirkovics was done at a constant Reynolds number which is no longer constant after conversion.

$$Re_{Mi} = const. = Re_{Da} \frac{d_{Mi}}{d_A} \quad (90)$$

as is obvious from the equation above for different  $d_{Mi}$ , even if  $d_A$  are all identical. The terms  $NuPr^{(1/3)}$  are converted to the same Reynolds number using  $(\frac{Re_{Da}}{Re_{Da_i}})^{0.67}$

for  $Da_i = Da_2, Da_3, Da_4$ , etc. The same method is used for  $Re_{ch}$ , in which the diameters  $d_{Mi}$  and  $d_{ch}$  are different. 0.29 is the resulting exponent of  $\frac{t_R - s_R}{h}$  at  $Ku_{Da4}$  and 0.48 for the calculation with  $d_{ch}$  to. For  $Ku_{ch}$  this results in:

$$Ku_{ch2} = Nu_{ch2} Pr^{(-1/3)} \left( \frac{h}{t_R - s_R} \right)^{0.48} Kf_t^{-1} \quad (91)$$

The measurement values of ITE and of Mirkovics are presented in the form of  $Ku_{ch2}$  above  $Re_{ch}$  in a double-logarithmic diagram, as seen in figure (25). From this, 0.75 is resulting exponent of  $Re_{ch}$ . In the representation of  $Ku_{ch}$  as well, the measurement values of ITE are approx. 26% higher than those of Mirkovics. The difference increases with Reynolds numbers higher than  $Re_{ch} = 1000$ . A relation generated from the measurement values of ITE for heat transfer using  $d_{ch}$  would therefore result in:

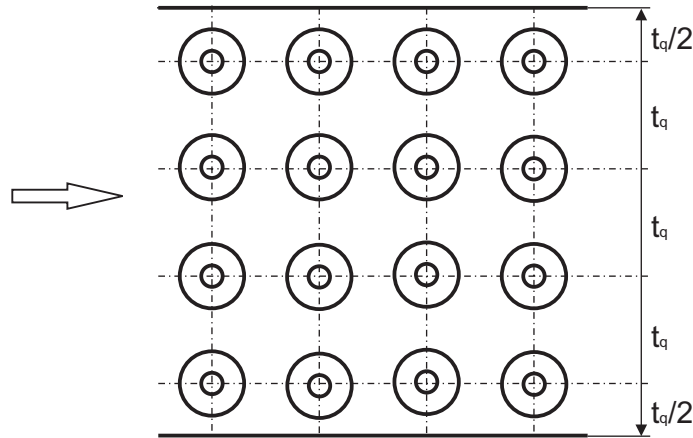
$$Nu_{ch} = 0.0845 Re_{ch}^{0.75} Pr^{(1/3)} \left( \frac{h}{t_R - s_R} \right)^{-0.48} Kf_t \quad (92)$$

From the explanations above it can clearly be seen that an analysis of the heat transfer at finned tube bundles with different characteristic lengths is possible and worthwhile. Depending on the selection of the characteristic length, the exponent generated with this Reynolds number in general differs in value, as do exponents in other terms from geometrical factors, as for example  $(t_R - s_R)/h$  or  $t_l/t_q$ , which occur in the formulas for the calculation of heat transfer. When comparing figures (22), (23), (24) and (25), it may be observed that in those figures in which the measurement values of Mirkovics are plotted above  $Re_{Da}$  (i.e. figure (23) and figure (24)), Mirkovics' scatter plot disintegrates into two parts. These scatter plots show to a large extent the same gradient but different heights. The single scatters lie like roofing tiles on top of each other. The upper scatter plot seems to be closer than the lower one to the measurement values of ITE, and thereafter the difference is only approx. 14%. This phenomenon does not occur when plotted above  $Re_{Mi}$  or  $Re_{Ch}$ . One can assume that between these two scatter plots a hardly negligible change occurred in the experimental geometry.

## 3.2 In-line tube arrangements

### 3.2.1 Enumeration of equations

Much fewer test series have been carried out for in-line tube arrangements than for staggered tube arrangements, and therefore fewer relations for heat transfer have been published. According to detailed information from Schmidt [1], heat transfer at in-line tube arrangements is around 1/3 less than at staggered arrangements.

Figure 26: **In-line finned tube arrangement**

Nevertheless, in-line tube arrangements have to be chosen sometimes for design reasons.

1. Th. E. Schmidt's formula [1] (MM)

The formula by Schmidt and Mannesmann for in-line tube arrangement is, except for the factor in front of the equation, identical with the formula for staggered arrangement. This factor is around 1/3 lower than for a staggered arrangement:

$$Nu = 0.30 Re^{0.625} Pr^{\frac{1}{3}} \left( \frac{A_{tot}}{A_R} \right)^{-0.375}. \quad (93)$$

With respect to the addition of the surface relation  $A_{tot}/A_R$ , the same applies here as was mentioned above in the case of the formula for staggered tube arrangement.

2. Mannesmann Carnoy Formula (MC)

The finned tube manufacturer Mannesmann adopted all of Schmidt's formulas, but in the course of the technical development finned tubes with welded spiral-fins arose, so that Mannesmann carried out their own heat transfer measurements on such tubes. From these measurements, the formula known as the Mannesmann Carnoy formula arose, which differs from Schmidt's formula through the constant coefficient of 0.387 instead of 0.30.

3. Formula from the VDI-Waermeatlas, 6th Edition 1991 [26] (WA)

This formula is similar to the formulas presented above, however, it shows other numerical values for the constants.

$$Nu = 0.22 Re^{0.60} Pr^{\frac{1}{3}} \left( \frac{A_{tot}}{A_R} \right)^{-0.15} \quad (94)$$

The constant 0.22 is valid for more than four consecutive tube rows. Up to three tube rows, a reduction of the constants is recommended to 0.20. Ebeling and Schmidt [35] set the constant at 0.23 for annular fins in more than three tube rows, but no information is given about spiral fins.

4. Brandt's formula [9] (BA)

Brandt's formula is structured differently from the other equations presented and also pursues different objectives, inasmuch as, by applying  $h = 0$  as the fin height, it results in the heat transfer value for a bare tube bundle. Accordingly, the expression

$$l' = \frac{\pi}{2} \sqrt{d_A^2 + h^2} \quad (95)$$

is used for the characteristic length. Defining  $d_A = 0$  should result in heat transfer for a flow along a group of longitudinal plates. Brandt's formula system is presented in section (3.1) for staggered tube bundles. The calculation for in-line tube bundles differs from this only through the use of the constants which are valid for in-line tube arrangements. These are also presented in section (3.1).

5. Calculation according to ESCOA [12] (EG)

The ESCOA equation for in-line arrangements of tubes with solid fins is:

$$Nu = 0.25 Re^{0.65} Pr^{1/3} \left( \frac{\vartheta_{gm} + 273.2}{\vartheta_{rm} + 273.2} \right)^{1/4} \left( \frac{D}{d_A} \right)^{0.5} C_3 C_5 \quad (96)$$

Here all factors are declared as in section 3.1.1.  $C_3$  is a factor which represents the influence of fin height and fin pitch.

$$C_3 = 0.20 + 0.65 \exp(-0.25 h / (t_R - s_R)) \quad (97)$$

$C_5$  accounts for the influence of transverse and longitudinal pitch in the fin bundle as well as the number of consecutive tube rows in the direction of flow.

$$C_5 = 1.1 - (0.75 - 1.5 \exp(-0.70 n_R)) \exp(-2.0 \frac{t_l}{t_q}) \quad (98)$$

ESCOA also specifies a formula for finned tubes with serrated fins arranged in line: (ES)

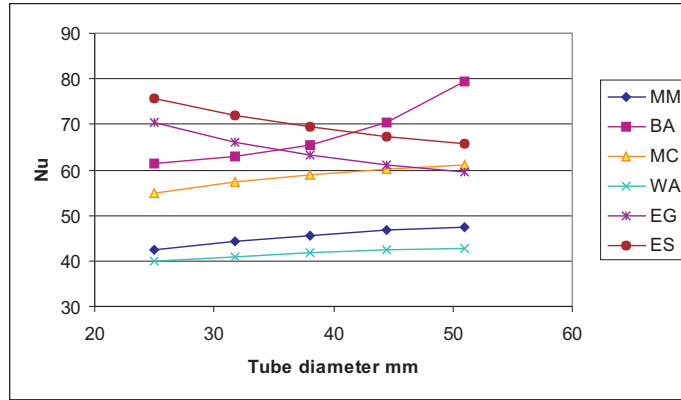


Figure 27: **Influence of tube diameter on heat transfer with constant Reynolds number (in-line arrangement)**

The formula for  $Nu$  with serrated fins is in this case identical with equation (96), and also the coefficient  $C_5$  remains unchanged, while another term applies for the coefficient  $C_3$  with serrated fins:

$$C_3 = 0.35 + 0.50 \exp(-0.35 h/(t_R - s_R)) \quad (99)$$

### 3.2.2 Evaluation of the influence of fin parameters with in-line tube arrangement

The influence of geometrical fin parameters on the external heat transfer coefficient is discussed here, also in comparison with staggered tube arrangement. Observations are made by referring to the example of an in-line tube arrangement with the parameters  $d_A = 0.038$  m,  $t_R = 0.00667$  m,  $s_R = 0.001$  m,  $h = 0.016$  m and the pitches  $t_q = t_l = 0.075$  m.

1. Influence of tube diameter at a constant Reynolds number: The influence is represented in figure (27) for constant fin geometry. This factor varies for the different equations. The heat transfer coefficient decreases with the diameter of the bare tube according to EG and ES, while for the other equations it increases; with MM, MC and WA it increases only slightly, with BA on the other hand considerably.
2. Influence of tube diameter at constant velocity  $w_E$  in the narrowest cross-section: See figure (28). Since the Reynolds number increases with  $d_A$ , an increase in the heat transfer coefficient with the tube diameter results for all equations; with BA this is particularly strong and positive.

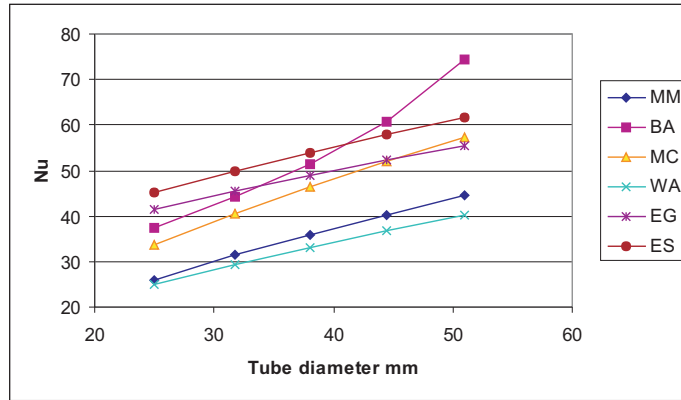


Figure 28: **Influence of tube diameter on heat transfer at constant gas velocity (in-line arrangement)**

3. Influence of tube diameter with  $t_q$  and  $t_l$  at  $Re = \text{const.}$ : If the tube diameter changes at constant fin geometry, transverse and longitudinal pitch each have to be adjusted so that there is enough space between each tube row. Alternatively, pitch values can be dimensioned according to the largest tube diameter and kept constant afterwards (this was done for the two preceding items). If one adapts the pitch in such a way that the distance between the fin edges remains constant (for example 5 mm), figure (29), similar to the first item, results: the heat transfer coefficient increases only moderately according to MM, MC and WA; with BA it increases strongly at first and remains constant afterwards; according to EG and ES it declines.

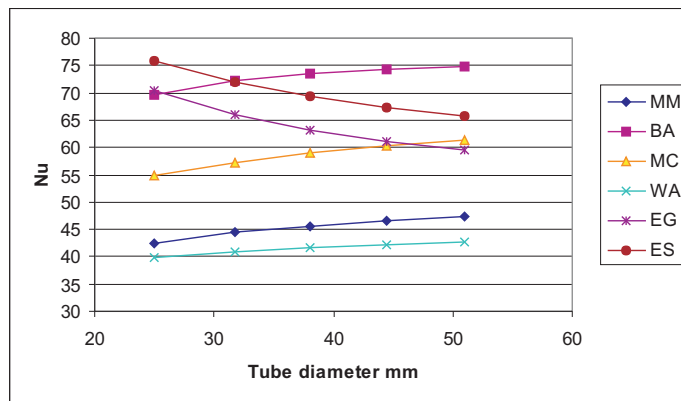


Figure 29: **Influence of tube diameter on heat transfer at constant Reynolds number and with adapted tube pitches (in-line arrangement)**

4. Influence of tube diameter with adapted pitches and with  $w_E = \text{const.}$ : If the pitches, but not the Reynolds number, are altered according to the tube diameter and the velocity in the narrowest cross-section is kept constant, then figure (30) results. Here the Nusselt number increases consistently for all relations with an increase in tube diameter.

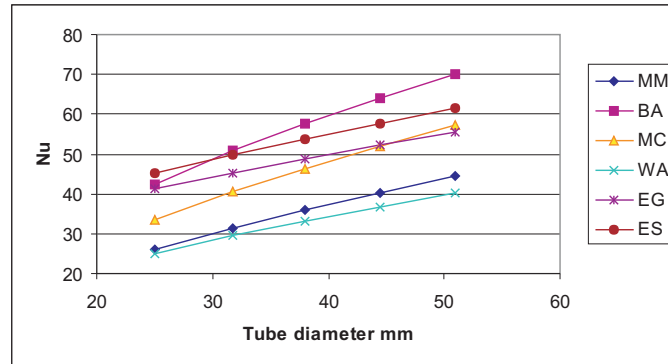


Figure 30: **Influence of tube diameter on heat transfer at constant gas velocity and with adapted tube pitches (in-line arrangement)**

5. Fin pitch: According to all relations, the heat transfer coefficient increases with the fin pitch, sharply at first and then more moderately, whereas the increase is small according to WA, moderate with MM, MC and BA, and strong according to EG and ES; see figure (31). The increase is not, however, strong enough to compensate for the decrease in the heating surface per m tube. For a compact heat exchanger, it would be preferable to select as a small fin pitch as possible while avoiding conditions leading to fouling.

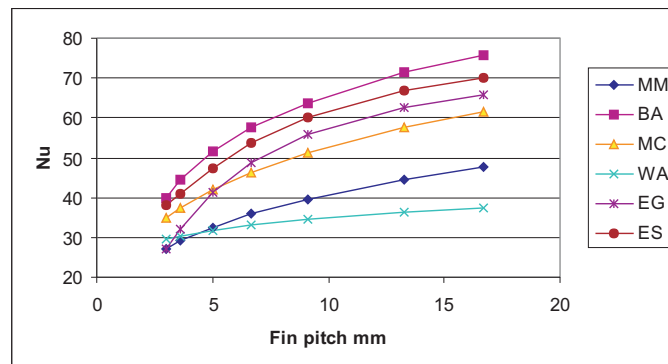


Figure 31: **Influence of fin pitch on heat transfer (in-line arrangement)**

6. Fin thickness: The influence of fin thickness is first examined without considering fin efficiency. According to EG, ES and BA, a decrease in the heat transfer coefficient is predicted with increasing fin thickness; according to MM, MC and WA, the decrease is hardly perceptible, meaning it remains virtually constant; see figure (32).

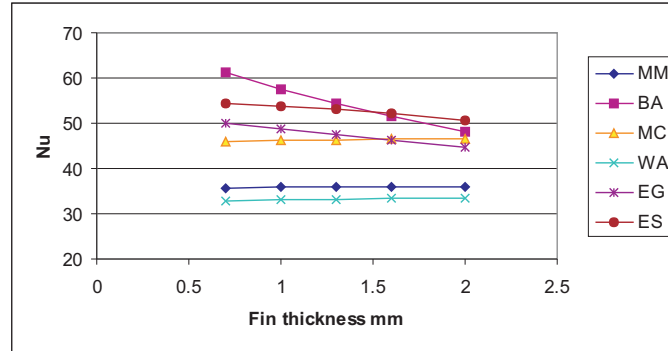


Figure 32: **Influence of fin thickness on heat transfer (in-line arrangement)**

If, instead of  $Nu_0$ , the apparent heat transfer coefficient  $\alpha$  is included, a different scenario results.  $\alpha$  can be derived from fin efficiency  $\eta_R$  and the real heat transfer coefficient  $\alpha_0$  (equation (35)) using equation (33). In this case the apparent heat transfer coefficient  $\alpha$  at first increases with fin thickness and achieves a maximum value. It then decreases according to some calculation equations, revealing an optimal fin thickness value. The resulting value for optimal fin thickness is not uniform among the different calculation equations, as figure (33) shows.

Furthermore, the value is considerably dependent on the thermal conductivity of the fin material. With a poor heat conductor as fin material, e.g. Austenite, the optimal fin thickness tends to be a higher value in comparison to e.g. St35.8, figure (34).

Optimal fin thickness values may similarly be obtained for staggered finned tube arrangements, but with differing numerical values, since fin efficiency  $\eta_R$  depends on the real heat transfer coefficient  $\alpha_0$ .

7. Fin height: For examining the influence of fin height, transverse and longitudinal pitch have to be dimensioned in a such way that the tallest fins still have enough space, which is, however, a waste of space with shorter fins and therefore not realistic. If one carries out an analysis, a decrease in heat transfer with rising fin height results for all equations with the exception of BA, for which the heat transfer rises with  $h$ ; see figure (35). Measurements

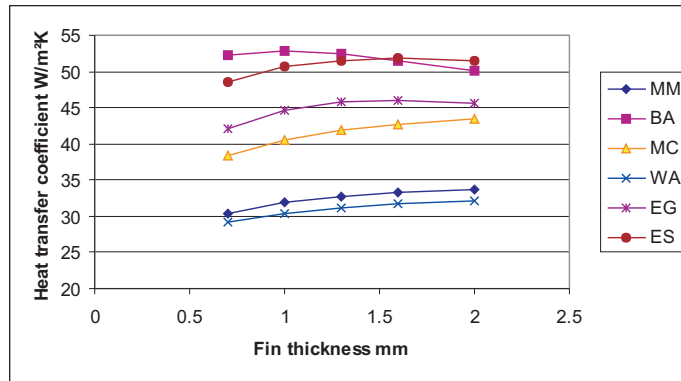


Figure 33: Optimum fin thickness with respect to heat transfer for St35.8 fins (in-line arrangement)

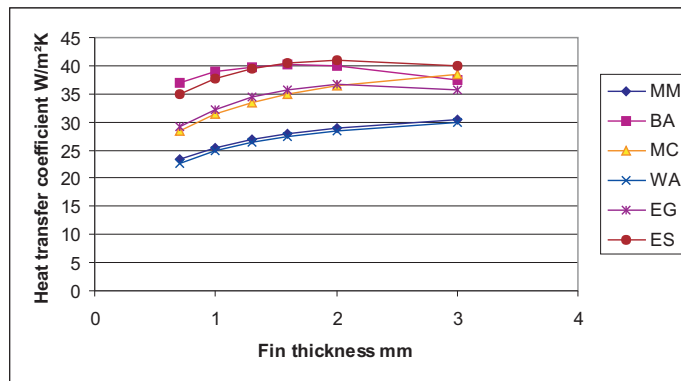


Figure 34: Optimum fin thickness with respect to heat transfer for Austenite fins (in-line arrangement)

by Stasiulevicius [3] and Mirkovics [5] on staggered arrangements revealed a decrease in heat transfer with increasing fin height. Brandt [9] also ascertains this for staggered tube arrangements. The same might also be valid then for in-line tube arrangements.

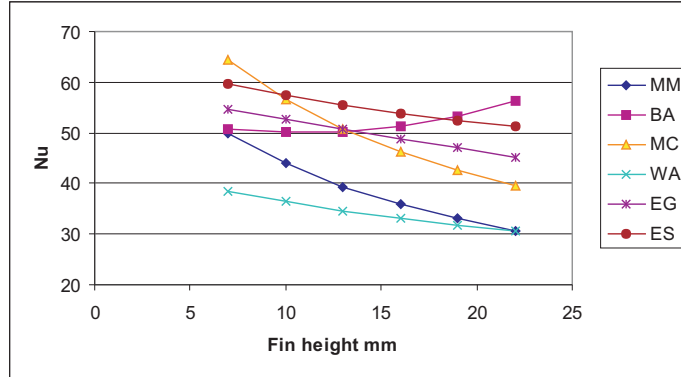


Figure 35: **Influence of fin height on heat transfer (in-line arrangement)**

8. Influence of fin height with varying transverse pitch: The transverse pitch is varied with the fin height so that the distance between the fin edges remains constant. The longitudinal pitch also remains constant and is dimensioned in such a way that the tallest fins still have enough space. Based on this assumption, heat transfer decreases more or less with increasing fin height, according to all equations, very moderately with WA, a little more strongly according to EG, ES and BA and by the greatest amount with MC and MM; this is presented in figure (36).
9. Influence of fin height with varying transverse and longitudinal pitch: If the longitudinal pitch as well as transverse pitch is increased with increasing fin height, heat transfer decreases. The decrease is quite similar for all equations, except for MM and MC, where the heat transfer decreases only moderately, as figure (37) shows.
10. Transverse pitch: In the equations MM, MC and WA, the influence of transverse pitch is not accounted for. According to EG and ES, heat transfer decreases with increasing transverse pitch. According to BA, heat transfer first declines strongly, then increases again. This occurs at a transverse pitch of  $t_q > 100$  mm at  $d_A + 2h = 70$  mm, which is very large and therefore hardly used; see figure (38).

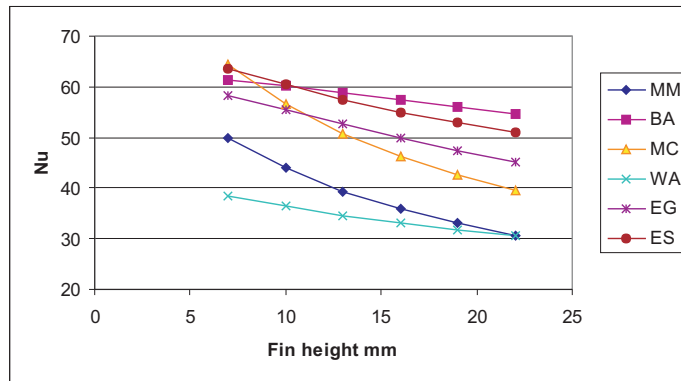


Figure 36: Influence of fin height on heat transfer at adapted transverse pitch (in-line arrangement)

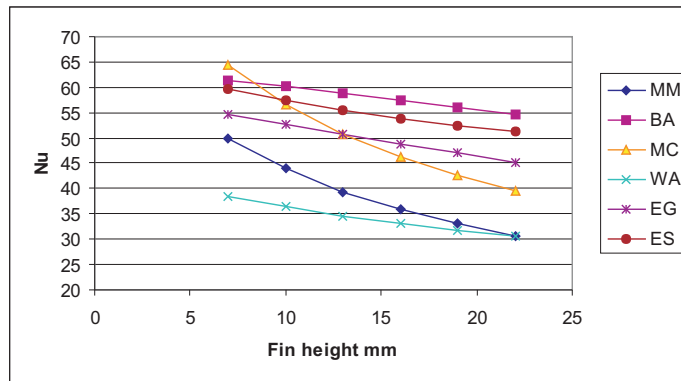


Figure 37: Influence of fin height on heat transfer at adapted tube pitches (in-line arrangement)

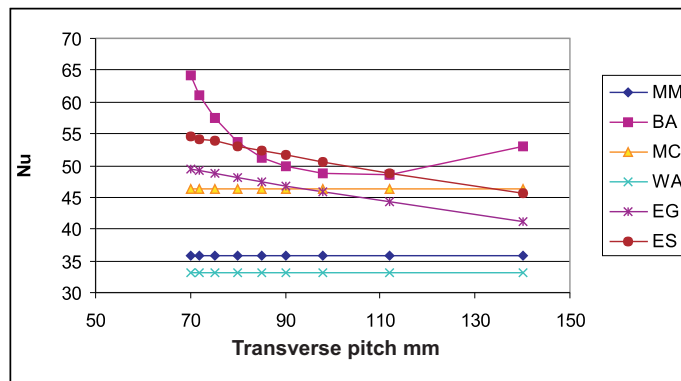


Figure 38: Influence of transverse pitch on heat transfer (in-line arrangement)

11. Longitudinal pitch: Only the equations EG and ES ascertain an influence of longitudinal pitch, whereby the heat transfer increases with increasing longitudinal pitch. This result matches the predictions that heat transfer decreases with the number of tube rows. This means that for greater longitudinal pitches every tube row appears to be a "first" tube row. In measurements done at ITE it also was possible to examine the influence of longitudinal pitch, at least for a single geometry. The observation stated above was confirmed, as figure (39) shows. According to our measurements, this dependence can be represented using the expression  $(\frac{t_l}{t_q})^{0.4}$ .

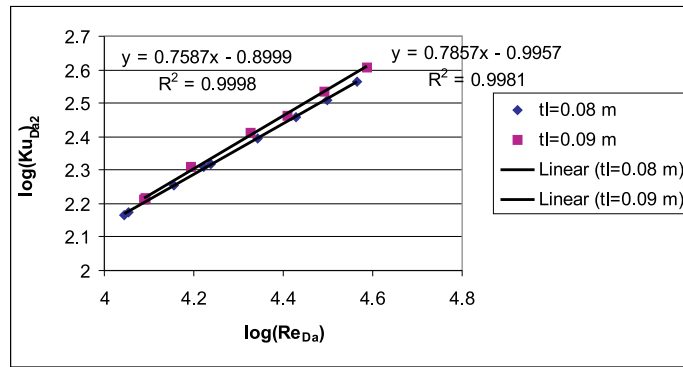


Figure 39: **Influence of the longitudinal pitch on heat transfer based on measurements by ITE (in-line arrangement)** (tube diameter 38 mm, 150 fins per m, 16x1 mm, transverse pitch 80 mm)

12. Influence of the Reynolds number: This influence is practically equal for all equations and lies in the range of the exponent of the Reynolds number between 0.60 to 0.65; figure (40). Measurements by ITE on spiral finned tube bundles revealed at 0.75 a somewhat higher exponent of the Reynolds number, however.

### 3.2.3 Proposal for an enhanced calculation formula

Based on measurements performed at ITE, an enhanced version of Schmidt's formula [1] is proposed as a calculation for predicting heat transfer at in-line finned tube bundles. The additions account for the influence of transverse and longitudinal pitch. It is valid for in-line bundles of spiral finned tubes with Reynolds numbers ranging between  $> 10000$  and  $< 40000$ .

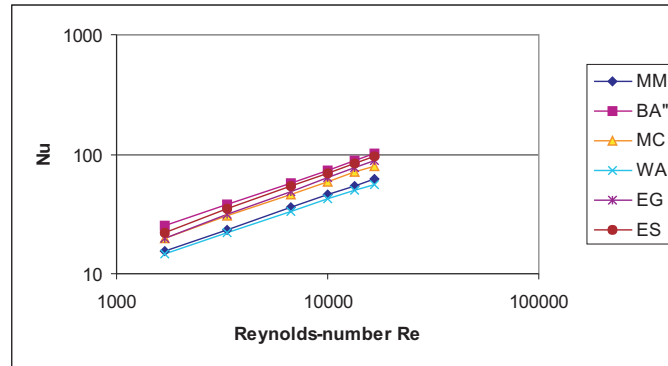


Figure 40: Influence of the Reynolds number on heat transfer at in-line arrangement

$$Nu = 0.1306 Re^{0.75} Pr^{\frac{1}{3}} \left( \frac{A_{tot}}{A_R} \right)^{-0.375} \left( \frac{t_q - d_A}{2h} \right)^{0.21} \left( \frac{t_l}{t_q} \right)^{0.4} \quad (100)$$

As figure (41) shows, the results of this equation (abbr. EM) lie within those for the other equations developed for spiral finned tubes. In line with measurements, the exponent of Re is somewhat greater.

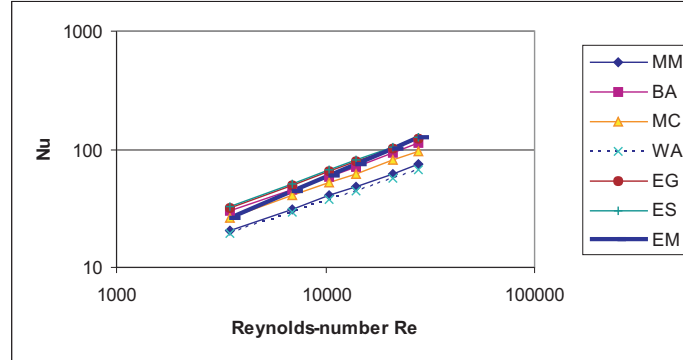


Figure 41: Results of the proposed equation (100) in comparison with available equations for heat transfer at in-line finned tube bundles

### 3.3 Selection method for finned tubes

If one poses the question as to the most preferable finned tube in general, no simple answer can be given. Rather, precise limiting conditions need to be specified. The requirement may be for the finned tube heat exchanger with the smallest

construction volume, with the lowest total cost (purchase price plus operating costs) for a given amount of heat or for the finned tube heat exchanger with the lowest material expense (mass) etc.... The answer will be different in each case. When the finned tubes are joined in a bundle, further variables arise in the way of longitudinal and transverse pitch as well as in-line or staggered arrangement. The influence of longitudinal and transverse pitch is not that great so as to favor a certain arrangement to the extent that this arrangement would achieve greater efficiency in relation to the construction volume than would be the case with the greatest possible packing density of finned tubes in that case. When designing a finned tube heat exchanger, especially for high pressures, longitudinal and transverse pitch need to accommodate available or producible U-bends. It must be pointed out that the design of a finned tube heat exchanger, especially with short single tube lengths, has to be done in such a way that the free space which arises around the connection bends without fins does not produce a harmful bypass flow. It would be best to place the connection bends of the single tubes on the outside of the flue gas channel. Such a design is, however, expensive to produce and very complicated to assemble. For this reason cheaper and simpler constructions are often chosen which do not achieve complete elimination of bypass flow at the connection bends.

According to Schmidt, a difference of 1.5 exists between in-line and staggered finned tubes arrangements. More recent research by the tube manufacturer Mannesmann Carnoy, as well as our measurements [6], reveal this difference to be a little smaller. Many studies have limited themselves to staggered arrangements because of the great advantage they have over in-line arrangements (so for example Mirkovics [5], Stasiulevicius [3]). Yet, in-line tube arrangements often have to be chosen, for example because of the cleaning capability provided by soot blowers or for design reasons (e.g. support structures for suspended tubes).

There is hardly ever a free choice of the most suitable finned tube, since this is often restricted more or less by the choice of a certain construction design or manufacturer. However, customers should become familiar with their own requirements as well as with the properties of the product offered in order to be certain of having selected the most suitable finned tube.

#### 1. Finned tube design type

A selection of finned tube construction design should be made based on the type of installation as well as on operating conditions:

- (a) Steam tube with welded spiral fins: suitable for high fluid pressures in the tube and, depending on the material of the fins, also for gas temperatures up to about 600 °C. Preferred area of application: steam generators and heat recovery boilers. The steel ribbon for the fins can

- also be twisted into a U shape, then wound around the tube and welded together, so that two fins are produced in a single working cycle.
- (b) Steam tube with fins separately welded to the tube, mostly with larger fin pitch for solid fuel furnace.
  - (c) Steam tube with fins wound and mounted only by pressure: suitable for gas temperatures up to approx. 350 °C. An improvement of heat transfer is achieved by subsequent hot-dip galvanization. Application: heat exchanger in plant engineering.
  - (d) High-alloyed steel tube with laser-welded spiral fins of high-alloyed steel: High-grade heat exchangers in process and refrigeration engineering, also suitable for high temperatures depending on materials used.
  - (e) Steel tube with forced-on, mounted fins of sheet steel: thinner fins, possibly also wavy in form, with small fin pitches can also be mounted by pressing i.e. flat tubes or oval tubes. For better heat conduction the fin base is often designed in an L- or T-shape and/or the finish of the finned tube is zinc-plated. For air-covered coolers and steam condensers up to approx. 30 bars for oval tubes.
  - (f) Copper tubes with copper fins (pressed on, can also be soldered) or aluminium fins (only pressed on) in ventilation and air conditioning installations, copper pipe with soldered copper fins also in refrigeration engineering.
  - (g) Copper tubes with one-piece pressed fins (rarely also of high-alloyed steel) have the advantage that the finned tubes can be twisted. These tubes can be manufactured in one piece as helical coils for heat exchangers.
  - (h) Finned tubes with continuous fins are often manufactured for cooler units in automotive engineering, for refrigeration installations and process engineering. The tubes are pushed through the fins and joined mostly only by force fit. Cu tubes and Cu fins can also be soldered. The fins can be also by wavy in form, both with angular and rounded waves.
  - (i) If requirements demand minimal gas-side pressure drop, elliptical tubes or flat tubes or even flat tubes with wing profiles may also be used as a base for fins.
  - (j) Finned tube elements with continuous fins for cooler units can be manufactured in one piece by plastic injection molding. With this application, temperatures and pressures are restricted, but it is corrosion-resistant.

## 2. Fin pitch

Fin pitch, or actually the clearance between the fins  $t_R - s_R$ , depends on the fouling factor of the gas which flows between the fins, and the minimum value is recommended as follows according to [25]:

Pure air	1.8-3	mm
Flue gas: Natural gas	3-4.2	mm
Low viscosity oil	4.2-6.3	mm
Heavy oil	5-8.5	mm
Solid fuels	12-25	mm

## 3. Fin thickness

Fin thickness is not so much dimensioned based on fin efficiency but rather on other criteria such manufacturing feasibility and strength of the fin materials during installation and operation. Standard fin thickness values:

Spiral fins	0.9-1.0-1.3	mm
Fins for solid fuels	1.6-2.5	mm
Fins for ventilation and air conditioning engineering also of Cu and Al	0.3-0.7	mm

## 4. Fin height

For compact and economic heat exchangers it is preferable to design fins as tall as possible, however other factors place restrictions.

- Fin efficiency decreases with increasing fin height.
- In manufacturing spiral fins, the exterior fibers of the fin band are subject to considerable strain, restricting the fin height.
- The tendency toward flow displacement out of the channels between the fins occurs especially with tall fins having a small distance between them, particularly when a large transverse pitch is involved. The result is reduced heat transfer at this point, while the flow around the outside of the finned tubes hardly participates in heat transfer. This is particularly important for only a single tube row or a few tube rows. According to [4] almost no flow displacement occurs when  $a = (t_q - (d_A + 2h))/t_q < 0.1$ , while on the other hand considerable displacement occurs in the range of  $0.1 < (t_q - (d_A + 2h))/t_q < 0.2$ , depending on the relative distance between the fin edges  $a$ ; for even higher values of  $(t_q - (d_A + 2h))/t_q$ , flow displacement does not further increase, as seen in figure (42). The quotient of the velocity between the fins  $w_R$  divided by mean velocity  $w_M = 1/2(w_0 + w_E)$  is used as a measure of flow displacement; this is calculated according to equation

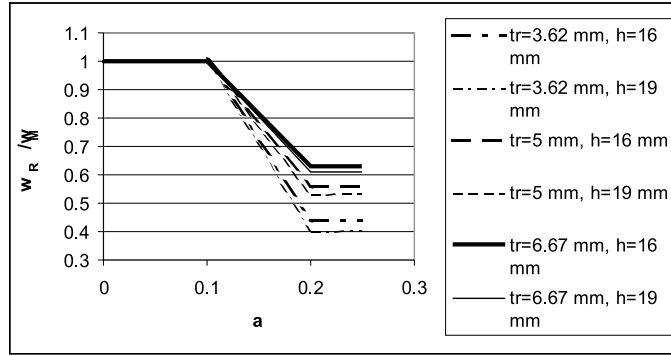


Figure 42: **Flow displacement in dependence of relative transverse pitch**  
 $a = (t_q - (d_A + 2h))/t_q$

(75) and equation (76).

The two restricting influences mentioned can be partly avoided by the application of serrated fins, since there is practically no elongation of the outside fibers when cuts are made in the fin band; flow displacement is also considerably reduced by the spaces between individual segments.

### 3.4 Substitution of fluid properties

The dimensionless groups  $Re$ ,  $Nu$ ,  $Pr$  include fluid properties that are generally temperature-dependent. For precise application of the calculation equations, it is necessary to define at which temperatures these fluid properties are to be applied. This especially holds true in the evaluation of test series.

Flue gas properties are calculated using the mean of wall temperature and average gas temperature in Schmidt's procedure [1]; this is also approximately the average boundary layer temperature.

$$\vartheta_{Bm} = (\vartheta_{Wa} + (\vartheta_{g1} + \vartheta_{g2})/2)/2 \quad (101)$$

The wall temperature of finned tubes differs above the surface of the fins. A mean wall temperature of the fin is calculated from the temperature at the fin base  $\vartheta_{RF}$  and the fin efficiency.

$$\vartheta_{mR} = \vartheta_{RF} + \frac{k}{\alpha}(1 - \eta_R)(\vartheta_{gm} - \vartheta_{wm}) \quad (102)$$

The average wall temperature is, in analogy to equation (6), therefore:

$$\vartheta_{Wa} = \frac{(\vartheta_{mR}A_{Ri} + \vartheta_{RF}A_{Ro})}{A_{Ri} + A_{Ro}} \quad (103)$$

For the temperature at the fin base, the FDBR formula [10] may be used:

$$\vartheta_{RF} = \vartheta_{wm} + \frac{A_{tot}}{A_R} \left( \frac{k d_A}{\alpha_i d_i} + \frac{k d_A}{2 \lambda_{Ro}} \ln \frac{d_A}{d_i} \right) (\vartheta_{gm} - \vartheta_{wm}) \quad (104)$$

When determining the Reynolds number in heat transfer calculations, the viscosity value at the temperature  $\vartheta_{Bm}$  is used, yet the velocity value at the mean gas temperature  $\vartheta_{gm}$  is used. Attention has to be paid to this, especially if in the place of the formula

$$Re = \frac{w d}{\nu}, \quad (105)$$

the following expression is used:

$$Re = \frac{\dot{m} d}{\eta} \quad (106)$$

In this formula, the rule given above for the calculation of  $Re$  is not implemented and has to be supplemented by a multiplicative factor  $(\vartheta_{Bm} + 273.2)/(\vartheta_{gm} + 273.2)$  when the dynamic viscosity  $\eta$  at the mean boundary-layer temperature is used.

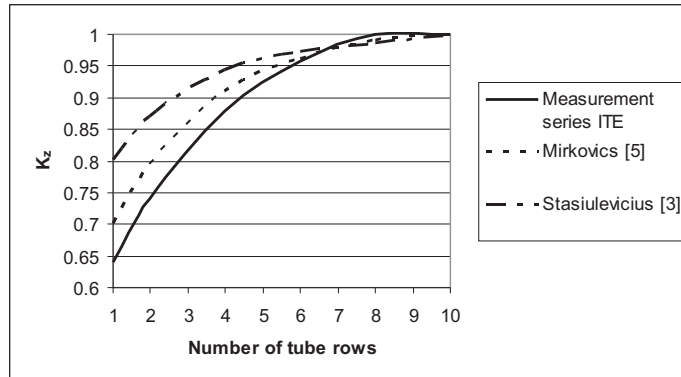


Figure 43: Reduction coefficient for heat transfer with a small number of consecutive tube rows (staggered arrangement)

### 3.5 Heat exchanger with a small number of consecutive tube rows

The formulas for heat transfer at finned tubes are generally valid for a certain minimum number of consecutive tube rows. This number varies according to the authors from 4 to 12 in the literature for staggered tube arrangements and from 4 to 20 for in-line tube arrangements. A reduction of heat transfer at staggered tube arrangements is generally assumed for smaller tube row numbers (see [2],[3],[5]); for in-line tube arrangements no such agreement exists; see [2],[3],[6]. The approaches and difficulties will be presented first by referring to the staggered tube arrangement because more papers exist for this problem case.

#### 3.5.1 Reduction methods for staggered tube arrangements as presented in tables and diagrams

Diagrams are presented for staggered tube arrangements in [6]. There the reduction of the heat transfer coefficient for a small tube row number in relation to the value  $\alpha_\infty$  (heat transfer coefficient for more than 8 tube rows) is shown; figure (43).

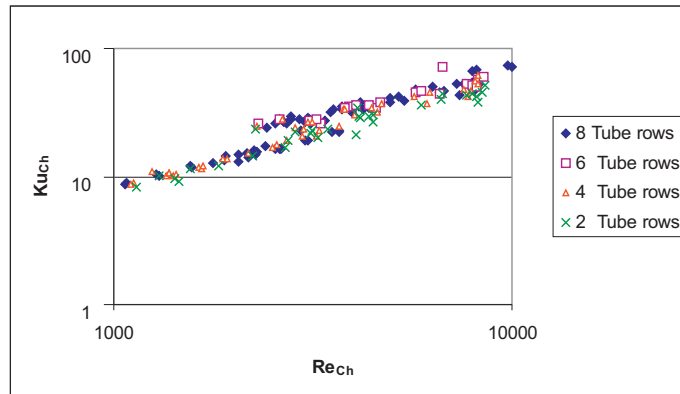


Figure 44: **Heat transfer with 8, 6, 4 and 2 consecutive tube rows with  $d_{Ch}$  as characteristic dimension (staggered arrangement)**

Depending on the longitudinal pitch  $t_l$ , the heat transfer coefficient differs for various tube bundles, thus different values are obtained for a heat exchanger with only a single tube row by using the reduction coefficients in figure (43), even though one tube row is only characterized by the transverse pitch  $t_q$  and can therefore show just one value for  $\alpha$ . This is a fundamental deficiency of this concept which can be avoided by other methods of calculation, i.e. according to Weierman [8], who states the reduction coefficients in dependence of  $t_l/t_q$ , or according to ESCOA, where the coefficients are calculated using the equations.

Table 2: Function  $E(n_R)$ 

$n_R$	1	2	3	4	5	6	7	8
$E(n_R)$	1.0	0.48	0.28	0.17	0.10	0.045	0.015	0.0

This method takes into account the considerations mentioned above, but cannot be added to other calculation formulas than the one given. In order to be able to include the considerations mentioned above, it is necessary to have a calculation method for heat transfer at a single finned tube row. This is the case with the 1984 edition of VDI Waermeatlas, pages Mb 1-5 [9], however, this method is less suitable for the calculation of finned tube bundles. In order to enable comparison of the results of the calculation with those of Mannesmann, a matching coefficient of 0.9 is introduced. For the dimensioning of a heat exchanger with less than eight consecutive tube rows, a correction factor  $K_z$  is proposed, which is substituted as a multiplier into the equation for heat transfer.

$$K_z = \left( \frac{Nu_{0,\infty}}{Nu_{0,1}} \right)^{-E(n_R)} \quad (107)$$

With this function, a reduction characteristic of the same amount is introduced for all heat transfer coefficients. For  $E(n_R)$  a value chart (table 2) is given, which is calculated from the heat transfer measurements by ITE with 1, 2, 4 and 6 tube rows and compared to 8 tube rows (see figure (6) in [6] on this).

The Nusselt number for  $n_R$  consecutive tube rows, with  $n_R$  less than 8, is calculated as:

$$Nu_{0,n_R} = Nu_{0,\infty} K_z \quad (108)$$

### 3.5.2 Calculations according to measurements on staggered finned tube bundles with less than 8 tube rows

The heat transfer measurements at finned tubes were almost always carried out at ITE on 8 consecutive tube rows. Afterwards, additional measurements were usually performed on 6, 4 and 2 tube rows. In one case, even measurements for a single tube row were performed, which was only possible through manipulation of the test rig, because the system is only designed for an even number of tube rows.

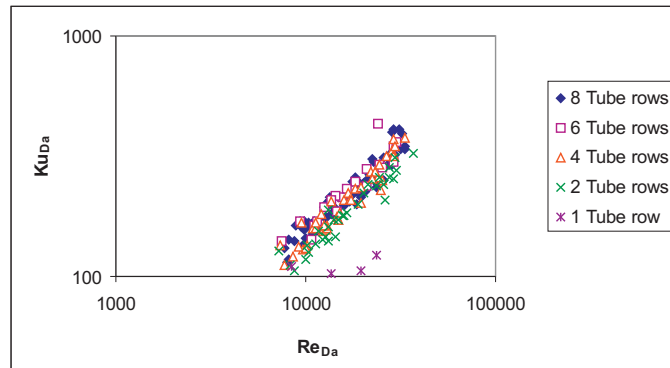


Figure 45: **Heat transfer with 8, 6, 4 and 2 consecutive tube rows with  $d_A$  as characteristic dimension (staggered arrangement)**

The experimental data of the measurements with a reduced number of tube rows was also evaluated. The results are presented in figures (44), (45) and (46). The evaluation was done according to different approaches with respect to the characteristic dimensions of the finned tube, i.e. using the outside tube diameter  $d_A$ , the hydraulic diameter of the flow channel between the fins  $d_{Ch}$  and the characteristic diameter according to Mirkovics  $d_{Mi}$ .

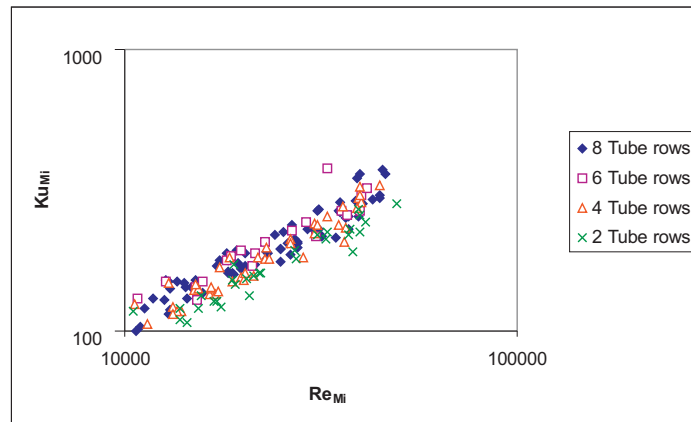


Figure 46: **Heat transfer with 8, 6, 4 and 2 consecutive tube rows with  $d_{Mi}$  as characteristic dimension (staggered arrangement)**

This has proven to be useful, since, depending on the approach, various measurement criteria became evident in each case. In figure (44) for example, where  $Ku_{Ch}$  according to equation (91) is plotted above  $Re_{Ch}$ , it is apparent that, in the range of Reynolds numbers 1000 to 2000, the difference between the measured values with 8 and 4 and/or 2 tube rows is relatively small, in any case considerably smaller than anywhere else in the figure. A comparison of the table of measured values with figure (44) shows that these values are for finned tubes

with a fin pitch of 3.62 mm, whereas the remaining measurement points are for finned tubes with a fin pitch of 6.67 mm. One can draw the conclusion that the reduction of heat transfer with a small number of tube rows is dependent on the fin pitch. This reduction would be low for small fin pitches while higher for large fin pitches. This hypothesis has to be verified, however, by further test series.

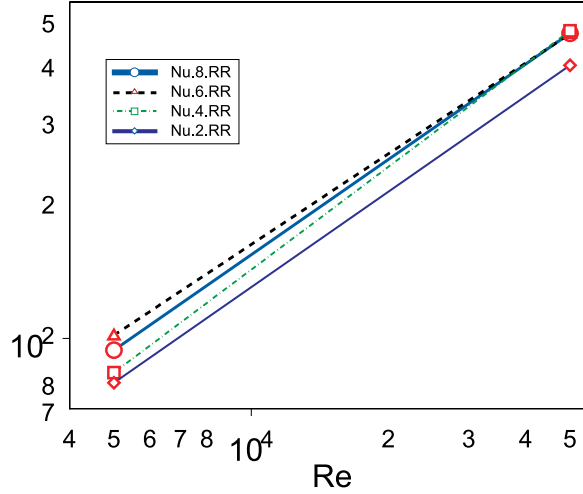


Figure 47: **Averages for heat transfer with 8, 6, 4 and 2 consecutive tube rows with  $d_A$  as characteristic dimension (staggered arrangement)**

In figures (45) and (46) it can be seen that the measurement points with 2 tube rows are clustered around a lower constant ratio than those with 8 and 6 tube rows. The values for measurements with 4 tube rows with low Reynolds numbers (approx. 5000) are closer to those with 2 tube rows, while for higher Reynolds numbers (approx. 50000) they near those for 8 and 6 tube rows. For a better visualization of this tendency, the linear mean values of measurements with 8, 6, 4 or 2 tube rows are plotted in figure (47). This tendency can be clearly seen there. Heat transfer with a small number of tube rows would therefore depend on both the number of tube rows and the Reynolds number. This fact is revealed again in a different manner in figure (48), whereas the measurement data for a single tube row has also been added. It in this case a reduction coefficient is plotted which indicates the decrease in heat transfer for a certain number of consecutive tube rows smaller than 8.

$$K_z = 0.82 - 0.3464z - 0.1736z^2 + (0.045 + 0.4144z + 0.3889z^2)y' + (0.025 - 0.0523z - 0.2677z^2)y'^2 + (0.01 - 0.0158z + 0.0525z^2)y'^3 \quad (109)$$

From this diagram an equation was generated which characterizes this diagram in an arithmetic form. For  $K_z$  a polynomial of the variable  $y'$  is given, which

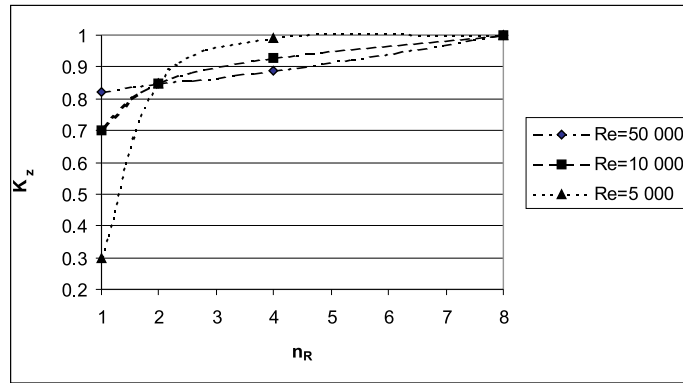


Figure 48: Reduction coefficient  $K_z$  for heat transfer with 8, 4, 2 and 1 consecutive tube rows (staggered arrangement)

depends on the number of tube rows  $n_R$  ( $y' = \frac{\log n_R}{\log 2}$ ) and on the variable  $z$ , which in turn depends on the Reynolds number ( $z = \log \frac{Re}{5000}$ ).

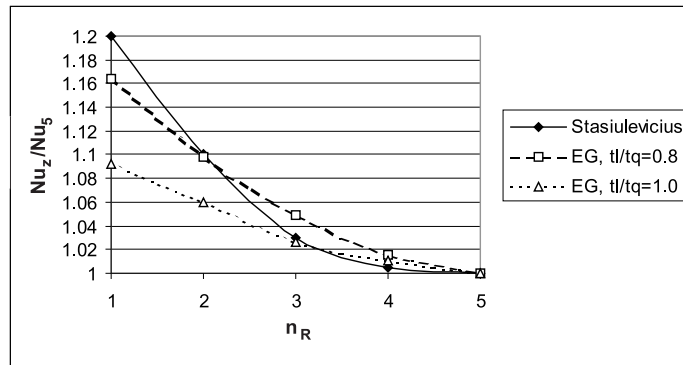


Figure 49: Heat transfer with small number of consecutive tube rows and in-line arrangement

### 3.5.3 Heat exchanger with small number of consecutive tube rows in in-line arrangement

A small number of consecutive tube rows influences heat transfer differently in in-line arrangements than in staggered arrangements. The first tube row shows the highest heat transfer coefficient in in-line arrangements, whereas it decreases for the following tube rows, since these are in the wake area of the previously arranged tube rows. Heat transfer decreases therefore up to the fourth tube row, behind this the asymptotic range is reached, according to [3]. This is represented in figure (49). According to [12], the asymptotic range is not reached before

the 5th tube row, the decline in heat transfer depends, however, additionally on the ratio of longitudinal to transverse pitch. For  $t_l/t_q > 1.1$  there is virtually no dependence of heat transfer on the number of the tube rows, but there is a noticeable dependence for  $t_l/t_q < 1.0$  which increases further with declining  $t_l/t_q$ . The diagram in figure (49) is misleading: the heat transfer coefficient cannot depend on the parameter  $t_l/t_q$  for a single tube row because no longitudinal pitch exists for a single tube row. The following figure (50) reveals this fact even more clearly.

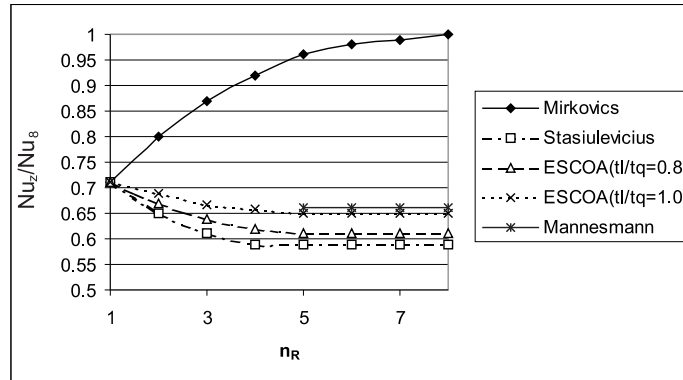


Figure 50: **Reduction coefficient for heat transfer with a small number of consecutive tube rows in in-line and staggered arrangement**

Figure (50) takes advantage of the fact that a single tube row shows a certain amount of heat transfer which is valid for both in-line and staggered tube arrangements. Thus, the curves, which characterize the dependence of heat transfer on the number of the tube rows for both geometrical arrangements, start from the same point. The reduction curve derived by Mirkovics [5] is thus plotted in figure (50) for staggered tube arrangements, as well as those from Stasiulevicius [3] and ESCOA [12] for in-line tube arrangements. In addition to this, the asymptotic value according to the Mannesmann formula [1], which results from the comparison of the constants for in-line and staggered tube arrangements to  $2/3$ , is plotted.

### 3.6 Serrated fins

For the manufacturing of spiral finned tubes, an initially straight steel strip, which forms the fins, needs to be bent around its larger axis and formed into a helical winding, whereby it is stretched on the outside and compressed or shaped on the inside in a wave-like manner as in figure (3). Therefore, the choice of the material for the fins is restricted to very ductile materials. (For example deep-drawing sheets among other things must sometimes be used, in spite of their unfavorable properties high temperatures.)

An alternative to this is to partially cut the steel strips (up to half the width) in short intervals on the outside before winding to generate a finned tube with serrated fins (figure (51)). Permanent elongation of the material is thus reduced. Hence materials with better high-temperature strength and better scaling resistance, yet less ductility, can be used for the fins.

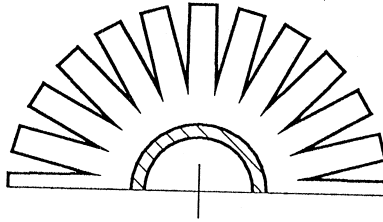


Figure 51: **Sectional view of a finned tube with serrated fins**

Finned tubes with serrated (also named segmented) fins show somewhat higher heat transfer coefficients than those with smooth fins because the boundary layer is built up anew at each segment, which results in better heat transfer. On the other hand, the pressure drop is a somewhat greater. Weierman [8] specifies reference values in graphical form for the calculation of such finned tubes. It follows from this that heat transfer in staggered tube arrangements increases only little for small values of  $h/(t_R - s_R)$  at and is considerably greater at  $h/(t_R - s_R) \geq 4$ ; see figure (52).

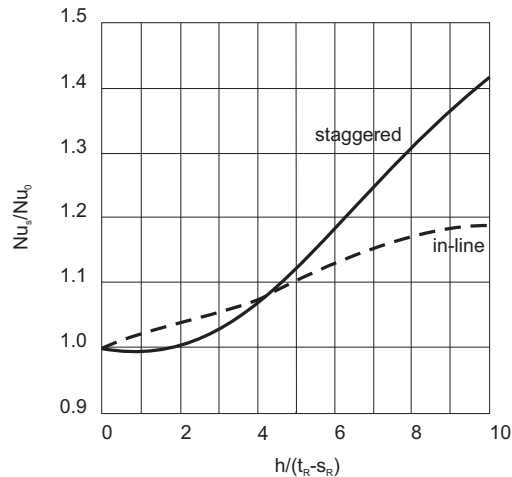


Figure 52: **Comparison of Nusselt numbers for finned tubes with serrated and annular fins**

The pressure drop coefficient is noticeably greater for small values of  $h/(t_R - s_R)$  (figure (53)), so that for  $h/(t_R - s_R) < 4$  no advantage in general is to be expected for finned tubes with serrated fins (no reduction of the heating surface at a large pressure drop).

For  $h/(t_R - s_R) > 6$ , heat transfer is around 20% better for a greater pressure drop of around 18% as related to common spiral finned tubes in staggered arrangement. An insignificant gain would be realized at the heating surface. With in-line tube arrangements, the increase in pressure drop for serrated fins is greater than the increase in heat transfer, which is seen in figure (52) and figure (53). It follows from this that in-line finned tube bundles with serrated fins are hardly to be preferred. The amount of loss, due to the serrated fins, at the heat-transferring surface depends on the width of the remaining fin volume and amounts to 7 ÷ 14% when 1/4 steel strip is retained, as given in the relation  $h/d_A$ .

A gain in specific power of the heat exchanger can therefore only be achieved with tall fins and a staggered tube arrangement. Equations for the determination of finned tubes with serrated fins were also developed by ESCOA (Extended Surface Corporation of America [17], a manufacturer of finned tubes with smooth fins and serrated fins; see the corresponding chapters) as well as by Nir [18].

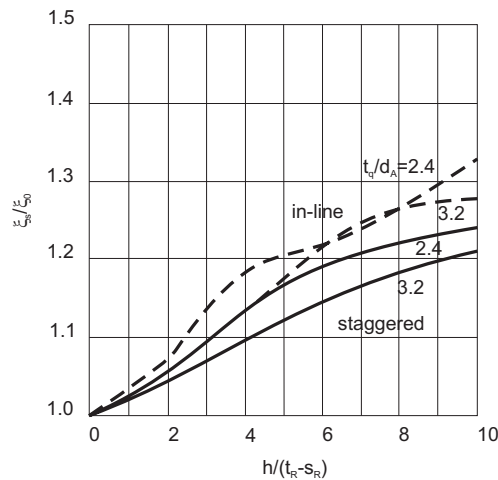


Figure 53: Comparison of pressure drop coefficients for finned tubes with serrated and annular fins

### 3.7 Geometrical arrangement of tubes in a bundle

The geometrical arrangement of tubes within a bundle noticeably influences heat transfer and pressure drop in finned tube arrangements. This fact is not always as obvious as in the heat transfer formulas by Schmidt [1], in which a factor of

0.45 appears for staggered arrangement and of 0.30 for in-line arrangements in otherwise identical equations.

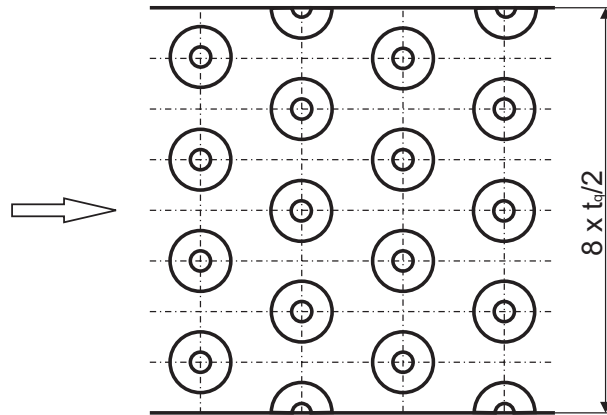


Figure 54: **Staggered finned tube arrangement with semi-tubes on the channel wall**

One has to distinguish between in-line and staggered tube arrangement, as presented in figure (26) and figure (54). In [26] a partly staggered arrangement is presented which differs from the staggered arrangement in that the following tube row is offset from the center of the transverse pitch of the preceding tube row; figure (56).

Semi-tubes should be arranged on the channel wall, especially in staggered tube arrangements, and with few parallel tube rows, in order to prevent a detrimental bypass flow through the otherwise empty space. In order to fully achieve this effect, these semi-tubes should also participate in heat transfer, which requires a very complicated design for the water side. The simpler construction design, as seen in figure (55), is usually chosen therefore.

A more general approach is to be attempted here, whereby a staggered arrangement is not achieved in the same way as the partly staggered arrangement, i.e. by transversely shifting every second tube row of an originally in-line arrangement, but rather by a slight shift in longitudinal direction; see figure (57). Strictly speaking, this alignment concept is no longer an in-line tube arrangement but rather a staggered tube arrangement.

A conceptual discrepancy arises here which does not exist physically, therefore another point of view is justified: the angle  $\alpha$  is used to characterize the arrangement, whereas it follows that:

$$\tan \alpha = \frac{t'_l}{t'_q} \quad (110)$$

The pitches  $t_q$  and  $t_l$  are the distances between the tube centers, whereas the pitches  $t'_q$  and  $t'_l$  are the distances between one tube center and an intersection of

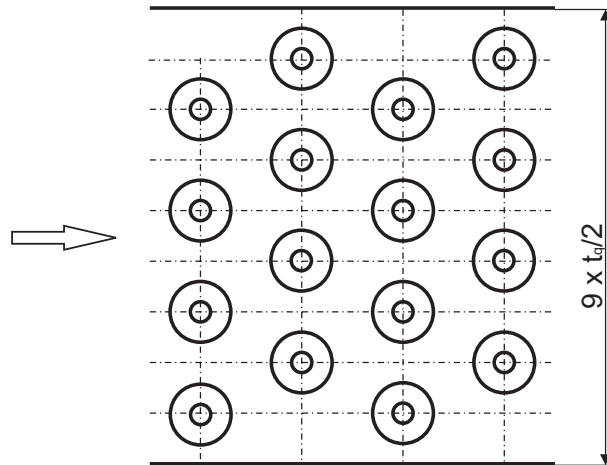


Figure 55: Staggered finned tube arrangement

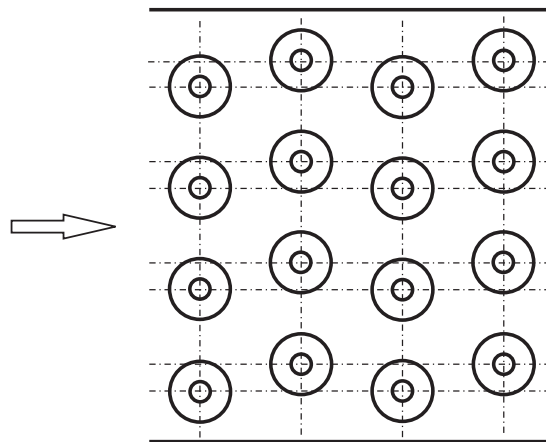


Figure 56: Partly staggered finned tube arrangement

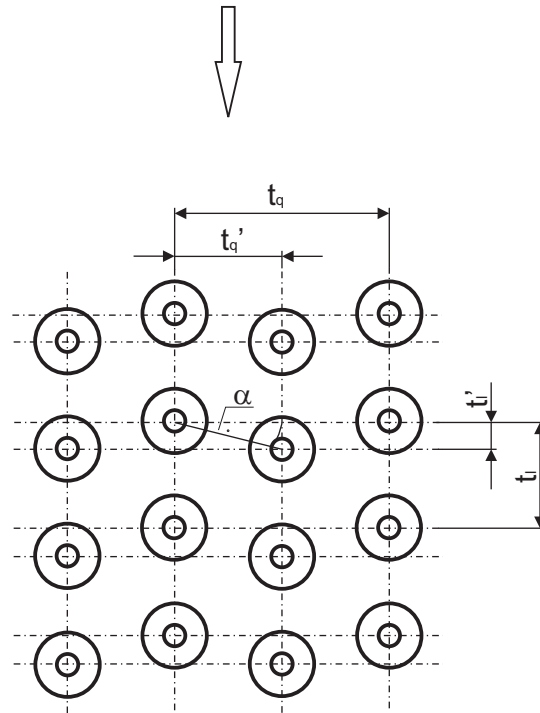


Figure 57: **Transition from an in-line to a staggered finned tube arrangement**

sleeve axes. With in-line arrangements  $\alpha$  is 0 and  $t'_l$  is also 0, and bundle geometry is determined by the specification  $t_l$  and  $t'_q$ . With staggered arrangements this is determined by the specification  $t_q$  and  $t'_l$ , where it often (but not necessarily) holds that:  $2t'_l = t_l$ . Except for partly staggered bundles,  $2t'_q = t_q$  is otherwise valid.

The characteristics of the dimensionless heat transfer coefficient  $Nu$  and the dimensionless pressure drop coefficient  $\xi$  in dependence on the angle  $\alpha$  could be determined through a series of experiments using the same finned tubes at a fixed transverse pitch but with a variable angle  $\alpha$ . Hence a relationship between in-line and staggered tube bundles would arise. Unfortunately, such a series of measurements has to date not been made. The function curve can be only partially plotted. In particular, no measurements are known for the determination of the area of angles  $\alpha$  smaller than 30 to 0 degrees.

Stasiulevicius and Skrinska [3] have done some measurements with the same finned tubes for  $\alpha = 35$  to 57 degrees, but unfortunately not for a smaller angle or for 0 degrees (in-line tube arrangement). The measurement series by [3] is presented in figure (58) with the angle  $\alpha$  from figure (57).

In the measurement series by ITE on staggered arrangements, still only a small interval for the angle  $\alpha$  was considered, while one measurement value for an in-line arrangement could be added using  $\alpha = 0$  for two different finned tubes with

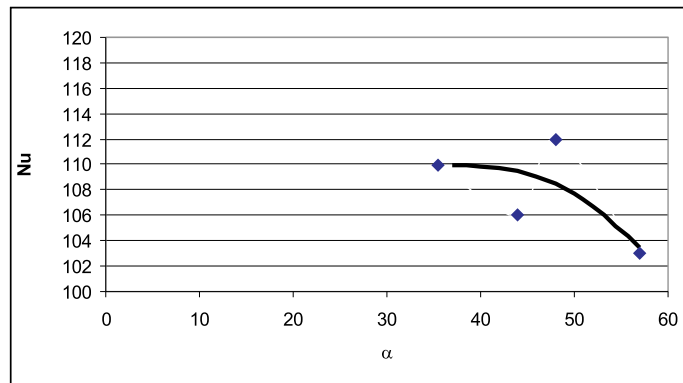


Figure 58: Heat transfer measurements of Stasiulevicius in dependence of the angle  $\alpha$  according to figure (57)

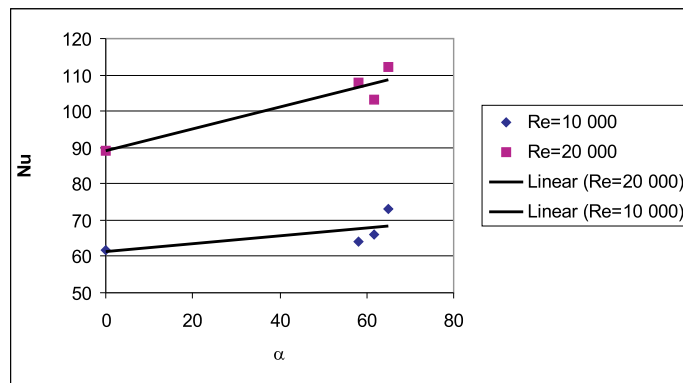


Figure 59: Heat transfer measurements by ITE in dependence of the angle  $\alpha$  according to figure (57). Tube diameter 31.8 mm

diameters of 31.8 mm and 38 mm; see figure (59) and figure (60) on this.

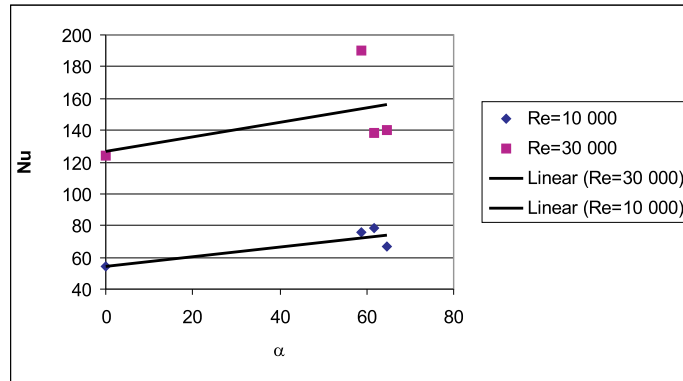


Figure 60: **Heat transfer measurements by ITE in dependence of the angle  $\alpha$  according to figure (57). Tube diameter 38 mm**

It is also interesting to produce the same diagram by means of a calculation equation. In this case calculation according to ESCOA would suggest itself, since first of all a relationship between transverse and longitudinal pitch exists and furthermore calculation can also be performed for in-line arrangements using a consistent equation. The result is presented in figure (61) and the curve matches the measurement values in the previous figures.

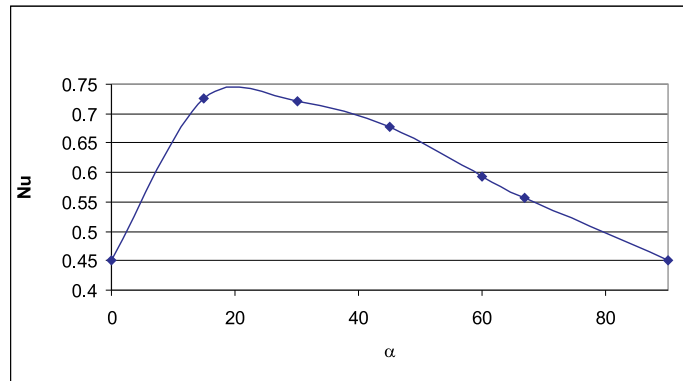


Figure 61: **Heat transfer calculated according to ESCOA in dependence of the angle  $\alpha$  according to figure (57)**

The test series by Stenin and Kuntysh [36] should also be mentioned. The tube rows in the direction of flow, originally in in-line arrangement (position I), are rotated by a certain angle, i.e. approx.  $7^\circ$  (position II),  $16^\circ$  (position III),  $24^\circ$  (position IV) and  $30^\circ$  (position V). The last arrangement represents equilateral triangular pitch, when a suitable longitudinal pitch is chosen; figure (62).

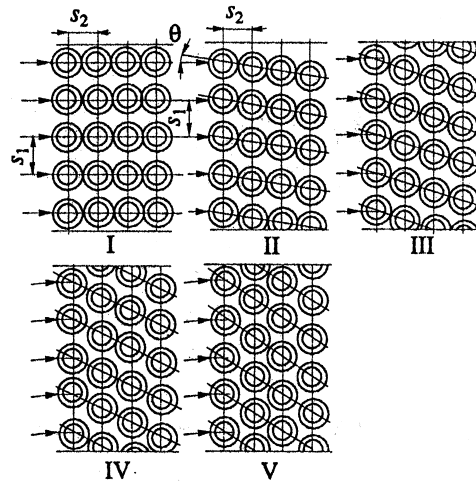


Figure 62: **Schematic representation of the experimental setup by Stenin and Kuntysh [36]**

The results of this test series are presented in figure (63). It can be seen that heat transfer shows a maximum for an angle of  $24^\circ$  and then decreases again by approx. 4% up to an angle of  $30^\circ$  (which is an equilateral triangular pitch).

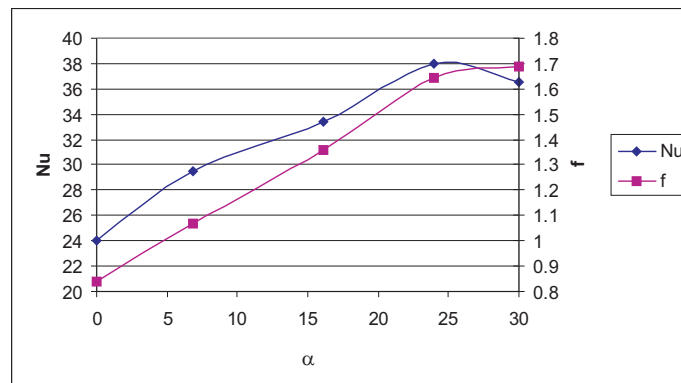


Figure 63: **Experimental results of Stenin and Kuntysh [36]**

### 3.8 Summary of heat transfer

Finned tubes with fins attached orthogonally to the sleeve axis on the outside are used for heat exchange between a gas with relatively unfavorable heat transportation properties and a liquid. The gas-side heating surface per m tube is

extended by the fins, so that a heat exchanger of smaller construction volume is attained than with smooth tubes. As a result of thermal conduction resistance in the fins, a reduction factor, so-called fin efficiency, is adopted for the calculation of heat transfer at finned tubes. This is derived from the geometrical dimensions and the thermal conductivity coefficient of the fin material as well as the gas-side heat transfer coefficient.

In the formulas for calculating heat transfer, the dimensionless Reynolds and Nusselt groups must be calculated using a characteristic length. This length is not as naturally evident as with the diameter of smooth tubes. In addition to more complex expressions, the base diameter of the finned tube has become the established measure of characteristic length in spite of some obvious deficiencies. The formulas consist of more terms than formulas for smooth tubes as a result of the greater number of characteristic dimensions of finned tubes. Attention has to be paid to the choice of the temperature value at which the thermal properties of the fluid are applied. According to Schmidt's equations, this could for example be the mean boundary temperature. Finned tube heat exchangers with few consecutive tube rows in a gas flow require a correction of the heat transfer coefficient.

## 4 Finned tube bundles with continuous fins

Particularly in air-conditioning and refrigeration engineering as well as for cooling units, but sometimes also in the case of general applications, finned tube bundles with continuous fins (also termed louvers- tube bundle) are used. In this case, the fins have the dimensions of a whole heat exchanger or a heat exchanger package. The tubes are inserted into the fins in adapted holes, whereby the heat-conducting connection between fin and tube is achieved by pressing the tubes onto the fins, expanding the tubes or by means of soldering or welding. In this case, the fins are often made of a different material from the tubes, for example aluminum fins with steel or copper tubes, or copper fins with steel tubes. In order to achieve a further improvement of heat transfer, the fins may also be wavy and approximately orthogonal to the gas flow direction. Apart from circular tubes, elliptical or flat tubes are also used to reduce gas-side pressure drop in particular; figure (64).

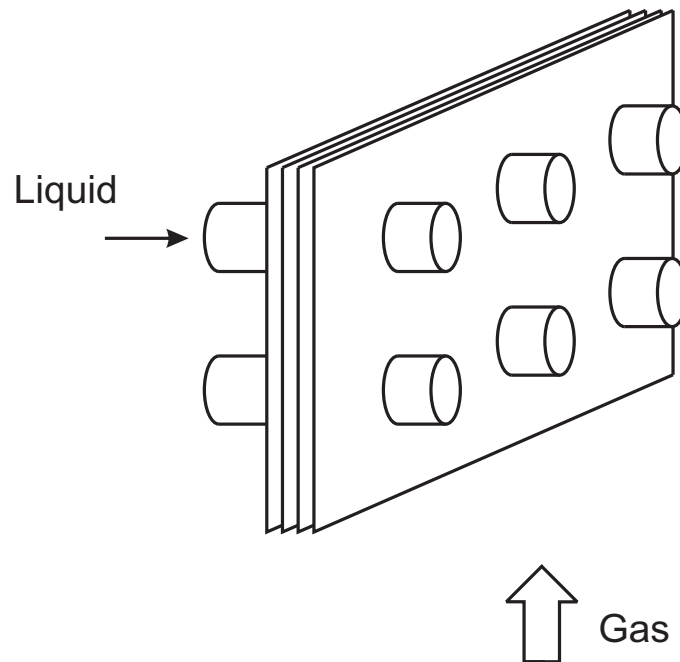


Figure 64: Circular tubes with continuous fins

## 4.1 Finned tube bundles with continuous smooth fins and circular tubes

For finned tube bundles with continuous smooth fins and circular tubes, calculation equations exist for both staggered and in-line tube arrangements.

1. In-line tube arrangement: the calculation equations use a characteristic length which is calculated as a hydraulic diameter of the single flow channel.

$$d_{ae} = \frac{4.V.\Psi}{A_{tot}} \quad (111)$$

The individual terms here are: porosity  $\Psi$  which represents the void fraction in relation to the total volume:

$$\Psi = 1 - \frac{s_R}{t_R} - \frac{\pi d_A^2 (t_R - s_R)}{4t_q t_l t_R} \quad (112)$$

The effective heating surface  $A_{tot}$  is expressed as:

$$A_{tot} = 2(t_q t_l - d_A^2 \frac{\pi}{4}) + d_A \pi (t_R - s_R) \quad (113)$$

The volume  $V$  is the product resulting from transverse pitch, longitudinal pitch and fin pitch  $t_q t_l (t_R - s_R)$ . For heat transfer at an in-line arrangement, the following relationship is given in dimensionless notation by Kaminski and Gross [19], however it also agrees with Haaf [20]:

$$Nu(d_{ae}) = C_1 Re(d_{ae})^{0.625} Pr^{\frac{1}{3}} \left(\frac{d_{ae}}{t_l}\right)^{\frac{1}{3}} \quad (114)$$

The dimensionless number  $Re(d_{ae})$  in this case is calculated using the hydraulic diameter  $d_{ae}$ , already defined, and, deviating from common procedure, calculated using the mean gas velocity in the bundle  $w_m$ :

$$w_m = w_0 / \Psi \quad (115)$$

where  $w_0$  is the velocity of the free fluid flow.

Kaminski and Gross [19] and Haaf, in the handbook of refrigeration engineering Vol. 6A [20], present the same values for the constant  $C_1$  in an in-line tube arrangement:  $C_1 = 0.20$  for more than 5 consecutive tube rows, while Kaminski and Gross [19] present a table for  $C_1$  for fewer than 5 tube rows. Haaf [20], on the other hand, states that fewer than 5 tube rows do not often occur and therefore no such specification is necessary.

2. Staggered tube arrangement: The equation shown (114) is also used for a staggered tube arrangement, however the specifications given for the constant  $C_1$  by the two sources above do not agree: Kaminski and Gross [19] specify the constant at  $C_1 = 0.24$  for staggered tube arrangements with a tube row number  $> 4$ , yet for Haaf [20]  $C_1 = 0.31$ . For a tube row number smaller than 4, a table for the constant  $C_1$  is specified in [19].

It is worthy of note that heat transfer is best for both in-line and staggered tube arrangements with only one tube row and decreases for several consecutive tube rows, until an asymptotic value is reached at 5 tube rows in in-line arrangement and/or 4 tube rows in staggered arrangement. On the other hand, for finned tube bundles with fins which are separately attached to the tubes in staggered arrangement, heat transfer increases with the number of the tube rows, until an asymptotic value is reached at 6-8 consecutive tube rows; see section 3.5.1 and 3.5.2 on this.

Pressure drop is calculated according to Kaminski and Gross [19] using the following formula,

$$\Delta p = \xi_{KG} n_R \frac{t_l}{d_{ae}} \frac{\rho_G w_m^2}{2} \quad (116)$$

which is adopted by Haaf [20] and based on Ward and Young [37].

The additional expression  $\frac{t_l}{d_{ae}}$  and the use of the ‘mean velocity  $w_m$  is a departure from prevalent notation for pressure drop in this field. Similar to the case of heat transfer, equivalent formulas are proposed for in-line and staggered tube arrangements. Only the pressure drop coefficients  $\xi_{KG}$  are different. The equations for the calculation of the pressure drop coefficients are identical, only the constant  $C_2$  varies according to the tube arrangement.

$$\xi_{KG} = C_2 Re(d_{ae})^{-\frac{1}{3}} \left(\frac{d_{ae}}{t_l}\right)^{0.6} \quad (117)$$

The specifications for the constant  $C_2$  given by different sources resemble each other for in-line tube arrangement, while considerable differences exist for staggered tube arrangement. Kaminski and Gross [19] set the constant  $C_2$  at 6.3 for in-line tube arrangements, while Haaf [20] specifies 6.0; i.e. only an insignificant difference of 5% exists between the two specifications. According to [19] the asymptotic value is  $C_2 = 8.1$  for 6 or more tube rows in staggered tube arrangement, while [20] specifies the value at  $C_2 = 10.5$  without stating any dependence on the tube row number. Similar to heat transfer, a difference of approx. 30 % exists. According to [19], a pressure drop table exists for  $C_2$  with fewer than 6 consecutive tube rows.

Table 3:  $C_1$  and  $C_2$  for few tube rows according to [19]

$n_R$	$C_1$	$C_2$	$C_1$	$C_2$
-	in-line		staggered	
1	0.31	12.9	0.31	12.9
2	0.25	8.8	0.28	10.5
3	0.22	7.5	0.26	9.4
4	0.21	6.9	0.24	8.7
5	0.20	6.5	0.24	8.4
6	0.20	6.3	0.24	8.1

## 4.2 Finned tube bundles with continuous wavy fins and circular tubes

Industrially manufactured heat exchangers often use finned tubes with wavy fins. These waves have two different designs, canted waves and round waves; see figure (65).

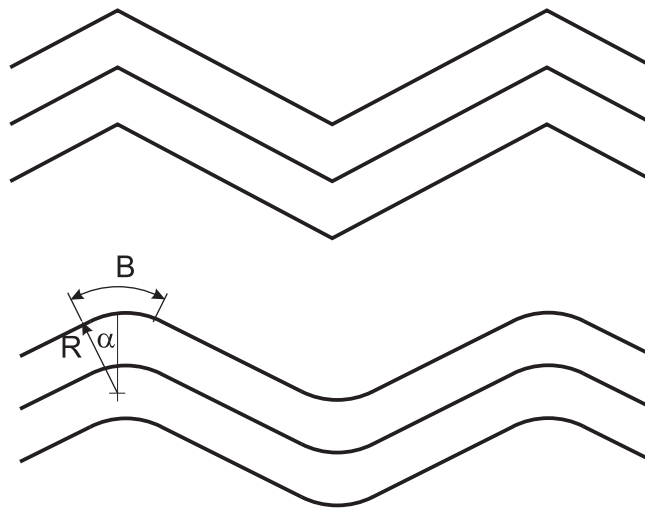


Figure 65: Wavy fins: corrugated or wavy form

The terms "corrugated fin" and "wavy fin" have also become established in German. The equations of Kaminski and Gross [19] are valid for round tubes and angular corrugation with wavelengths of 6.25 mm, in in-line tube arrangement, and 5.5 mm, in staggered tube arrangement, and an amplitude of 1.38 mm in each case. For in-line tube arrangements these equations are:

$$Nu(d_{ae}) = 1.28 Re(d_{ae})^{0.329} Pr^{(\frac{1}{3})} \left(\frac{d_{ae}}{t_l}\right)^{0.214} \quad (118)$$

The same notation applies as in the preceding section. The following equation holds for the pressure drop coefficient in this arrangement:

$$\xi_{KG} = 24 Re(d_{ae})^{-0.52} \left(\frac{d_{ae}}{t_l}\right)^{0.63} \quad (119)$$

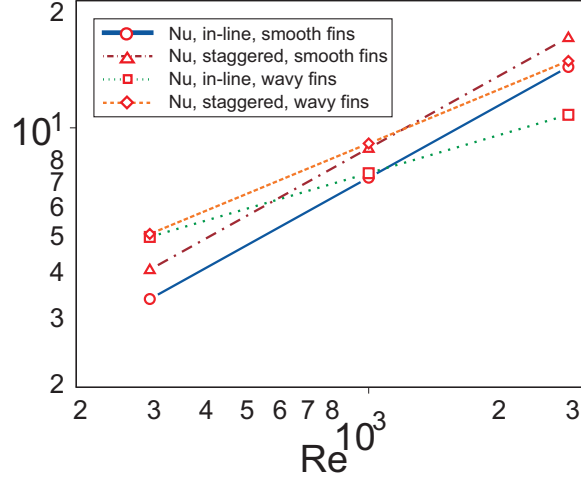


Figure 66: Comparison of Nusselt numbers for circular tubes with continuous smooth or wavy fins

Similar equations are valid for staggered tube arrangement, however with other constants. First, the one for heat transfer:

$$Nu(d_{ae}) = 0.597 Re(d_{ae})^{0.466} Pr^{(\frac{1}{3})} \left(\frac{d_{ae}}{t_l}\right)^{0.214} \quad (120)$$

The following is valid for the pressure drop coefficient:

$$\xi_{KG} = 7.8 Re(d_{ae})^{-0.32} \left(\frac{d_{ae}}{t_l}\right)^{0.63}. \quad (121)$$

A comparison of Nusselt numbers in these equations with the equations for smooth fins in figure (66) shows that, with in-line tube arrangements, heat transfer is only better for wavy fins than for smooth fins in the Reynolds number range < 1000.

The pressure drop coefficient for  $Re < 1000$  is also a little higher, and wavy fins therefore provide a somewhat more compact heating surface; see figure (67).

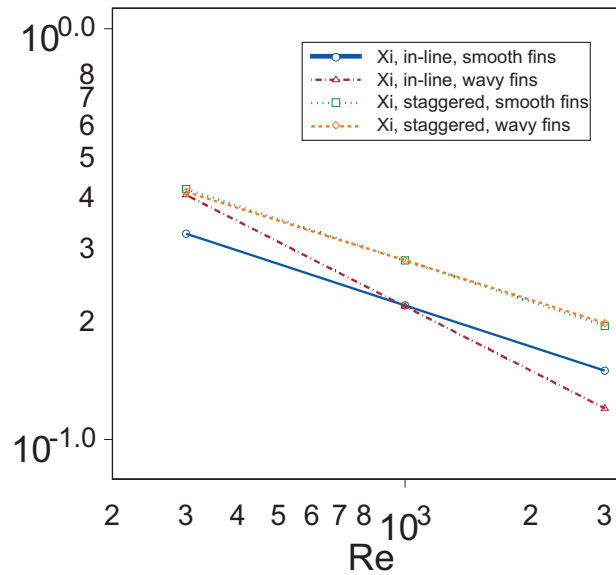


Figure 67: Comparison of pressure drop coefficients at circular tubes with continuous smooth or wavy fins

For higher Reynolds numbers, wavy fins are not as good as smooth fins both for in-line tube as well as for staggered tube arrangements, even though staggered are better than in-line arrangements, as can be seen by comparing the performance numbers ( $Pn$ ) for circular finned tubes according to equation (132) in figure (68).

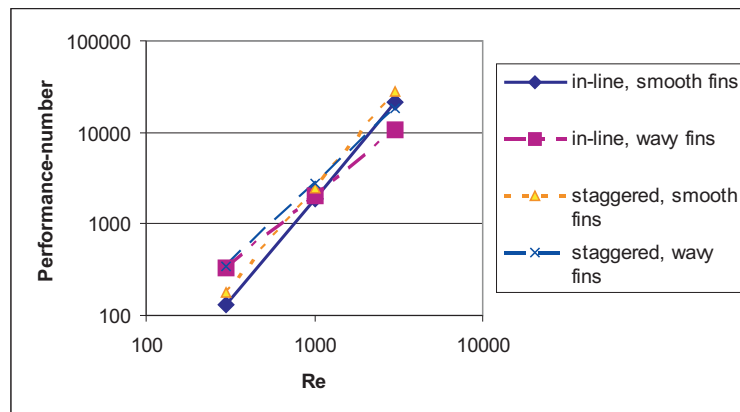


Figure 68: Comparison of performance numbers according to equation (132) for circular tubes with continuous smooth or wavy fins

Sparrow and Hossfeld [27] examined the influence of rounding the angular waves and discovered that for a small rounding radius (see figure (65) for the terms), i.e. when  $R/B < 0.55$ ,  $Nu$  decreases by about 3%, while for a larger radius, i.e.

$0.55 < R/B < 0.972$ ,  $Nu$  decreases by about 8%. The pressure drop coefficient decreases in the first case by about 21%, however, and in the second case by as much as 44%, so that the rounded wavy fins are obviously to be preferred.

### 4.3 Finned tube bundles with non-circular tubes and continuous smooth fins

Finned tube bundles with continuous fins as well as single tubes with fins are often manufactured from elliptical or flat tubes in order to reduce the gas-side pressure drop. Yet these tubes show considerably less strength against internal and external overpressure, particularly flat tubes, which consist of two semicircles with straight lines joining them in the cross-section; see figure (69). For these finned tube bundles only few measurement values are available, those by Kays and London [21] for flat tubes and those by Geiser [30] for flat tubes and other tube designs, while no suitable calculation equations exist.

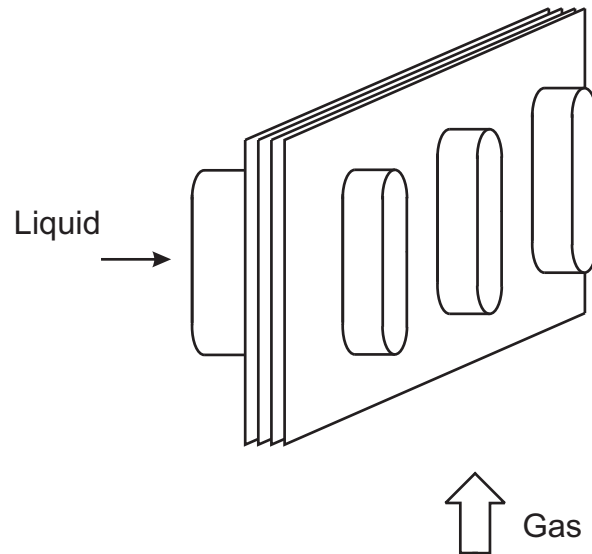


Figure 69: **Flat tubes with continuous fins**

The task of developing calculation equations mainly from the above-mentioned measurements by Kays and London [21] is even more difficult when flat tubes with a very small axial ratio of 0.138 to 0.136 (small to big axis) are used and this relation is not varied. Thus, the difference in geometry compared to a circular tube is considerable. When merely the design of the tubes used is considered, a comparison between measurements on flat tubes with the measurements on circular tubes does not seem to be possible. However, the equivalent diameters  $d_{ae}$  of the different tube bundles are not that far apart (4.9 mm to 5.2 mm). A comparison for staggered arrangement according to the diagrams of Kays and

London [21] can be nevertheless done if one accepts a greater uncertainty of the resulting equations.

This comparison shows that heat transfer is a little smaller for flat tubes than for cylindrical tubes. No statement can be made about a possible influence of the axial ratio  $a/b$  of the flat tubes. The following approximate equation for heat transfer may be specified based on the explanations given above for flat tubes in staggered arrangement with continuous smooth fins by drawing on the equation for cylindrical tubes by [19]:

$$Nu(d_{ae}) = 0.438 Re(d_{ae})^{0.531} Pr^{\frac{1}{3}} \left(\frac{d_{ae}}{t_l}\right)^{\frac{1}{3}} \quad (122)$$

According to the information in [21], the Reynolds number was also determined using  $d_{ae}$ , but with the velocity in the narrowest cross-section  $w_E = w_0/A_f$ , at which the proportional free cross-section results as:

$$A_f = \left(\frac{t_q - a}{t_q}\right) \left(\frac{t_R - s_R}{t_R}\right) \quad (123)$$

The hydraulic diameter of the fluid channel is ascertained using  $d_{ae} = d_h = 4V/F$ :

$$d_{ae} = \frac{4((t_R - s_R)(t_q t_l - (a(b - a)) - a^2 \frac{\pi}{4}))}{A_{Ftot}} \quad (124)$$

$A_{Ftot}$  in this case is the heating surface:

$$A_{Ftot} = 2(t_q t_l - a(b - a) - a^2 \frac{\pi}{4}) + (2(b - a) + a\pi)(t_R - s_R) \quad (125)$$

For the development of a calculation equation for flat tubes with staggered tube arrangement, measurement values are available from cylindrical tubes for comparison. Such measurements are not available for in-line tube arrangements. Heat transfer equations for in-line flat tube bundles may only be determined based on measurement values and will therefore show a greater uncertainty. A comparable approximate equation representing heat transfer for flat tubes with continuous smooth fins arranged in line is thus as follows:

$$Nu(d_{ae}) = 0.0842 Re(d_{ae})^{0.7} Pr^{(\frac{1}{3})} \left(\frac{d_{ae}}{t_l}\right)^{\frac{1}{3}} \quad (126)$$

A comparison shows that heat transfer for lower Reynolds numbers is considerably better in staggered arrangement. For higher Reynolds numbers, on the other hand, a smaller difference exists. The representation of the Nusselt number, depending on  $Re$  and  $Pr$  in the formulation of the equations given above is,

however, a simplification, since the measurement values do not form a straight line in the double-logarithmic diagram of the measured values as the above formula would demand, instead they show a curved characteristic. Strictly speaking, the formulas are only valid in the range between  $1000 < Re < 10000$ , that is, approximately for air at ambient temperatures with a velocity from 3 m/s up to 30 m/s. The gas-side pressure drop for a flat tube bundle with continuous fins could be estimated with the measured pressure drop coefficients provided by Kays and London [21]. Relations of the same variety as for circular tube bundle with continuous fins can according to [19] be expressed for smaller ranges of Reynolds numbers. Such an equation for in-line flat tube arrangement with smooth fins in the same range of Reynolds number as above ( $10^3 < Re < 10^4$ ) would be as follows:

$$\xi = 0.70 Re(d_{ae})^{-0.339} \left(\frac{d_{ae}}{t_l}\right)^{0.6} \quad (127)$$

For a staggered or partially staggered arrangement the equation reads as follows:

$$\xi = 1.523 Re(d_{ae})^{-0.414} \left(\frac{d_{ae}}{t_l}\right)^{0.6} \quad (128)$$

In contrast to the section on circular tubes, the pressure drop coefficients  $\xi$  in this case are defined for  $n_R$  tube rows according to the following relationship:

$$\xi = \frac{\Delta p}{n_R \rho_G \frac{w_E^2}{2}} \quad (129)$$

using the velocity in the narrowest cross-section  $w_E$  and without the expression  $\frac{t_l}{d_{ae}}$ .

The equations specified above are, however, only applicable for tube arrangements which do not differ geometrically too much from the examined tube bundles. In particular, the aspect ratio  $a/b$  of the flat tubes seems to be worthy of note. An immediate comparison of the pressure drop coefficients of in-line and staggered arrangements is not helpful, since the free flow cross-section is not identical. A comparison of the quotient  $\xi/A_f^2$  in each case better expresses the relationship between in-line and staggered arrangements, where  $A_f$  is the fraction of the free cross-section of the tube arrangement. To answer the question as to whether flat tube bundles show a lower effective pressure drop than circular tube bundles, the velocity occurring in the respective free cross-section needs to be considered. In this case, comparable conditions should be assumed, for example the available flow cross-section ought to be identical for the medium in the tubes.

A more complex calculation would result if it is assumed that the pressure drop for the medium in the tubes is identical in both geometries. When for example

Table 4: Flat tubes with differing profiles according to Geiser [30]

Profile type	Profile-length [mm]	Nu	$\zeta$ (for Re=1000)	Performance coefficient
R4K	300	11.8	7.4	222
PRSK-V	300	11.8	5.4	304
PRSK-H	300	11.8	7.7	213
PKSK	300	11.8	5.2	316
GEK	300	11.9	5.3	318
GSK-V	300	11.3	5.8	249
837KK-V	320.5	10.8	6.7	188
479K-V	253	11.8	4.8	342

the calculation is performed under the first condition for flat tube bundles of 5 x 20 x 1 mm (equivalent circular tube 9.4 x 1 mm), only approx. a quarter of the pressure drop of the circular tubes results for the flat tubes. In this respect the usage of flat tube bundles is certainly advantageous when thermodynamic and/or economic and/or design advantages can be achieved through the smaller pressure drop on the gas-side, as long as the strength of the flat tubes allows them to be used in the face of the internal pressure of the medium.

The flat tubes examined by Kays and London [21] all consist of two semicircles joined by straight lines. Investigations of flat tubes with other profiles also exist, revealing even less pressure loss. Geiser [30] investigated, through experiments and calculations, tubes of different profiles with rectangular mounted fins. The pressure drop was measured directly on the models manufactured of metal and plastic. Heat transfer on the other hand was determined via the analogy between mass and heat transfer using a small amount of ammonia in the gas and the discoloration of test papers at the fins.

Here only those profiles are presented for which both pressure drop values and heat transfer numbers are available. These include 8 different profiles starting from the simple flat tube. All profile tubes are 60 mm thick, the length is mostly 300 mm. Only a few are shorter or longer. The fins are 150 mm wide and 357 mm long. The clearance between the fins is 12 mm and the transverse pitch  $t_q$  is therefore 150 mm. The flat tubes were analyzed on an enlarged scale and are presented in figure (70) with the most important data and performance coefficients (table (4)).

For the evaluation of different profiles of tubes, as well as in general for different geometrical arrangements of heat exchangers, heat output is related to blower power, which is necessary for the processing of the gas-side pressure drop. As a standard for efficiency, the criterion suggested by Stephan and Mitrovic [31] can

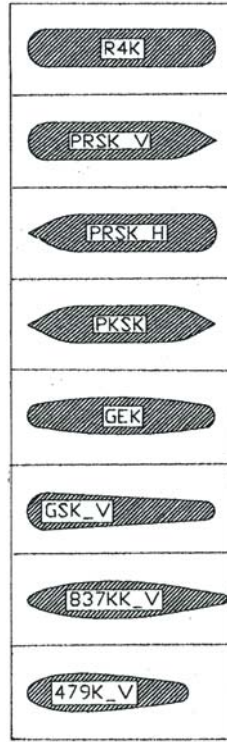


Figure 70: Flat tubes with differing profiles according to Geiser [30]

be used.

$$\frac{St^3}{\xi} \quad (130)$$

According to Geiser [30], for finned tubes the Stanton number has to be multiplied by fin efficiency.

$$\frac{(St \eta_R)^3}{\xi} \quad (131)$$

Since in this comparison  $Re$  and  $Pr$  remain constant and fin efficiency will also be almost constant, the expression for the performance number, which is easier to determine, can be used for the comparison as an approximation.

$$Pn = \frac{Nu^3}{\xi} \quad (132)$$

The profile  $R4K$  (see figure (70)) is the familiar flat tube with two semicircles and straight lines joining them. Here the length-to-width ratio is about 5 (with Kays and London [21] somewhat higher than 7). The next profile  $PRSK-V$  has

Table 5: Circumference and surface of profile flat tubes

Profile type	F( $m^2 10^{-4}$ )	U(m)
R4K	172.27	0.669
PRSK-V	158.07	0.647
PRSK-H	158.07	0.647
PKSK	143.86	0.626
GEK	148.05	0.644
GSK-V	132.42	0.651
837KK-V	139.09	0.67
479K-V	118.32	0.528

a spike on the downstream side and is therefore more advantageous with regard to pressure drop because of the smaller vortex in the wake region. The reverse profile *PRSK – H* with the spike at the upstream side is not advantageous, the symmetrical profile *PKSK* with two tips downstream and upstream is again very advantageous, even more than the profile *PRSK – V*. The profile *GEK* is an elliptical profile, approximated by circular arcs. *GSK – V* is a spheroid profile with moderate performance; the profile *837KK – V* is supposed to be advantageous from a fluid mechanical point of view, but actually considered not efficient due to its excess length, whereas the shorter profile *479K – V* seems to be the best of all. The Reynolds number, according to Geiser [30], is determined using the mean velocity in the bundle as well as the hydraulic diameter of the flow channel. For the calculation of  $d_{ae}$ , the circumference (U) and the cross-section area (F) of the profiled flat tubes is given in table (5).

#### 4.4 Finned tube bundles with flat tubes and continuous wavy fins

Finned tube bundles consisting of flat tubes with continuous wavy fins are sometimes used. Yet also single finned tubes with wavy fins are employed. In this way the heat transfer coefficients according to Kays and London [21] may be increased. For in-line tube arrangements of flat tubes, the Nusselt number increases with Reynolds numbers between 300 and 3000 by around 38% at a wave height of 0.635 mm and a wavelength of 6.35 mm. For continuous wavy fins only the experimental values of Kays and London [21] exist. They used flat tubes for their investigations. For circular tubes, investigations of corrugated fins by Kaminski and Gross [28] exist. The wavy fins examined by Kays and London have all the same wave geometry, with a wave height of 0.635 mm and a wavelength of 6.35 mm. There is only little information for converting this result to other wave

geometries. According to Mirth and Ramadhyani [29], heat transfer and pressure drop depend on the geometry of the waves, however the use of additional parameters like wave height and wavelength does not improve the adaptation of the equations to the measured values, so that it can therefore be assumed that the influence is small. Should any influence of the corrugation parameters nevertheless be considered, this could be attempted for the flow in tubes and channels with wavy walls with the help of equations (11.1) and (11.2) on page 11.12 of the Handbook of Heat Transfer, 3rd edition 1998 [39]. According to the restrictions mentioned above, the approximate relationship is valid for heat transfer in in-line flat tube bundles with rounded wavy and continuous fins:

$$Nu(d_{ae}) = 0.1452 Re(d_{ae})^{0.6576} Pr^{\frac{1}{3}} \left(\frac{d_{ae}}{t_l}\right)^{\frac{1}{3}} \quad (133)$$

For the pressure drop coefficient of the arrangement listed above, the following results from the diagrams of measurements:

$$\xi = 0.56 Re(d_{ae})^{-0.261} \left(\frac{d_{ae}}{t_l}\right)^{0.6} \quad (134)$$

For the corresponding flat tube bundles in staggered arrangement with wavy fins, an equation the heat transfer would be:

$$Nu(d_{ae}) = 0.164 Re(d_{ae})^{0.678} Pr^{\frac{1}{3}} \left(\frac{d_{ae}}{t_l}\right)^{\frac{1}{3}} \quad (135)$$

The pressure drop coefficient for a staggered arrangement of flat tubes with wavy fins results as:

$$\xi = 0.9094 Re(d_{ae})^{-0.313} \left(\frac{d_{ae}}{t_l}\right)^{0.6} \quad (136)$$

For the example listed above, the pressure drop coefficients are presented in figure (71).

The equations for heat transfer and pressure drop are valid with sufficient accuracy for staggered flat tube arrangement with wavy fins in the case of different fin pitches. This may be considered as evidence that an approach using the equivalent hydraulic diameter  $d_{ae}$  is in principle correct.

The following may be stated with regard to the selection of finned flat tubes: in view of the Nusselt numbers in figure (72), the staggered tube arrangement is invariably better than the in-line tube arrangement. For in-line arrangement, wavy fins are always better, but for staggered arrangements and Reynolds numbers  $< 1000$  not as preferable as smooth fins, while for higher Reynolds numbers slightly better. For comparison the performance numbers for flat tubes according

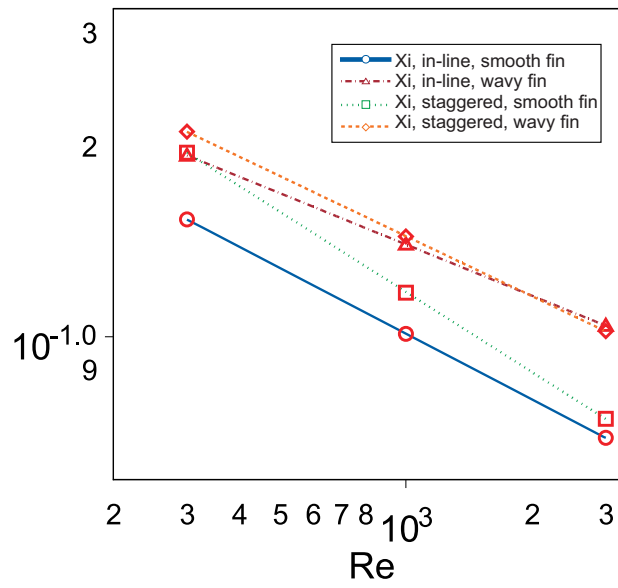


Figure 71: Pressure drop coefficients of flat tubes with continuous fins

to equation (132) are presented in figure (73). These display same behavior as described for the Nusselt numbers.

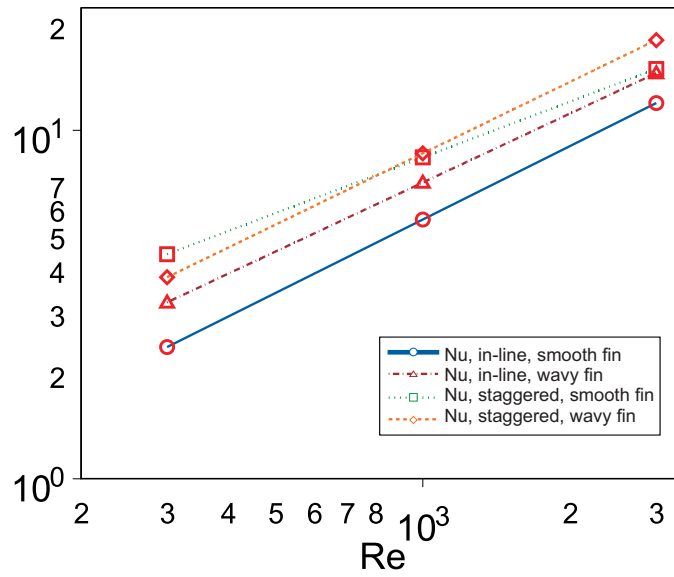


Figure 72: Nusselt-numbers at flat tubes with continuous fins

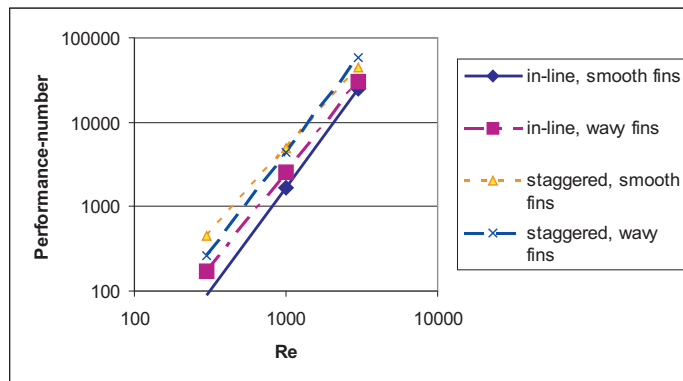


Figure 73: Performance numbers according to equation (132) for flat tubes with continuous fins

## 5 Pressure drop

### 5.1 Fundamentals for the determination of pressure drop at finned tubes

For the design and construction of finned tube heating surfaces, knowledge of the gas-side pressure drop is just as important as knowledge of the heat transfer coefficient. For fossil-heated steam generators it does not make a great difference whether the pressure drop of a heating surface differs from the design value, because the flue gas blowers are almost always amply designed. The arrangement of finned tube heating surfaces in heat recovery boilers behind gas turbines results in a pressure drop which directly influences the capacity, the efficiency and the performance of the machine, whereas the entirety or almost the entirety of the heating surface often consists of finned tubes. In combination with smoke gas scrubbers, finned tube heater exchangers are often arranged as a heat-shifting system, for example for reheating flue gases in front of a flue. In this case the available pressure drop is often minimal and the pressure drop of the heat exchanger has to be able to be calculated exactly. The number of useful measurement values for the pressure drop coefficient of finned tubes is, however, much smaller than those for the heat transfer coefficients, and thus the reliability of the calculation equations is lower. Furthermore, discrepancies may be observed between specific pressure drop measurements, which are carried out mostly at ambient temperatures, and the pressure drop measurements, which are taken in the course of a heat transfer test run. The following considerations are intended to contribute toward a solution of the problems that occur.

### 5.2 Problems with test result evaluation

Both heat transfer and pressure drop measurements were carried out at the same time on spiral finned tube bundles by ITE. The pressure drop coefficients were obtained not only at different Reynolds numbers, but also at different temperatures within the gas stream, the boundary layer region and at the wall. When the pressure drop coefficients were plotted above the Reynolds number in a diagram, another curve often resulted than the one described in the literature [1,2,3] or a scatter-plot, without any recognizable ordering principle, was obtained. According to the literature cited, pressure drop coefficients decrease by  $Re^{-0.25}$  with a rising Reynolds number. For measurements with heat transfer they either rise with the Reynolds number or remain constant. It should be mentioned that in our tests of variation of the Reynolds number not only gas velocity but also gas temperature was changed. Specifically, gas temperature had to be increased to obtain low Reynolds numbers in order to avoid measuring instrumentation error

and for precise measurement of small gas flow and small pressure differences. Whenever these discrepancies were identified, pressure drop measurements were repeated without cooling of the tubes, which means without heat transfer and at a little above ambient temperature. In this case a typical curve for pressure drop coefficient was obtained comparable to the literature, however with a quantitatively changed value of the pressure drop coefficient. After this, a measurement series with heat transfer was carried out for the last tube arrangement, which in this case substantiated previous results for pressure drop. Gross measurement errors can therefore be ruled out. The question thus arises as to how pressure drop measurements with heat transfer can be correlated with such measurements without heat transfer. In order to consider the phenomenon described, the available literature was reviewed and the following was ascertained:

1. In Zukauskas' book about finned tubes [3] it is noted that pressure drop coefficients were measured at ambient temperature or a little above this and without any heat transfer. The equations which were developed from this attained further publicity through inclusion in the HEDH [2], which was created in cooperation with Zukauskas.
2. In the case of pressure drop at smooth pipe bundles, HEDH [2] distinguishes between a fluid flow with the same temperature in the boundary layer region as in the free flow and one with a different temperature, as occurs during heat transfer. In the latter case, a correction factor for the pressure drop coefficient is introduced, by taking the ratio of dynamic viscosity at mean flow temperature to the viscosity at boundary layer temperature to the power of  $n$ .

$$\frac{\xi_a}{\xi_W} = (\eta_{\vartheta_{gm}}/\eta_{\vartheta_{Gr}})^n \quad (137)$$

The exponent  $n$ , according to HEDH [2], depends on the Reynolds number in that  $n$  for a small Reynolds number of 500 is approx. 0.4 and at  $Re = 5 \cdot 10^3$  becomes almost 0.

3. Mirkovich [5] also reports that pressure drop measurements were taken at ambient temperature or a little above (this minor heating was apparently caused by the fans).

If test runs with same geometrical arrangement and same Reynolds number exist for both cases, i.e. with heat transfer and such without heat transfer, the exponent  $n$  can be determined according to following equation:

$$\xi_a/\xi_W = (\eta_{\vartheta_{gm}}/\eta_{\vartheta_{Gr}})^n \quad (138)$$

If one carries out the evaluation above with the values measured by ITE, one obtains exponents for  $n$  which are almost always  $> 1$  and reach values of  $0.9 - 4.5$ ; see figure(74).

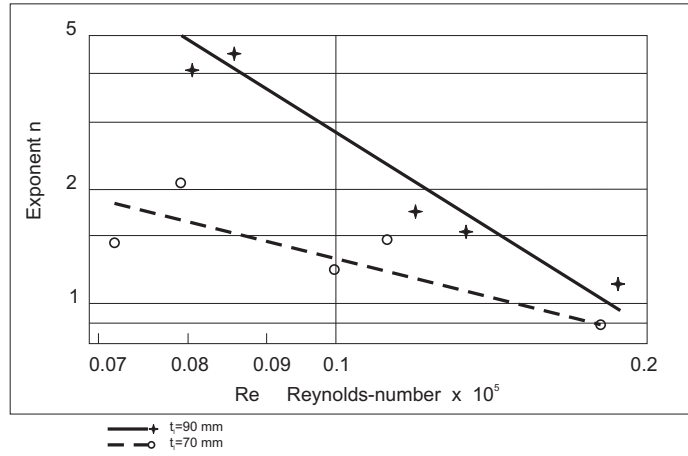


Figure 74: **Exponent  $n$  according to equation (138), tube diameter 38 mm, 150 fins per m (16 x 1 mm),  $t_q=85\text{mm}$**

Since this method is thus not satisfactory, Scholand's [13] was tested. Scholand postulates that those pressure drop coefficients measured during adiabatic experiments and those with heat transfer are equal, if the ones with heat transfer are calculated with the density at gas inlet temperature.

Up to now pressure drop coefficients  $\xi_m$  have been calculated with the density  $\rho_m$  at the mean gas temperature and  $w_E$  using  $\rho_m$  in the narrowest cross-section:

$$\xi_m = 2 \Delta p / (\rho_m w_E^2) \quad (139)$$

$$\vartheta_{gm} = (\vartheta_{g1} + \vartheta_{g2}) / 2 \quad (140)$$

$$\rho_m = \rho_0 273.2 / (273.2 + \vartheta_{gm}) \quad (141)$$

When the gas cools  $\rho_1 < \rho_m$ , thus  $\xi > \xi_m$ :

$$\rho_1 = \rho_m (273.2 + \vartheta_{gm}) / (273.2 + \vartheta_1) \quad (142)$$

See purpose figure (75) on this: measurement values converted according to Scholand's method [13] are signified by the symbol +. The conversion does not completely result in the pressure drop coefficients measured without heat transfer, rather it tends to reveal only values in the middle between those with and without heat transfer.

After converting the values, by using  $(273.2 + \vartheta_{gm})/(273.2 + \vartheta_{Wa})$ , i.e. with the ratio of the absolute average gas temperature to the absolute average wall temperature, pressure drop coefficients without heat transfer are obtained; see figure (75).

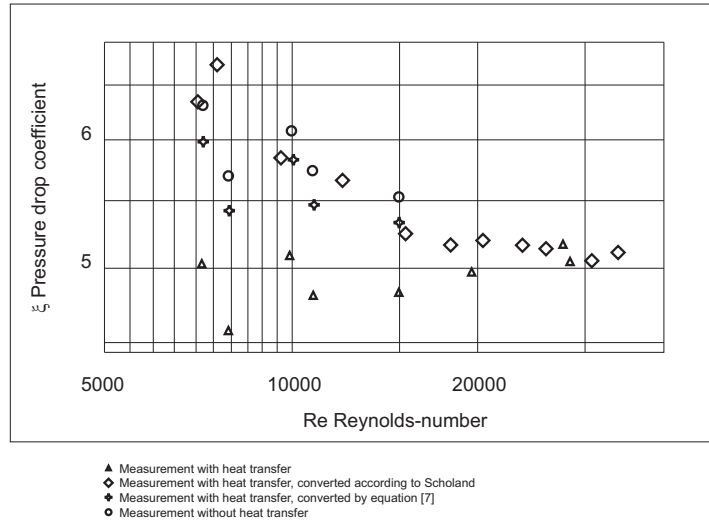


Figure 75: **Pressure drop measurements with and without heat transfer. Tube diameter 38 mm , fins 16 x 1 mm,  $t_q=85$  mm. Eq.(7) in the figure is identical with equation (143)**

If the density  $\rho$  (referred to as  $\rho_m$  in equation (141)) is calculated with the mean wall temperature  $\vartheta_{Wa}$  of the finned tubes, often a good correspondence is obtained between the pressure drop measurements with and without heat transfer; figure (76). The results of measurement with heat transfer, calculated with  $\rho(\vartheta_{gm})$ , are represented by the symbols + and x. These values, which have been converted according to equation (143), are represented by  $\triangle$  and  $\square$ . These fit together well with the measurement values without heat transfer to produce a curve.

The correction factor, according to HEDH [2], Eq.(1)  $\eta_{\vartheta_{gm}}/\eta_{\vartheta_{Gr}}$  can also be approximately replaced by the factor  $\vartheta_{gm}/\vartheta_{Gr}$ , since the dynamic viscosity  $\eta$  is almost a linear function of the gas temperature. This relates the proposals for the conversion of the pressure drop coefficients for smooth pipe bundles made by HEDH to Scholand's for finned tube bundles. According to our own test cases, however, better correspondence can be observed by using the temperatures  $\vartheta_{gm}$  and  $\vartheta_{Wa}$ . It is therefore suggested to convert the pressure drop coefficient, which is determined from tests with heat transfer, using the factor  $(\vartheta_{Wa} + 273.2)/(\vartheta_{gm} + 273.2)$ . The pressure drop coefficients from calculation equations, which are based on tests without heat transfer, would have to be converted using the reciprocal.

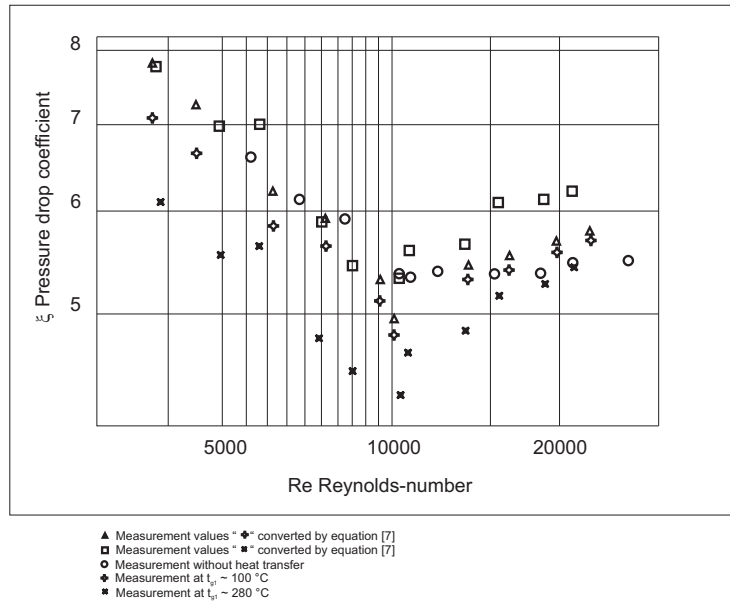


Figure 76: Correlation of pressure drop measurements at different gas temperatures. Tube diameter 31.8 mm, 200 fins per m, 15 x 1 mm. Eq.(7) in the figure is identical with equation (143)

$$\xi_W/\xi_a = (\vartheta_{Wa} + 273.2)/(\vartheta_{gm} + 273.2) \quad (143)$$

### 5.3 Evaluation of pressure drop for staggered finned tube bundles

The pressure drop for finned tube bundles is calculated in a manner similar to that for smooth tube bundles according to the equation

$$\Delta p = \xi \frac{\rho}{2} w_E^2, \quad (144)$$

which specifies the pressure drop per tube row. For the evaluation of pressure drop in a tube bundle, equation (144) has to be multiplied by the number of consecutive tube rows. The pressure drop is calculated using the velocity  $w_E$  in the narrowest cross-section, the mean density of the gas in the bundle and the pressure drop coefficient  $\xi$ . The pressure drop coefficient  $\xi$  depends on both the Reynolds number of the gas flow in the tube bundle and on the geometry of the finned tube bundle. The coefficient can be ascertained using equations derived from test cases done on finned tubes. Although many heat transfer measurements for finned tubes have been performed, only few pressure drop measurements have been recorded.

### 5.3.1 Equations for pressure drop in staggered finned tube bundles

While 12 different equations were able to be found for heat transfer with staggered arrays, only 8 different relations can be presented for the pressure drop coefficient.

1. FDBR Handbuch 1980 [10]. First of all, a hydraulic diameter is determined:

$$d_h = (a_{Ri} d_q + a_{Ko}(d_A + 2h) + a_{Ro} d_A) / (a_{Ri} + a_{Ko} + a_{Ro}) \quad (145)$$

where

$$d_q = \sqrt{t_R a_{Ri} / 2} \quad (146)$$

$a_{Ri}$  is the surface area per m tube of the fin flanks,  $a_{Ko}$  of the fin tops and  $a_{Ro}$  of the bare tube. The geometrical measurements of the fin tube bundle are accounted for in the factors  $E1$  and  $E2$ . Any effect on the pressure drop coefficient is attributed to the transverse tube pitch, while the longitudinal pitch has no effect and therefore does not occur in  $E1$  and  $E2$ .

$$E1 = (t_q - d_A) / (t_R - s_R) \quad (147)$$

$$E2 = d_h / (t_q - d_A) \quad (148)$$

The Reynolds number  $Re$  is derived from the hydraulic diameter  $d_h$  as well as from the velocity in the narrowest cross-section  $w_E$ .

$$Re = \frac{w_E d_h}{\nu(\vartheta_{gm})} \quad (149)$$

The kinematic viscosity  $\nu$  is to be selected at the mean gas temperature  $\vartheta_{gm}$  according to calculation procedures. The pressure drop coefficient is then calculated for a single tube row.

$$\xi = 1.463 (E1 + 1)^{0.7} E2^{0.9} Re^{-0.245} \quad (150)$$

According to FDBR, it is assumed that the pressure drop coefficient is independent of the number of consecutive tube rows. The pressure drop for  $n_R$  tube rows is calculated by multiplying equation (150) with  $n_R$ .

## 2. HEDH(Heat Exchanger Design Handbook [2])

The Reynolds number is derived using the diameter of the bare tube.

$$Re = \frac{w_E d_A}{\nu(\vartheta_{gm})} \quad (151)$$

The pressure drop coefficient for Reynolds numbers in the range of  $10^4 < Re < 10^5$  is

$$\xi = 13.1 \left(1 - \frac{t_R}{d_A}\right)^{1.8} Re^{-0.25} \left(\frac{t_q}{d_A}\right)^{-0.55} \left(\frac{t_l}{d_A}\right)^{-0.50} \left(1 - \frac{h}{d_A}\right)^{-1.4} \quad (152)$$

Attention has to be paid in applying the formula, since in HEDH [2] the constant is given with 13.1, in Stasiulevicius [3], however, misleadingly with half the value, i.e. 6.55! In addition, the equation above indicates the pressure drop coefficient for only a single tube row. The influence of the tube row number is mentioned in the previous section. For higher Reynolds numbers ( $10^5 < Re < 10^6$ ) the following holds:

$$\xi = 0.74 \left(1 - \frac{t_R}{d_A}\right)^{1.8} \left(\frac{t_q}{d_A}\right)^{-0.55} \left(\frac{t_l}{d_A}\right)^{-0.50} \left(1 - \frac{h}{d_A}\right)^{-1.4} \quad (153)$$

The pressure drop coefficient for this range of  $Re$  is independent of the Reynolds number. A determination of an intersection point for the equation given above with equation (152) results in a fixed and geometry-independent value for the Reynolds number at  $Re = 0.982 \cdot 10^5$ . It must be mentioned that in reality no sharp bend occurs when the pressure drop coefficient is plotted above the Reynolds number, rather all values gradually converge in a constant. The sharp bend only appears because a relatively simple equation for the pressure drop coefficient intersects a horizontal axis-parallel straight line.

## 3. Mirkovics [5]

The Reynold number for the calculation of pressure drop is derived according to Mirkovics' method using an hydraulic diameter which is calculated using the free volume in the tube bundle and the heating surface, per meter tube in both cases.

$$d_{hMi} = 4 \frac{t_q t_l - d_A^2 \frac{\pi}{4} - (d_A + h) h \pi s_R / t_R}{A_{tot}} \quad (154)$$

$$Re_{Mi} = \frac{w_E d_{hMi}}{\nu(\vartheta_{gm})} \quad (155)$$

The pressure drop coefficient is then:

$$\xi = 3.96 \left(\frac{t_q - d_A}{d_A}\right)^{0.14} \left(\frac{t_l - d_A}{d_A}\right)^{-0.18} \left(1 - \frac{s_R}{t_R}\right)^{-0.20} Re_{Mi}^{-0.31} \quad (156)$$

#### 4. ESCOA Spiro Gills [12]

The pressure drop coefficient has been converted from the relation given in [12], in American notation, for the Fanning friction factor into the more well known European notation. The Fanning friction factor  $f_f$  is generally known as:

$$f_f = \frac{\xi}{4} \quad (157)$$

For  $\xi$ , the equation

$$\xi = 4 C_2 C_4 C_6 \left(\frac{D}{d_A}\right)^{0.5} \quad (158)$$

is obtained.  $D$  in this case represents the diameter above the fins, which is  $d_A + 2h$ . The constants  $C_2$ ,  $C_4$  and  $C_6$  account for the influence of the Reynolds number and the finned tube geometry.

$$C_2 = 0.07 + 8.0 Re^{-0.45} \quad (159)$$

Re also is derived using  $d_A$

$$C_4 = 0.11 \left(0.15 \frac{t_q}{d_A}\right)^{(-0.7(\frac{h}{t_R - s_R})^{0.20})} \quad (160)$$

$$C_6 = 1.1 + (1.8 - 2.1 e^{-0.15 n_R^2}) (e^{-2\frac{t_l}{t_q}}) - (0.7 - 0.8 e^{-0.15 n_R^2}) (e^{-0.6\frac{t_l}{t_q}}) \quad (161)$$

The coefficient  $C_4$  represents the influence of  $\frac{t_q}{d_A}$  and of  $\frac{t_R - s_R}{h}$ , whereas the influence of  $\frac{t_q}{d_A}$  upon pressure drop is higher with small fin pitches and vice versa.

The coefficient  $C_6$  accounts for the influence of transverse and longitudinal tube pitch, as seen in  $\frac{t_l}{t_q}$ , and of the number of tube rows  $n_R$ .

#### 5. M. Brockmann: Druckverlust bei Stroemungen quer zu Rippenrohrbuendeln. VDI Progress Report, Series 6, No. 431 [38]

More recent, extensive measurements of pressure drop in finned tube bundles for both in-line and staggered arrangements are presented. The measurements were carried out in a channel with a cross-section of approx. 0.45 m x 0.45 m, with 6 or 7 tube rows in consecutive order. The channel was operated at ambient temperature and the air is sucked in through the test apparatus by a fan. Only tubes with a diameter of 25 mm and spiral fins of different pitches and heights were used. The fins were not welded to the tubes but merely pressure-wound around them. The pitches of the tubes in the bundle were varied, both for in-line and staggered arrangement. The results of the measurement series have been presented in form of equations:

For Reynolds numbers  $1000 < Re < 8000$

$$\xi = z_0 \sqrt{\left(\frac{1600}{Re}\right)^2 + \left(\frac{Re}{1600}\right)^{m_0}} \quad (162)$$

and for Reynolds numbers  $10000 < Re < 10^5$

$$\xi = z_1 \left(\frac{Re}{10000}\right)^m \quad (163)$$

For Reynolds numbers ranging from 8000 to 10000, the pressure drop coefficients  $\xi$  are interpolated linearly between equation (162) and equation (163). For this equation the Reynolds number is derived using the flooding length  $l = \frac{\pi}{2} \sqrt{d_A^2 + h^2}$  and the velocity of free flow  $w_0$ .  $m_0$  and  $m$  are constants, while  $z_0$  and  $z_1$  are related in a complex manner to up to 24 constants which are different for in-line and staggered arrangements. For the purpose of varying any geometrical value of the finned tube bundle, this system of equations is not readily transparent. However, it supplies comparable values for pressure drop in comparison with other relationships. Yet one major exception exists: the pressure drop coefficient according to VDI 431 [38], which depends on fin height  $h$ , has at  $h \approx 0.36 d_A$  a distinct minimum in each case which amounts to only approx. 1/3 to 1/4 of neighboring pressure drop coefficient values, as seen in figure (77).

A comparable progression of pressure drop coefficient values appears neither in any other pressure drop equation cited here nor could one be found through our own measurements. These also include a finned tube with a diameter of 44.5 mm and fins with 16 mm height, which is  $h = 0.36 d_A$ . A comparison of the experimental values for the 44.5 mm tube with finned tube diameters of 38 mm and 31.8 mm and fin height of 15 mm shows no decrease in pressure drop coefficient. Care should thus be taken when using this low pressure drop coefficient in the case of finned tubes with  $h \approx 0.36 d_A$ .

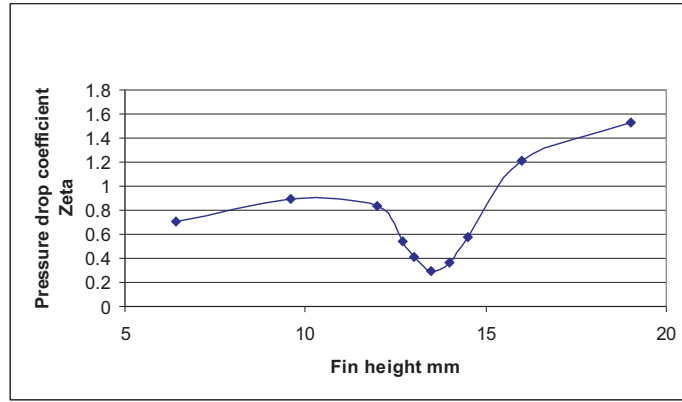


Figure 77: **Pressure drop coefficient in dependence of fin height according to VDI 431 [38]. Tube diameter 38 mm, 150 fins per m,  $t_q = 85$  mm,  $t_1 = 75$  mm, staggered arrangement**

6. Pressure drop for finned tubes (with smooth fins) in staggered arrangement, according to J. Vampola [14]

Vampola specifies the following equation for the pressure drop coefficient for finned tube bundles (with smooth fins) in staggered arrangement:

$$\xi = 1.463 Re_h^{-0.245} \left( \frac{t_q - d_A}{t_R - s_R} + 1 \right)^{0.7} \left( \frac{t_q - d_A}{d_A} \right)^{-0.9} \left( \frac{d_h}{d_A} \right)^{0.9} \quad (164)$$

Here the Reynolds number is also derived using the hydraulic diameter according to Vampola, equation (69). Vampola's formula is very similar to the equation for the pressure drop coefficient according to FDBR (150) and only written differently. Yet Vampola's equation (69) for hydraulic diameter is different from that of FDBR (145). The underlying difference is that, in the case of FDBR, the heating surface of the fin is accounted for separately, using the particular diameter  $d_A + 2h$ , in the equation for  $d_h$ , while Vampola includes it in the heating surface  $A_{Ripp}$  with its diameter. The difference in pressure drop coefficient is insignificant.

7. Pressure drop calculation according to A. Nir [18]

Nir applies the usual approach for pressure drop using  $Re^{-0.25}$ . He expresses the relationship of finned tube and bundle geometry using the parameter  $W$  as well as  $R_d$ , which were already used for heat transfer (see the equation (65)).

$$\xi = 2.12 Re_d^{-0.25} W^{0.45} (2.08 - 0.83 R_d) \quad (165)$$

The parameter  $R_d$  indicates the ratio of the diagonal flow cross-section to the frontal flow cross-section.

8. Pressure drop calculation for finned tube bundles in cross-flow, according to VDI Waermeatlas, 8th Edition 1997, Bl.Ldb1-4 [33]

These formulas are similar to the HEDH equations [2]. They also make use of the diameter of the bare tube and the velocity in the narrowest cross-section for calculation of the Reynolds number.

The formula is valid for a Reynolds number within the range of  $10^2 < Re < 10^3$ :

$$\xi = 290 Re_d^{-0.7} e_q^{-0.55} e_l^{-0.5} \left(1 - \frac{t_R}{d_A}\right)^{1.8} \left(1 - \frac{h}{d_A}\right)^{-1.4} \quad (166)$$

For a Reynolds number in the range of  $10^3 < Re < 10^5$  the following then applies:

$$\xi = 13 Re_d^{-0.25} e_q^{-0.55} e_l^{-0.5} \left(1 - \frac{t_R}{d_A}\right)^{1.8} \left(1 - \frac{h}{d_A}\right)^{-1.4} \quad (167)$$

For even higher Reynolds numbers, i.e.  $10^5 < Re < 1.410^6$ , the pressure drop coefficient becomes constant and independent of the Reynolds number:

$$\xi = 0.74 e_q^{-0.55} e_l^{-0.5} \left(1 - \frac{t_R}{d_A}\right)^{1.8} \left(1 - \frac{h}{d_A}\right)^{-1.4} \quad (168)$$

$e_q$  in this case is  $e_q = \frac{t_q}{d_A}$  and  $e_l$  is  $e_l = \frac{t_l}{d_A}$ . As one can see, the formulas for higher Reynolds numbers are virtually identical with the HEDH formulas, only the range of validity has been altered partially.

### 5.3.2 Discussion of cited pressure drop equations

Among all of the arrangements considered, the pressure drop coefficients calculated according to FDBR, HEDH and ESCOA are situated relatively closely together as compared to the Mirkovics' values. These values are only about half as high. Dependence is calculated for the individual factors using the data listed below by way of example and discussed:

Tube diameter	$d_A$	=	38	mm
Fin thickness	$s_R$	=	1	mm
Fin pitch	$t_R$	=	6.67	mm
Transverse pitch	$t_q$	=	85	mm
Longitudinal pitch	$t_l$	=	75	mm
No. of tube rows	$n_R$	=	8	
Velocity of gas in the narrowest cross-section	$w_E$	=	8	m/s
Temperature of gas	$\vartheta_G$	=	100	°C

1. Influence of tube diameter  $d_A$ : When considering the influence of the tube diameter on the pressure drop coefficient, two cases need to be distinguished: first, the tube diameter is varied at constant gas velocity in the narrowest cross-section, in which case the Reynolds number also varies since it is based on  $d_A$ ; or second, examination is done using a constant Reynolds number. As seen by comparing figure (78) ( $w_E = \text{const.}$ ) and figure (79), the difference between these two cases is not very significant. The pressure drop coefficient generally increases with tube diameter. Only with HE and WA does the pressure drop coefficient initially decline somewhat, for small diameters less than 32 mm, and then increases. In the case of constant velocity  $w_E$ , the increase in pressure drop coefficient proportional to diameter  $d_A$  coincides with a decrease in pressure drop coefficient with increasing Reynolds number, resulting in a smaller increase. Among Brockmann's values, an anomaly is evident at  $h = 0.36 d_A$ .

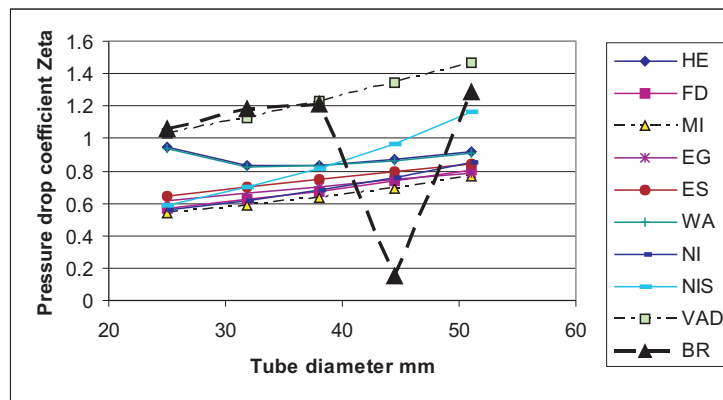


Figure 78: **Influence of tube diameter upon the pressure drop coefficient at constant velocity in the narrowest cross-section (staggered arrangement)**

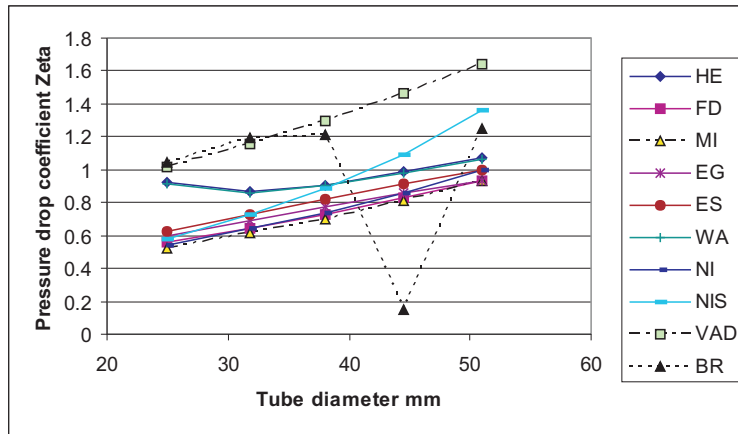


Figure 79: **Influence of tube diameter upon the pressure drop coefficient at constant Reynolds number (staggered arrangement)**

2. Influence of tube diameter with varying transverse pitch:

When analyzing different tube diameters, transverse pitch should be dimensioned according to the largest tube diameter. This should be done in a such way that there is enough space between the fins, whereas the transverse pitch is too great for smaller tubes and heat transfer is not optimal. It is helpful to choose a transverse pitch value ensuring a constant distance between fin flanges, for example 5 mm. In figure (80), the influence of tube diameter is shown under this condition and for  $w_E = \text{const}$ . The pressure drop coefficient rises only very little with tube diameter. According to the HE equation, it declines at diameters smaller than 38 mm and then remains constant. The pressure drop coefficient according to Brockmann declines with increasing tube diameter, with an anomaly at  $h = 0.36 d_A$ .

The pressure drop coefficient increases slightly with tube diameter at constant Reynolds numbers. With HE, the pressure drop coefficient declines first and then increases again. With Brockmann, the pressure drop coefficient increases somewhat, while displaying the anomaly already mentioned in between (figure (81)).

3. Influence of fin thickness  $s_R$ :

According to FD and MI, as well as EG and ES, the pressure drop coefficient increases moderately with fin thickness. According to HE, on the other hand, it remains constant. However, this increase in fin thickness of 0.7 mm to 1.0 mm or 1.0 mm to 1.3 mm is only approx. 3% of the pressure drop coefficient for FD and only 2% for other relations. The latent uncer-

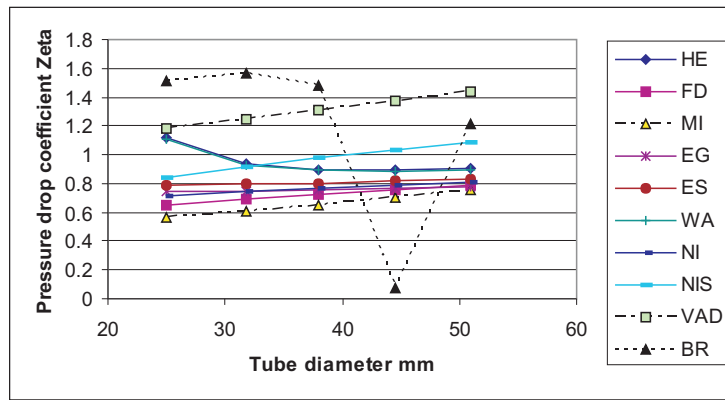


Figure 80: Influence of tube diameter upon the pressure drop coefficient at constant velocity in the narrowest cross-section and adapted varied transverse pitch (staggered arrangement)

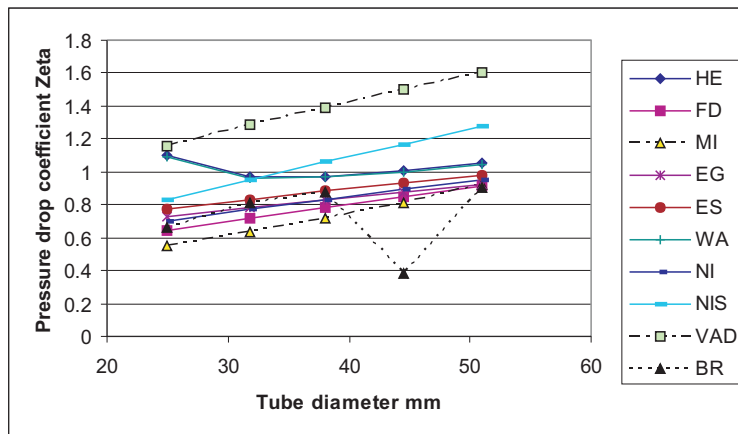


Figure 81: Influence of tube diameter upon the pressure drop coefficient at constant Reynolds number and varied transverse pitch (staggered arrangement)

tainty of pressure drop coefficients is at least  $\pm 15\%$ . Thus, the amount of error seen with HE, resulting from neglecting the influence of  $s_R$ , would still be acceptable. The influence of fin thickness is more distinct according to Brockmann [38]. The pressure drop coefficient increases by approximately 4% with an increase in fin thickness from 1 mm to 1.3 mm, according to figure (82).

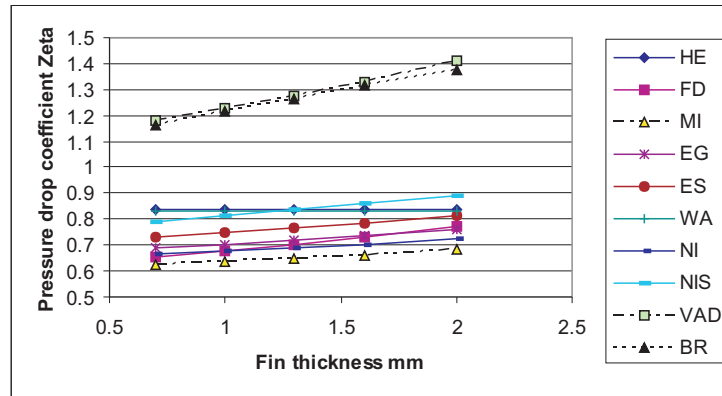


Figure 82: Influence of fin thickness upon the pressure drop coefficient (staggered arrangement)

It should be mentioned that the calculation equations with regard to the influence of fin thickness are based only on measurements by Mirkovics. In these tests, fin thickness was varied from 1.27 mm to 1.57 and up to 2.03 mm for otherwise identical finned tube geometries. From these three measurement points (Symbol  $\square$ ), shown in figure (83) it becomes apparent that the pressure drop coefficient declines with greater fin thickness. A diagram with pressure drop coefficient plotted above the parameter  $\frac{t_R - s_R}{h}$  shows that this variation is too small for any clear result; figure (83). A sufficiently wide margin was achieved for the parameter stated above by the addition of further measurement points (Symbol  $\diamond$ ), whereby  $t_R$  and  $h$  also change, and a different result was obtained. In the case of other measurements, the fin thickness was not changed or this was not documented, except for the new measurements by Brockmann [38] mentioned above.

#### 4. Influence of the fin pitch $t_R$ :

Decreasing for small fin pitches, the influence of  $t_R$  upon pressure drop seems to be better captured by HE than by FD, EG and ES. Pressure drop declines with increasing fin pitch more or less according to the shape of a hyperbola. For FD, EG and ES, the decline continues in a linear way and in the same way for Mirkovics, as seen in figure (84). The Brockmann's

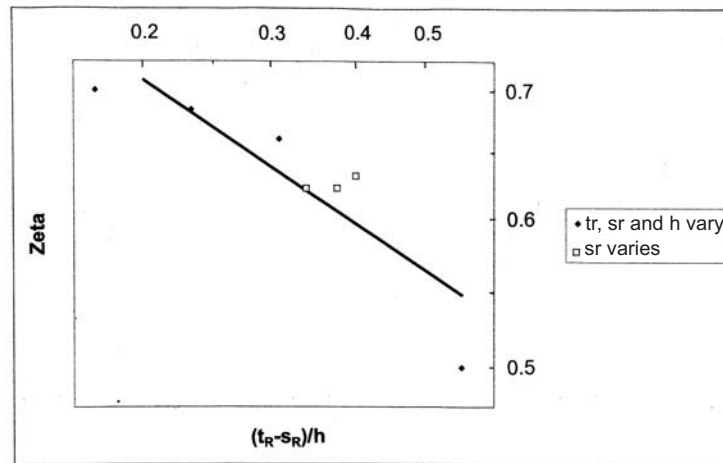


Figure 83: Influence of fin thickness upon the pressure drop coefficient according to measurements by Mirkovics

relation [38] does not correlate well with the others, because the pressure drop coefficient first rises and then starts to decline again (through changing the fin pitch from 3.6 mm to 5 mm), whereas the slope increases even further for a greater fin pitch.

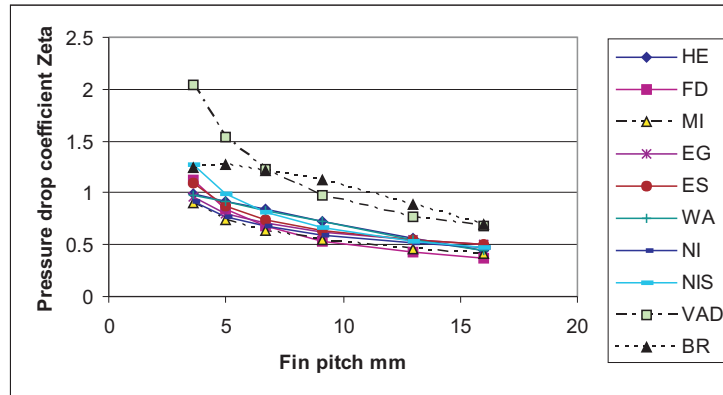


Figure 84: Influence of fin pitch upon the pressure drop coefficient (staggered arrangement)

5. Influence of fin height  $h$ :

The pressure drop coefficient increases with  $h$  according to all relations mentioned above. According to the HE equation, the increase for fin heights  $> 16$  mm becomes so steep so as to assume that the range of validity of the equation has been exceeded. See figure (85) on this, which shows that

the pressure drop coefficient according to Brockmann, in contrast, [38] rises more with fin height than with the remaining formulas. On the other hand it also shows a very distinct minimum at  $h \approx 0.36 d_A$ , which does not occur with any other relation.

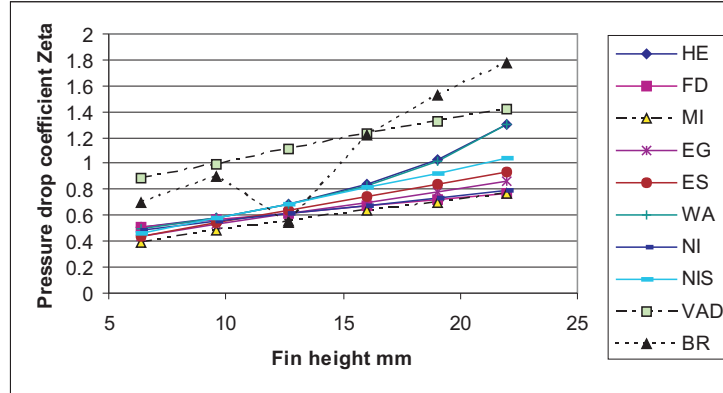


Figure 85: Influence of fin height upon the pressure drop coefficient (staggered arrangement)

6. Influence of fin height  $h$  and transverse pitch  $t_q$ :

When only the influence of fin height is considered, transverse pitch should be chosen in such a way that even the tallest fins can be accommodated. Such an arrangement is, however, unrealistic for shorter fins, since free space is wasted in this case. The influence of a changing fin height is examined, whereby the transverse pitch is varied so that the distance between fin flanges is constant, e.g. at  $t_q = d_A + 2h + 5$  mm. The result in figure (86) shows that, in comparison with figure (85), the pressure drop coefficient increases with smaller fin heights, with the increase becoming less sharp with decreasing fin height  $h$ .

7. Influence of transverse pitch  $t_q$ :

For staggered finned tube arrangements, the pressure drop coefficient decreases with increasing transverse pitch for all equations. This decline is very small according to the Mirkovics' relationship and is almost imperceptible, as figure (87) shows. Brockmann's equation [38], on the other yields an above-average decline.

8. Influence of longitudinal pitch  $t_l$ :

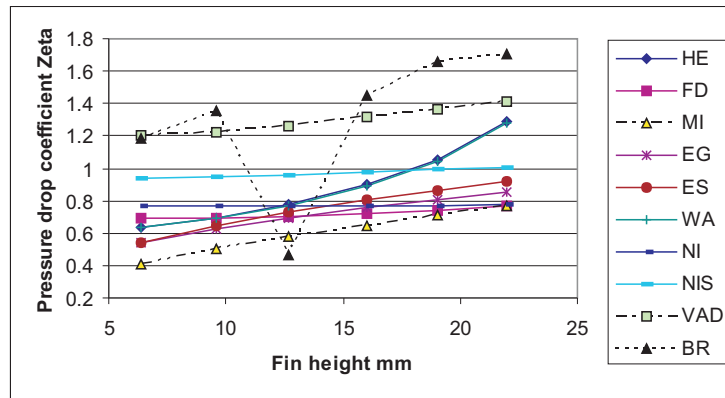


Figure 86: Influence of fin height and varied transverse pitch upon the pressure drop coefficient (staggered arrangement)

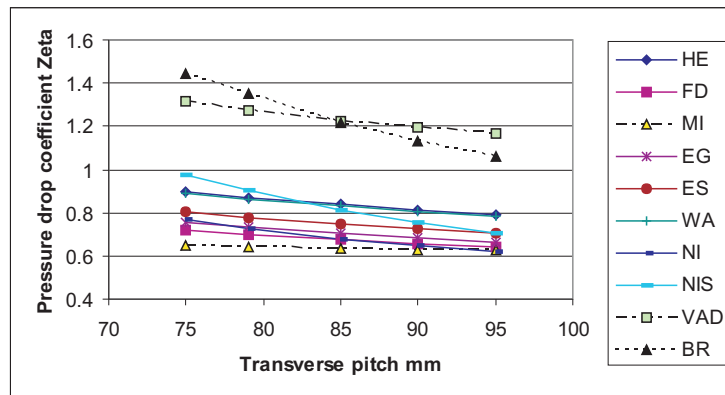


Figure 87: Influence of transverse pitch upon the pressure drop coefficient (staggered arrangement)

According to FD [10] and Nir [18], there is no influence of longitudinal pitch on the pressure drop coefficient. According to other relations it declines with increasing longitudinal pitch, as emerges from figure (88). This confirms the measurement values obtained by ITE in figure (91) and figure (92).

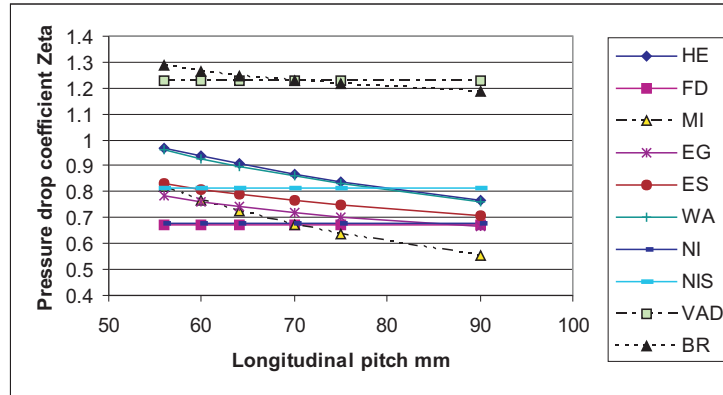


Figure 88: Influence of longitudinal pitch upon the pressure drop coefficient (staggered arrangement)

9. Influence of the number  $n_R$  of consecutive tube rows:

Except for EG and ES [12] and Brockmann [38], all relationships concur that no influence of the tube row number on the pressure drop coefficient exists for staggered tube arrangements. According to EG and ES, the pressure drop coefficient, as seen in equations and diagrams, is clearly influenced by the number of tube rows  $\leq 4$ : the pressure drop coefficient increases with a decreasing number of tube rows by about 20% for  $\frac{t_l}{t_q} > 0.68$ , but declines by about 20% for  $\frac{t_l}{t_q} < 0.68$ . According to Brockmann, the pressure drop coefficient decreases with fewer tube rows. Several series of experiments with 8, 6, 4 and 2 tube rows have been carried out at ITE, a definite influence of the number of tube rows on the pressure drop coefficient could not, however, be observed.

10. Triangular pitches:

The pressure drop coefficient for triangular pitches decreases with increasing pitch according to all cited formulas; see figure (89). Since heat transfer remains approximately constant according to most of the formulas, no disadvantage is incurred when, due to construction reasons (e.g. feasible tube bending radii), the pitch is somewhat greater than the minimum value. In

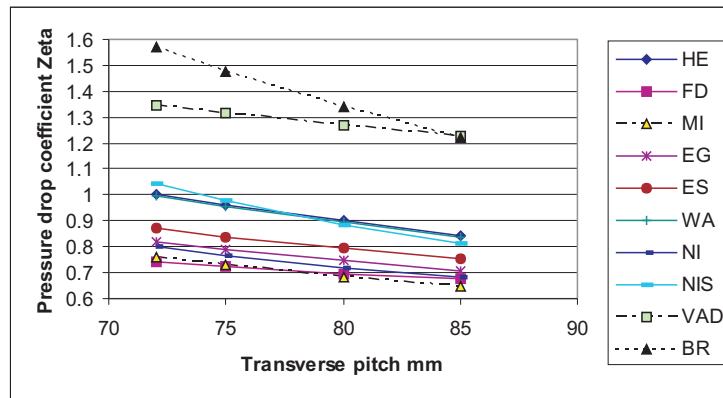


Figure 89: Influence of magnitude of triangular pitch upon the pressure drop coefficient

this way the quotient of pressure drop through heat transfer improves, while the specific power of the heat exchanger decreases slightly.

Comparison with the measurements performed by ITE: Our own measurements do not exhaustively cover all influences listed above since they mainly concern the use of finned tubes in steam generator construction. Measurements exist only for the influence of  $t_R$ ,  $t_l$  and  $n_R$ .

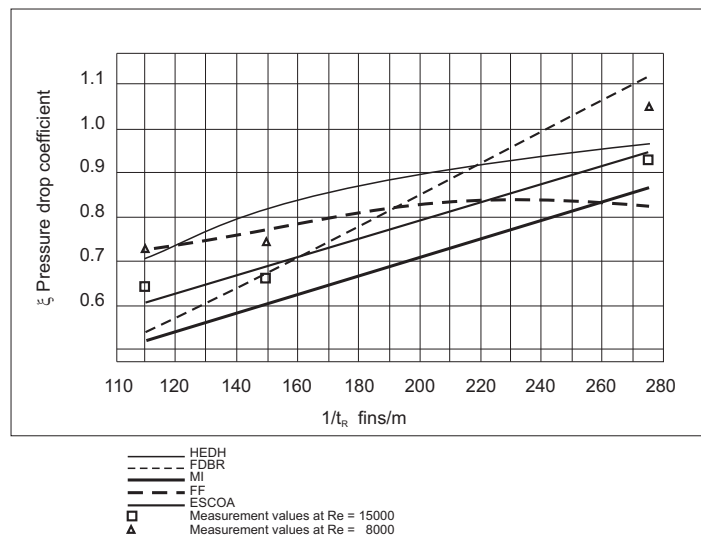


Figure 90: Influence of fin pitch upon the pressure drop coefficient: comparison of measured values and calculation. Tube diameter  $d_A=38$  mm, fins  $16 \times 1$  mm

For a variation of fin pitch  $t_R$ , an influence of the same type as described in the

equations can be seen in figure (90) and even of approximately the same amount as predicted. Three different fin pitch values of 110, 150 and 276 fins per m, with the same geometrical measurement of bare tubes, were analyzed by ITE. The influence of longitudinal pitch could be examined for: a tube diameter of 31.8 mm with a constant transverse pitch of 75 mm and three different longitudinal pitches of 60, 70 and 80 mm; as well as for bare tubes with a diameter of 38 mm, a transverse pitch of 85 mm and three longitudinal pitches of 70, 80 and 90 mm. The results, presented in figures (91) and (92), do not confirm the FDBR equation [10], assuming that longitudinal pitch has no influence on pressure drop, nor do they entirely concur with the assumption that pressure drop decreases with increasing longitudinal pitch (HE [2], Mirkovics [5] and EG [12]). The pressure drop coefficients calculated according to the equations given above are presented in figure (88).

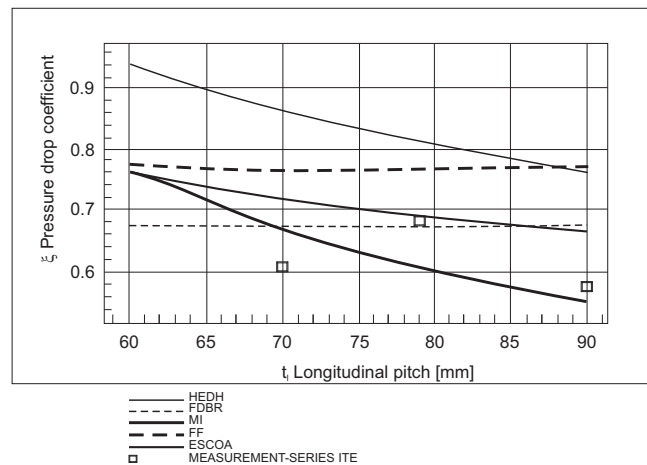


Figure 91: **Influence of longitudinal pitch upon the pressure drop coefficient. Comparison of measured values and calculation for  $d_A=31.8$  mm**

In figure (93), the pressure drop coefficient is plotted in dependence of the Reynolds number. The results of the calculation, according to HE, FD and EG, lie quite close together, whereas the results according to MI are considerably lower. The results according to Brockmann [38] meanwhile, represent the highest values by far.

It is to be noted for the characteristics of the pressure drop coefficient in dependence of the Reynolds number that the relationships of FD, MI and EG assume a constant decline in pressure drop coefficient with an increase in Reynolds number. HE and Stasiulevicius [3] predict a constant pressure drop coefficient above a certain Reynolds number of approx.  $10^5$ . This point of discontinuity in the characteristics of the pressure drop coefficient depends on the geometrical data of the finned tube bundle (see on this the diagrams of the measurement results

by Zukauskas [3]). Some of our own pressure drop measurements indicate such a discontinuity, as do measurements by Scholz [16].

### 5.3.3 Recommendation for a calculation to predict pressure drop at staggered finned tube bundles in cross-flow

The explanations given above reveal weak points in each of the four most suitable equations, i.e. HE, FD, EG and MI. With HE, the influence of fin thickness, which is not very significant, is not considered. In the FD equation the influence of longitudinal pitch is neglected. In the case of EG, the influence of the number of tube rows is apparently somewhat overestimated. While these criticisms do not apply to Mirkovics' formula, in this case the influence of transverse pitch is not appropriately described.

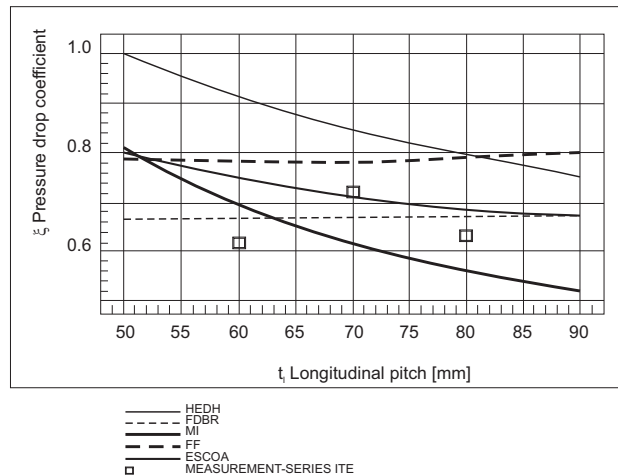


Figure 92: Influence of longitudinal pitch upon the pressure drop coefficient. Comparison of measured values and calculation for  $d_A=38$  mm

Furthermore, since it is not yet certain how the design of the finned tubes or the way they are manufactured affects the pressure drop coefficient, one should exercise caution when using the formulas.

The FDBR formula, based on the work of Vampola [14], represents an average for a large number of different finned tube designs. The HEDH formula arose from the work of Stasiulevicius and Skrinška [3], where only tubes with annularly milled fins of trapezoid cross-section are used. It cannot be presupposed that these finned tubes behave in the same way as finned tubes with welded spiral fins. While Mirkovics [5] also used spiral fins, he does not mention anything in regard to the way they were manufactured.

For an equation with a higher degree of accuracy for the pressure drop coefficient in finned tube bundles, one would presumably have to alter or supplement each of the formulas.

In the HEDH formula, the influence of fin thickness could be accounted for by an additional term for instance, whereas the constant would have to be adjusted accordingly.

The fact that no influence of fin thickness  $s_R$  upon the pressure drop coefficient is mentioned in the HEDH formula may probably be attributed to the experiments by Stasiulevicius and Skrinska, which used annular fins with a homogeneous, trapezoid-shaped cross-section with a fin thickness of 2 mm at the foot and 1 mm at the top but with variable height. Apparently no influence of fin thickness upon the pressure drop coefficient was assumed a priori. If the formula is to be supplemented by accounting for the influence of fin thickness, this could only be done using measurements by another author. It would then have to be taken into account that the measurements, for example those by Mirkovics, were of finned tubes of other designs.

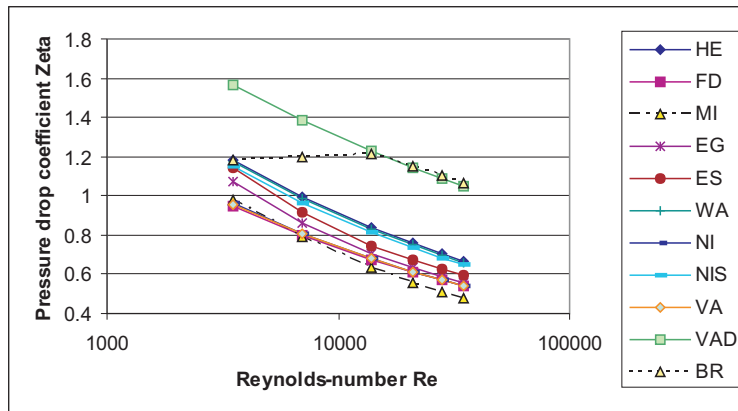


Figure 93: **Influence of the Reynolds number upon the pressure drop coefficient (staggered arrangement)**

In order to be able to compare the values measured by Mirkovics with those by ITE, the values must be taken from the diagram and converted to the Reynolds number derived using the hydraulic diameter  $d_h$  to  $Re(d_A)$ . These converted measured values, originating with Mirkovics, were then evaluated in order to obtain a formula for the pressure drop coefficient similar in terms to the HEDH formula but with other coefficients. The result is as follows:

$$\xi = C Re(d_A)^{-0.31} \left(\frac{t_q}{d_A}\right)^{0.05} \left(\frac{t_l}{d_A}\right)^{-0.71} \left(1 - \frac{h}{d_A}\right)^{-2.0} \left(\frac{t_R}{d_A}\right)^{0.75} \left(\frac{s_R}{d_A}\right)^{-0.16} \quad (169)$$

Departing from HE with  $(1 - \frac{t_R}{d_A})$ , the influence of  $t_R$  was changed to the term  $\frac{t_R}{d_A}$  because the expression  $(1 - \frac{t_R}{d_A})$  would result in a huge exponent which would magnify inaccuracies too much. A comparison of the coefficients in the formula given above with the HE equation (152) indicates that these are nevertheless similar in range but different in amount. On the other hand, evaluations of our own measurements show an exponent of 1.21 for  $(1 - \frac{t_R}{d_A})$  and an exponent of 0.56 for  $\frac{t_l}{d_A}$ . Our own measurements confirm the HE function at  $t_R$ , yet at  $t_l$  they do not confirm this function, whereas the values converted according to HE by Mirkovics [5] and the results of Stasiulevicius and Skrinska [3] lie close together.

When the pressure drop equations for smooth tube bundles in cross-flow are considered in comparison, a different question arises. For both FDBR 1980 [10] and VDI Waermeatlas 1994 [15] the pressure drop coefficient declines with increasing  $t_q$ , whereas in FDBR the pressure drop coefficient also declines with increasing  $t_l$ , but in VDI-Waermeatlas it increases.

With regard to the influence of transverse pitch  $t_q$ , the number  $t_q/d_A$  would seem to reflect the experimental values better than the dimensionless number  $t_q/d_E$ .  $d_E$  is the diameter with equal area in the profile of the finned tube.

$$d_E = d_A + \frac{2 h s_R}{t_R} \quad (170)$$

This is because with few short and thin fins, almost no flow influence occurs; with many thick and long fins, however, a strong displacement of the flow from fin spacing takes place. Unexpectedly, a better correlation for  $\frac{t_q}{d_A}$  is obtained for  $\frac{t_q}{d_E}$  after evaluation of the data. In conclusion, it is suggested to use a modified form of the equation of Stasiulevicius and Skrinska (also defined in HEDH) [3] for a calculation of the pressure drop coefficient for spiral finned tubes because of its clarity. The equation could be supplemented on the one hand by an expression for the influence of fin thickness, and on the other hand by adapting constants to measured values for spiral finned tubes. The suggested formula would then be:

$$\xi = Konst Re(d_A)^{-0.25} \left(\frac{t_q}{d_A}\right)^{-0.50} \left(\frac{t_l}{d_A}\right)^{-0.55} \left(1 - \frac{t_R}{d_A}\right)^{1.8} \left(1 - \frac{h}{d_A}\right)^{-1.4} \left(\frac{s_R}{d_A}\right)^{-0.16} \quad (171)$$

The constant adapted to existing pressure drop measurements on spiral finned tubes results as  $Konst. = 7.07$ . Figure (94) results from a comparison of calculations according to this equation (SP denomination) with the results of the most important equations from the literature. The pressure drop coefficients according to equation (171) are situated among the other evaluated pressure drop coefficients, yet rather in the upper range. This could result from their origin in test cases with welded spiral finned tubes.

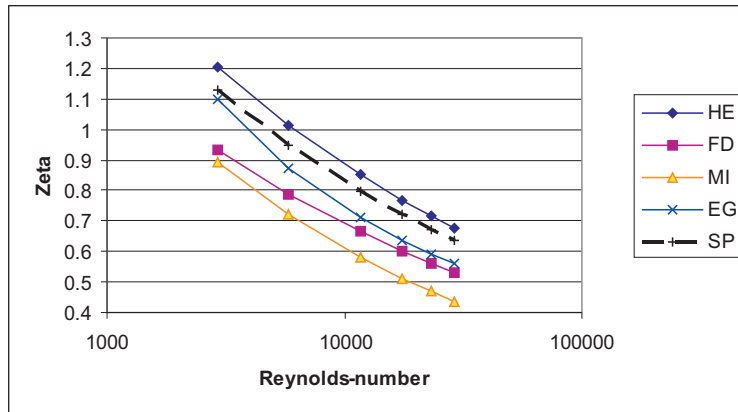


Figure 94: Comparison of the pressure drop coefficient calculated according to equation (171) with the results of equations from the literature

## 5.4 Calculation of pressure drop for finned tubes arranged in line

The pressure drop for finned tube bundles arranged in line is calculated in part with formulas similar to those for staggered arrangements, while only the coefficients show other values, or also with completely different equations. The basis of calculation for in-line arrangement, as in other cases too, is equation (139), whereas the task at hand is to determine the pressure drop coefficient  $\xi$  in dependence of the Reynolds number and geometrical characteristics.

### 5.4.1 Presentation of equations

#### 1. FDBR equation [10]

The FDBR equation for finned tubes arranged in line is quite similar to that for staggered tube arrangements.

$$\xi = 0.72 (E1 + 2)^{0.9} E2^{0.9} E3^{0.1} Re^{-0.245} \quad (172)$$

The Reynolds number is determined using the hydraulic diameter  $d_h$  as defined in section 5.3.1 for the staggered arranged finned tubes. The geometrical dimensions of the finned tube bundle are accounted for in the factors  $E1, E2$  and  $E3$  where:

$$E1 = (t_q - d_A)/(t_R - s_R) \quad (173)$$

$$E2 = d_h/(t_q - d_A) \quad (174)$$

$$E3 = (t_l - d_A)/(t_q - d_A) \quad (175)$$

$E3$  also accounts for longitudinal pitch, which is not included in the equation for staggered tube arrangement. The Reynolds number  $Re$  is derived using the velocity  $w_E$  in the narrowest cross-section, as well as using the hydraulic diameter  $d_h$ .

$$Re = \frac{w_E d_h}{\nu(\vartheta_{gm})} \quad (176)$$

The kinematic viscosity  $\nu$  has to be determined using the mean gas temperature  $\vartheta_{gm}$  according to calculation procedures.

## 2. HEDH equation [2]

This equation was developed on the basis of test cases with squared fins and annular fins and should therefore be used only with caution for spiral finned tubes.

$$\xi = 0.52 \left(\frac{d'}{d_A}\right)^{0.3} Re^{-0.08} \left(\frac{t_l}{d_A} - 1\right)^{0.68} C_z \quad (177)$$

$d'$  here is an equivalent diameter which is calculated using the surfaces of the fins, the fin tops and the bare tube per m tube:

$$d' = \frac{\pi d_A^2 + (a_{Ri} + a_{Ko})\sqrt{\frac{a_{Ri}t_R}{2}}}{a_{Ro} + a_{Ri} + a_{Ko}} \quad (178)$$

The Reynolds number in equation (177) for the pressure drop coefficient  $\xi$  is calculated meanwhile using the diameter  $d_e$ , which is obtained according to the following equation:

$$d_e = \frac{2(t_R(t_q - d_A) - 2h s_R)}{2h + t_R} \quad (179)$$

The expression  $C_z$  is introduced to account for the increased pressure drop in the first five tube rows and depends on the number of the tube rows  $n_R$  as a sum for 1 to  $n_R$  over the items in  $c_z$  as a function of  $n_R$ .

$$C_z = \frac{1}{n_R} \sum_1^{n_R} c_z \quad (180)$$

Wherein  $c_z$  is:

$$c_z = 0.738 \frac{1.509}{n_R - 0.25} \quad (181)$$

### 3. ESCOA equation [12]

The ESCOA pressure drop equation for finned tubes arranged in line is very similar to that for staggered arrangements. Only the functions  $C_4$  and  $C_6$  are different, which are responsible for the influence of geometry. This equation is valid for spiral finned tubes with smooth fins and was adapted from American syntax to European notation.

$$\xi = 4 (0.07 + 8.0 Re^{-0.45}) \frac{D}{d_A} C_4 C_6 \quad (182)$$

For  $C_4$  and  $C_6$  is valid

$$C_4 = 0.08 \left(0.15 \frac{t_q}{d_A}\right)^{-1.1 \left(\frac{h}{t_R - s_R}\right)^{0.15}} \quad (183)$$

$$C_6 = 1.6 - (0.75 - 1.5 e^{-0.7n_R}) e^{-0.2 \left(\frac{t_l}{t_q}\right)^2} \quad (184)$$

The influence of the number of consecutively arranged tube rows in this equation is implied within the coefficient  $C_6$ .

### 4. Equation according to VDI-Waermeatlas, 9th edition, Blatt Lda 1-4[33]

The equation of the VDI-Waermeatlas is valid for annular fins and spiral fins with approximately the same transverse and longitudinal pitches. Here the Reynolds number is also calculated using the diameter of the bare tube  $d_A$  and the velocity in the narrowest cross-section. For the range  $3000 < Re < 40000$  the following holds:

$$\xi = 5.5 Re^{-0.30} \left(\frac{t_q}{d_A}\right)^{-0.5} \left(\frac{t_R}{d_A}\right)^{-0.7} \left(\frac{h}{d_A}\right)^{0.5} \quad (185)$$

For higher Reynolds numbers, i.e.  $40000 < Re < 1400000$ , the pressure drop coefficient no longer changes with the Reynolds number and is thus:

$$\xi = 0.23 \left(\frac{t_q}{d_A}\right)^{-0.5} \left(\frac{t_R}{d_A}\right)^{-0.7} \left(\frac{h}{d_A}\right)^{0.5} \quad (186)$$

## 5. ESCOA equation for serrated fins [17]

The equation of ESCOA for in-line finned tube arrangements with serrated fins is very similar to that for smooth fins, whereas the factor  $C_4$  is different. The factor  $C_4$  differs only in the exponent of  $\frac{h}{t_R - s_R}$ , which increases from 0.15 for smooth fins up to 0.20 for serrated fins.

$$C_4 = 0.08 \left(0.15 \frac{t_q}{d_A}\right)^{-1.1} \left(\frac{h}{t_R - s_R}\right)^{0.20} \quad (187)$$

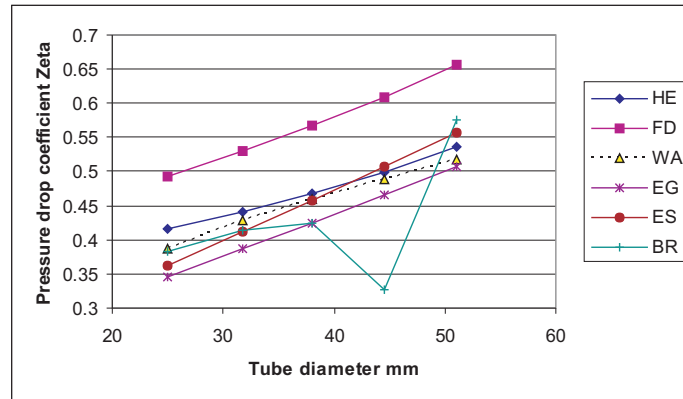


Figure 95: **Influence of tube diameter upon the pressure drop coefficient with constant velocity in the narrowest cross-section (in-line arrangement)**

## 6. According to M. Brockmann: Druckverlust bei Stroemungen quer zu Rippenrohrbuendeln, Progress Report VDI, Series 6, No. 431[38]

See also section 5.3.1, pressure drop for staggered finned tube arrangements, where the test cases and calculation equations of Brockmann are presented in details.

The results of the test series were depicted in the form of equations:

At Reynolds numbers  $1000 < Re < 8000$ , the following holds for the pressure drop coefficient  $\xi$ :

$$\xi = z_0 \sqrt{\left(\frac{1600}{Re}\right)^2 + \left(\frac{Re}{1600}\right)^{m_0}} \quad (188)$$

and for Reynolds numbers  $10000 < Re < 100000$

$$\xi = z_1 \left(\frac{Re}{10000}\right)^m \quad (189)$$

Between Reynolds numbers of 8000 and 10000, the pressure drop coefficient values  $\xi$  are linearly interpolated according to equations (188) and (189). The Reynolds number for this equation is derived, in contrast to all other authors, using the flooding length  $l = \frac{\pi}{2} \sqrt{d_A^2 + h^2}$  and the free superficial velocity  $w_0$ .  $m_0$  and  $m$  are constants,  $z_0$  and  $z_1$  are dependent in a complex way on approx. 24 further constants, whereby one set of the constants mentioned is valid for in-line tube arrangement. All of the observations in section 5.3.1 concerning the extremely low pressure drop coefficients for  $h \approx 0.36 d_A$  are also valid here for in-line tube arrangements.

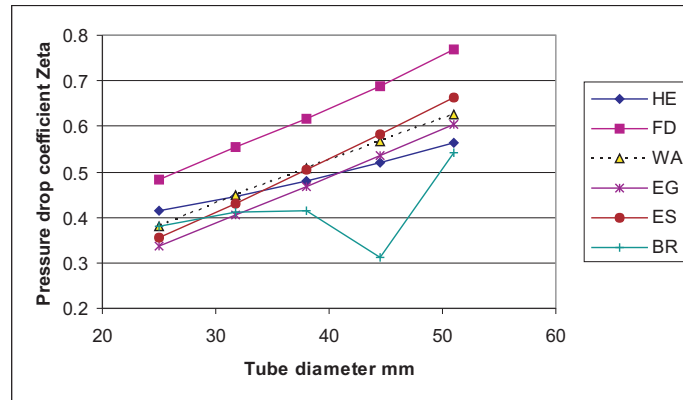


Figure 96: Influence of tube diameter upon the pressure drop coefficient with constant Reynolds number (in-line arrangement)

#### 5.4.2 Discussion of pressure drop equations for in-line tube bundle arrangements

##### 1. Influence of tube diameter

The influence of tube diameter on the pressure drop coefficient has to be considered for two different cases. First, it can be assumed that the velocity in the narrowest cross-section remains constant, then the Reynolds number increases with the diameter and, since the pressure drop coefficient decreases at about  $Re^{-0.25}$ , it increases only little in total if fin geometry is unaltered; see figure (95).

In the second case, in which the Reynolds number remains constant, the pressure drop coefficient increases more strongly with tube diameter; see figure (96).

##### 2. Influence of tube diameter with transverse pitch and longitudinal pitch

When changing tube diameter at a constant fin height, transverse and longitudinal pitch should also be altered for an optimal use of space. This has to be varied in such a way that the distance between fin edges remains constant. If the velocity in the narrowest cross-section is constant in this case, figure (97), the pressure drop coefficient increases for HE, FD, WA and BR, but for the other equations (EG and ES) it declines.

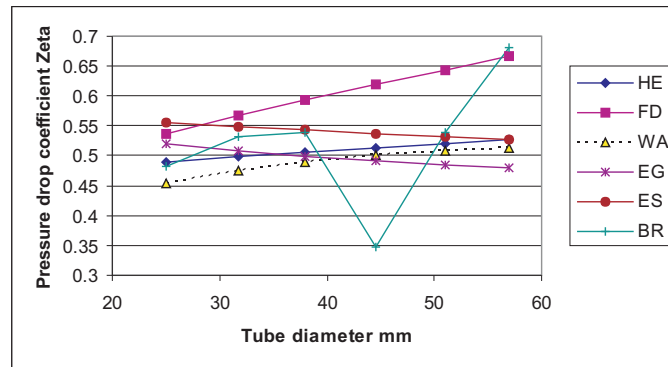


Figure 97: Influence of tube diameter upon the pressure drop coefficient with constant velocity in the narrowest cross-section and adapted transverse and longitudinal pitch (in-line arrangement)

For a constant Reynolds number, figure (98), the pressure drop coefficient increases slightly with the tube diameter with all formulas except BR.

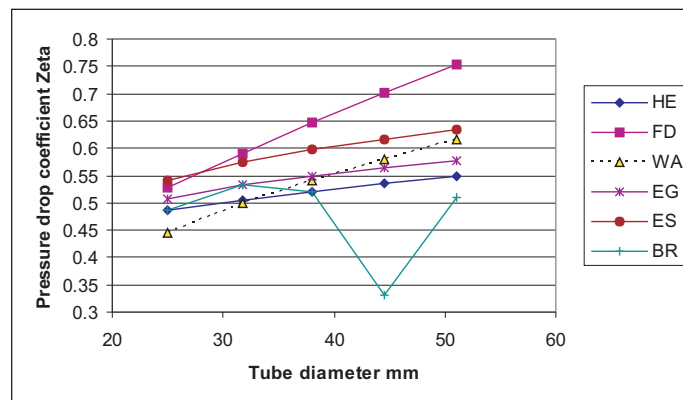


Figure 98: Influence of tube diameter upon the pressure drop coefficient with constant Reynolds number and at adapted transverse and longitudinal pitch (in-line arrangement)

### 3. Influence of fin thickness

With increasing fin thickness, the pressure drop coefficient generally increases for in-line tube arrangements; only the WA relation does not include any influence of fin thickness. For a change of the fin thickness from 1 mm to 1.3 mm, the pressure drop coefficient according to HE climbs by about 1.3 %, according to FD, however, by 4.5 %; figure (99).

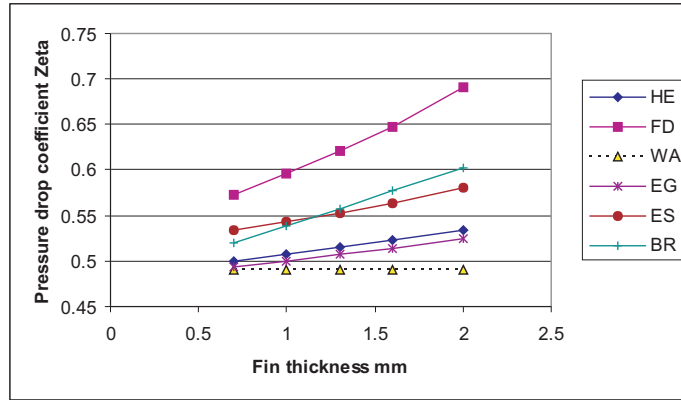


Figure 99: Influence of fin thickness upon the pressure drop coefficient (in-line arrangement)

#### 4. Influence of fin pitch

The pressure drop increases more strongly with a decreasing fin pitch, whereas the increase for fin pitches  $t_R < 5$  mm occurs almost exponentially. Only Brockmann [38] detects a small influence, in which case the pressure drop coefficient declines slightly for an increase in fin pitch from 3 mm to 7 mm; see figure (100).

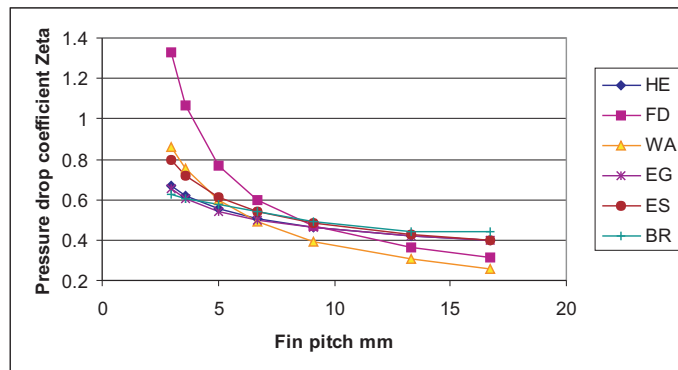


Figure 100: Influence of fin pitch upon the pressure drop coefficient (in-line arrangement)

## 5. Influence of fin height

With regard to the influence of fin height, almost all formulas consistently ascertain an increase in the pressure drop coefficient with fin height. The slope is almost identical for all of the equations. Only Brockmann's equations [38], which otherwise indicate a direct increase in pressure drop coefficient with fin height, show the anomaly at  $h = 0.36 d_A$ , already mentioned above in the form of a very distinct relative minimum (figure (101)).

## 6. Influence of fin height with transverse and longitudinal pitch

For determining the influence of fin height, the observed transverse and longitudinal pitch should be designed in such a way that even the tallest fins have enough space. If shorter fins are used, much space is lost. It is therefore helpful to choose pitch values with this in mind, so that the distance between the fins conforms to a certain dimension. Under this condition as well, the pressure drop coefficient increases with the fin height according to almost all of the equations; see figure (102). The only exception is Brockmann [38], where irregular curve results with a drop in the middle.

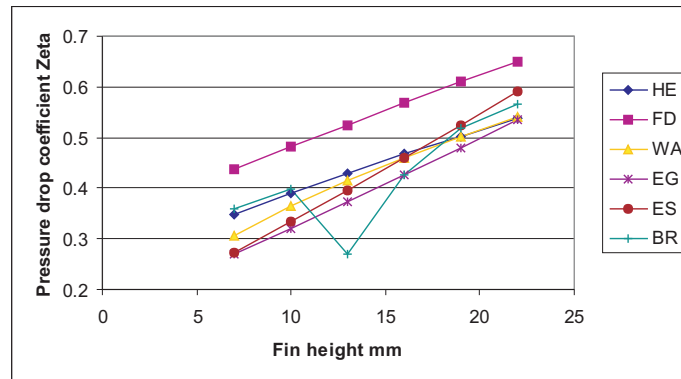


Figure 101: **Influence of fin height upon the pressure drop coefficient (in-line arrangement)**

When only transverse pitch is altered with fin height, a decline in the pressure drop coefficient is obtained with a increasing fin height, according to HE and Brockmann [38]. For FD, a decrease exists for fin heights smaller than 10 mm, whereas with FD the pressure drop coefficient is almost constant in total. The remaining formulas show an insignificant increase in the pressure drop coefficient with fin height, as can be seen in figure (103).

## 7. Influence of the Reynolds number

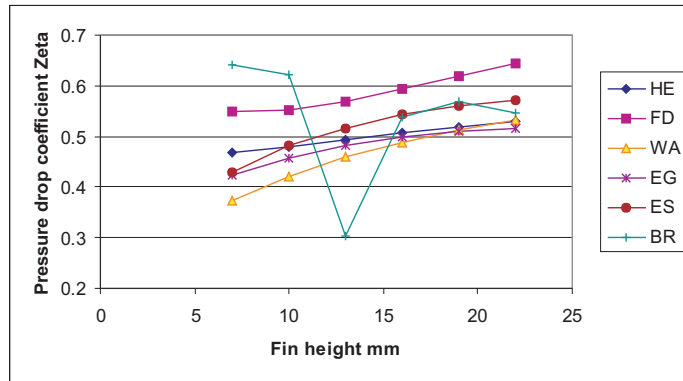


Figure 102: Influence of fin height upon the pressure drop coefficient at adapted transverse and longitudinal pitch (in-line arrangement)

One might suppose that at least the influence of the Reynolds number upon the pressure drop coefficient shows a uniform tendency according to the different formulas. This is not the case, as only the equations of FD, EG, ES and WA result in the expected decline of the pressure drop coefficient zeta at approx.  $Re^{-0.30}$ . For the HE equation, the exponent of Reynolds is only approx.  $-0.08$ , and for BR even a very slight rise is ascertained for smaller values of the Reynolds number, i.e. less than  $Re = 14000$ , followed by a similarly insignificant decrease in zeta for even higher Reynolds numbers; see figure (104).

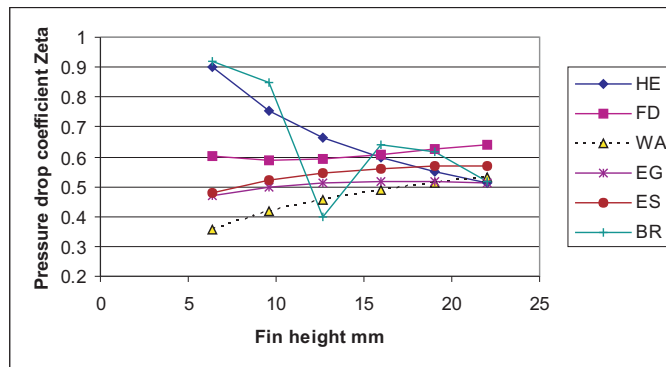


Figure 103: Influence of fin height upon the pressure drop coefficient with adapted transverse pitch (in-line arrangement)

### 8. Influence of transverse pitch

The pressure drop coefficient decreases with increasing transverse pitch in all equations. According to FD and WA, the decline is insignificant and

rather linear. In other equations, the pressure drop coefficient on the other hand is digressive, i.e. for a greater transverse pitch the pressure drop coefficient changes only little; see figure (105). This behavior does confirm expectations, however.

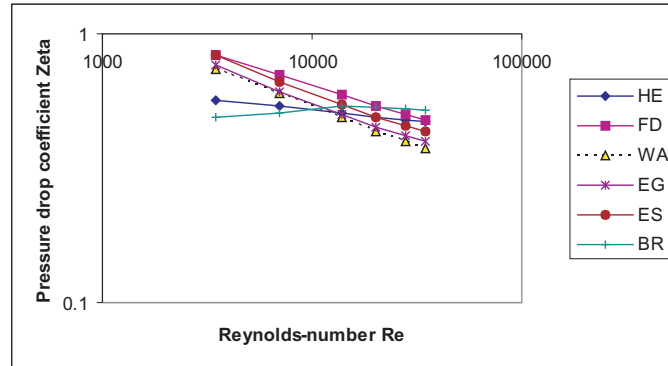


Figure 104: **Influence of the Reynolds number upon the pressure drop coefficient (in-line arrangement)**

#### 9. Influence of the longitudinal pitch

Except for the WA formula, where the pressure drop coefficient does not depend on longitudinal pitch, this variable with an increasing longitudinal pitch increases in all of the equations. This increase is moderate for FD, EG and ES, but considerable in the HE and BR equations; see figure (106) on this. We also found a small increase of the pressure drop coefficient with increasing longitudinal pitch through our own measurements.

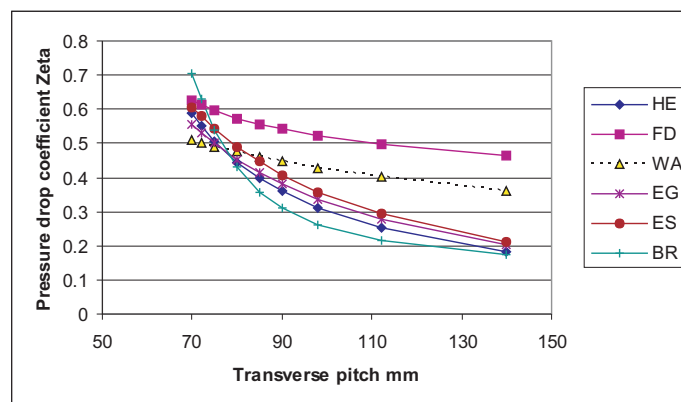


Figure 105: **Influence of transverse pitch upon the pressure drop coefficient (in-line arrangement)**

## 10. Influence of the number of consecutive tube rows

The pressure drop coefficient decreases with an increasing number of consecutive tube rows, at least according to the HE, EG and ES equations. The others do not show any such influence at all. According to BR, for an increasing number of tube rows up to a number of 8, zeta rises very little and then remains constant; see figure (107).

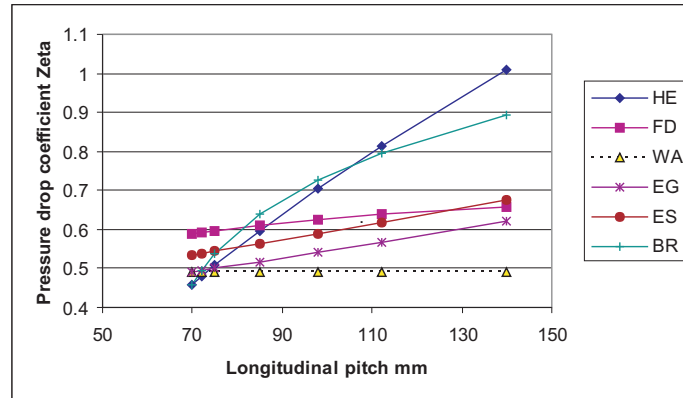


Figure 106: **Influence of longitudinal pitch upon the pressure drop coefficient (in-line arrangement)**

In our own test cases with in-line tube arrangements (unfortunately only 3 different geometries were analyzed, but each with 8, 6, 4 and 2 tube rows) it was found that, for Reynolds numbers of  $\approx 7000$  to  $\approx 25000$ , the pressure drop coefficient per tube row is slightly smaller for 6 tube rows than for 8, still a little smaller for 4 tube rows and apparently increases again slightly for 2 tube rows. Thus, the observation may not be entirely incorrect that the pressure drop coefficient does not depend on the number of consecutive in-line tube rows; see figure (108) on this.

It is however possible to draw a regression line through the four points which represent measurement values, as figure (108) shows. Thus, for 2 tube rows the pressure drop coefficient per tube row is approx. 90% of the value for 8 tube rows. This could also be accounted for through a reduction factor for a certain number of consecutive tube rows less than 8 as follows:

$$K_z = 1 - 0.1 \frac{8 - n_R}{6} \quad (190)$$

The relationship for the calculation of pressure drop in in-line tube arrangements shown below can be derived from our own measurement values. In this case

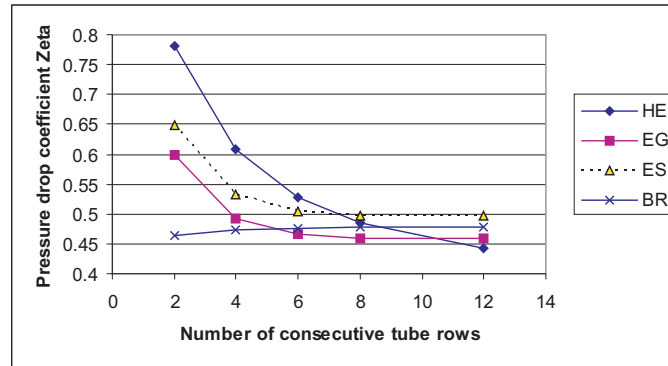


Figure 107: Influence of the number of consecutive tube rows upon the pressure drop coefficient (in-line arrangement)

the equation from the Waermeatlas [33] is taken as a basis and supplemented by a term that represents the influence of longitudinal pitch on the pressure drop coefficient. This expression is made dimensionless by multiplying it with  $t_l/d_A$ . The exponent has been determined as 0.40 from our own measurements. The exponent of the Reynolds number also results from measurements at ITE and is specified at about  $-0.34$  when all measurement points are averaged. The following equation for the pressure drop coefficient in in-line spiral finned tube arrangements results therefore:

$$\xi = 4.534 Re^{-0.34} \left(\frac{t_q}{d_A}\right)^{-0.5} \left(\frac{t_R}{d_A}\right)^{-0.7} \left(\frac{h}{d_A}\right)^{0.5} \left(\frac{t_l}{d_A}\right)^{0.4} \quad (191)$$

The pressure drop coefficient values that were determined using this equation are labeled with EM in figure (109); these values are distributed among those calculated according to the other equations from the literature. For higher Reynolds numbers they display a tendency towards the lower boundary of the range.

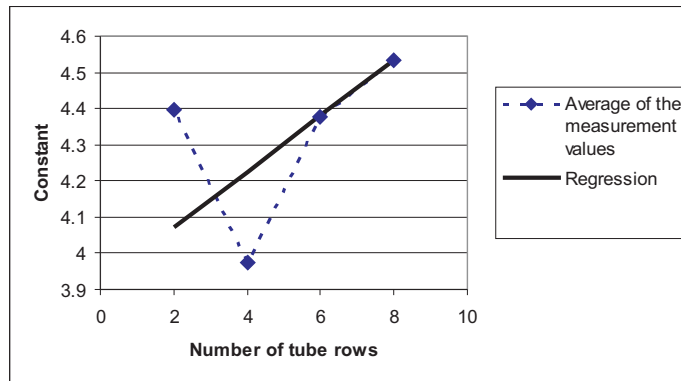


Figure 108: Constant of equation (191) calculated by measurement values of the pressure drop coefficient in dependence of the number of tube rows (in-line arrangement)

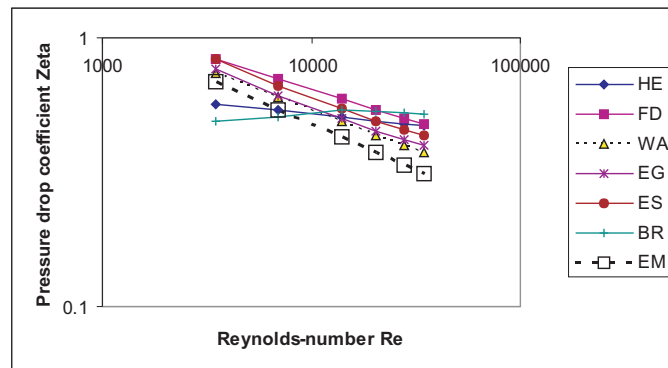


Figure 109: Pressure drop coefficient values according to equation (191) in comparison with the values for in-line arrangements from the literature

## Conclusion and recommendations

Heat exchangers with finned tubes in cross-flow are used to exchange heat between a gas with relatively poor heat transfer properties and a fluid with better heat transfer properties. The fluid used is usually a liquid but sometimes also a gas under high pressure. The goal is to minimize size or mass requirements in designing the recuperator as well as the pumping power required for the gaseous medium. The current state of scientific and technical knowledge allows such heat exchangers to be designed well in accord with their purpose. Yet one cannot be content with the particular state of knowledge, so that further research in this sector is worthwhile and appropriate.

While research into certain problem areas might result in further improvements to design safety, the following list makes no claim to being complete. The influence of the real local heat transfer coefficient at the surface of the fins, as a function of the radius and the angle of flow direction, on overall fin performance ought to be investigated for different tube arrangements as well as fin height and pitch values. Experimental research as well as finite volume calculations with efficient flow simulation programs could be used for this purpose. Some work has been done in this area, in which case local distribution of the heat transfer coefficient on the fin was determined based on the analogy between heat and mass transfer, e.g. by means of a naphthalene sublimation.

At ITE (Institute for Thermodynamics and Energy Conversion) such tests involving direct measurement of fin surface temperature at different positions have commenced but not yet been completed. Heat transfer and pressure drop in only a few consecutive tube rows has not yet been entirely investigated, neither for bundles of separate finned tubes nor for pipe bundles with continuous fins. In particular, knowledge is missing for bundles of flat tubes and other non-circular types of tubes with few tube rows.

With regard to wavy fins, there is very little published research concerning the influence of wave height and wavelength or wave design (i.e. whether round or corrugated waves) on heat transfer and pressure drop, either for single or continuous fins.

It might be worth examining the effects of the positioning of concentric fins in successive tubes, i.e. whether in-line, staggered or partially staggered configuration has any effect. In this case the possibility of fouling as well as cleaning options, with the aid of soot blowers, should also be considered. Initial steps toward such investigation have already been carried out at ITE for finned tubes with welded rectangular fins.

Further progress in the design of heat exchangers with finned tubes in cross-flow could therefore be certainly achieved, both through the options listed above as well as through other methods which have not been mentioned.

## Appendix: Test facility for heat transfer measurements

A test rig for heat transfer and pressure drop measurements at finned tube bundles in cross-flow has been in operation at the laboratory of the Institute for Thermodynamics and Energy conversion (ITE) at the Vienna University of Technology since 1989.

The layout of this test facility is presented in figure (110). The (finned) tube bundle under examination is admitted with up to 400 °C hot gas, which is generated by combustion of natural gas and air. Air intake is performed using a Venturi nozzle, which is also used for mass flow measurement of combustion air. Following a connecting piece with a bend, a variable incidence entry vane is mounted in front of the radial fan for mass flow regulation of air. The radial fan can produce a maximum pressure height of 5000 Pa and generates 45000 Nm<sup>3</sup>/h at 3500 Pa. The fan is powered by a 90 kilowatt three-phase alternator motor. The air flows through a three-meter conical connecting piece to the burner. The burner is designed as a duct burner, drawing its combustion air partly from the process air through ductings. The maximum temperature after the burner is 400 °C, maximum burner power is 1160 kilowatts.

Due to the overpressure in the burner, which is necessary for flue gas flow through the experimental rig, the natural gas, with approx. 20 mbar of overpressure in the gas pipe, has to be compressed to approx. 60-80 mbar by using a side-channel compressor with bypass control. The gas flows to the burner through a safety system with pressure switch and magnetic valves. Firing is initiated by an ignition burner with high voltage pulse. The flame is controlled by means of a flame detector. Temperature regulation is achieved through adjustable regulators which control a gas adjustment valve. Behind the burner, with a cross-section of 1000 x 750 mm, and following a tube with a diameter of 600 mm there is a transition section, in which two static mixer applications are installed as well as two 90° bends, resulting in the U-shaped the test rig layout; this is necessary due to length restrictions placed by the experimental laboratory. After this redirecting apparatus, there is an additional mixer application, followed by a transition piece to a rectangular cross-section 500 mm in width and 1000 mm in height containing a flow rectifier consisting of three fine wire meshes in close arrangement. After the flow rectifier, which serves to rectify the vortices caused by mixers and redirecting pipes, a 500 mm adjustment channel follows, which adapts the height of the experimental channel to the required value in each case (between 800 and 1000 mm), as well as a 2000 mm inlet channel, which serves to calm the flow. The finned tube heat exchanger with a tube length of approx. 500 mm is built into a 1500 mm channel piece. Behind this, a 1500 mm outlet channel with the same cross-section follows. A further adjustment channel follows the 500 x 1000 mm

rectangular cross-section. Then there is a piece connecting to a tube with a diameter of 500 mm which ends in a steel tube flue, into which flue gases are conducted.

The finned tube heat exchanger consists of a rectangular sheet steel channel in which the finned tubes are arranged horizontally with the required transverse and longitudinal pitch. The free channel width is fixed at 500 mm and the experimental tubes have to be prepared so that they only have fins along a length of 500 mm. The additional 50 mm at each end are smooth. The bare tubes which remain after the fins at the tube ends are cut off offer the advantage of allowing insertion through the sidewalls of the heat exchanger and in turn complete sealing using asbestos cord rings and conical pressure washers on the inside. The bends which connect the individual finned tubes to a coiled pipe are mounted outside of the gas channel, since this is the only arrangement allowing exact measurement of heat transfer at the small test section width of the coiled pipes. Measurements are thus not influenced by bypass flow through the space for the bends.

The bends have been soldered together using conventional copper fittings, as these maintain their dimensions well, and in order to facilitate ease in mounting and reassembly, and O-rings are used to achieve a tight seal with the finned tubes. For this purpose, the tubes are equipped with soldered pipe connections of brass with O-ring grooves, in which the copper fittings are mounted. The single coiled tubes are arranged one on top of the other and connected to the collectors in parallel on the water side. Depending on transverse pitch, 10 to 12 coiled tubes are connected in parallel; each individual one usually consists of 8 consecutive tubes. It is also possible to examine heat exchangers with 6, 4 and 2 consecutive tube rows, however, and in special cases even only with one tube row. An even flow in the coiled tubes is achieved by an arrangement of orifices after the inlet collector in every coiled tube.

The hot parts of the test facility are insulated to prevent heat loss and any accidental contact. The components containing hot gas are insulated using a 70 mm layer of mineral wool and, above that, an additional 50 mm layer of glass wool. Aluminium foil is used as external protection for the finish. The cooling water collectors and the inlets for the coiled tubes are insulated using polyurethane foam.

The test rig requires a number of measurements to be taken simultaneously in order to evaluate and determine the amount of heat transferred as well as gas-side pressure drop. The temperatures on the water side are measured for every coiled tube at the inlet and at the outlet using Pt-100 RTDs (resistance temperature detectors) so that boundary influences can be ascertained for the outside coiled tubes and considered in the evaluation. The thermocouples are directly immersed in the water and sealed by screw joints. Gas temperatures are measured by NiCr-Ni thermocouples. Four thermocouples are arranged and mounted in front of and

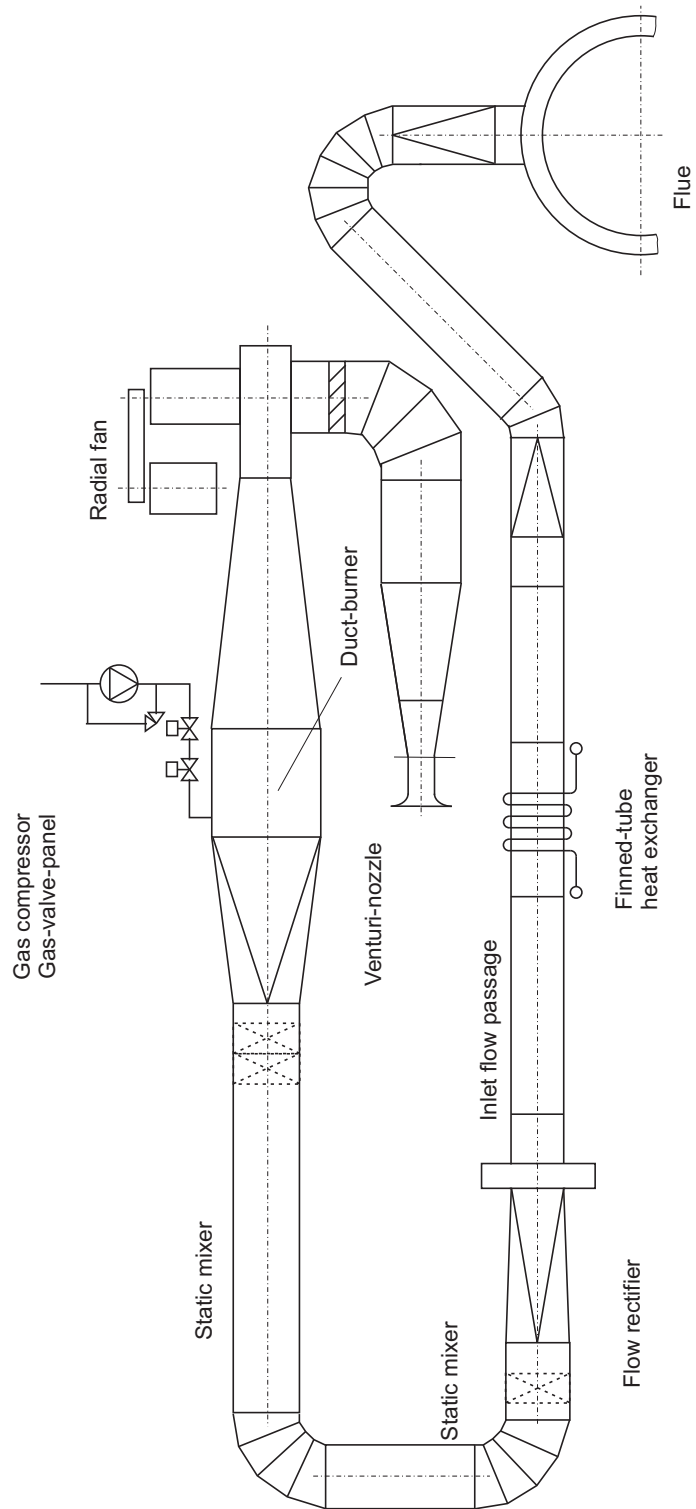


Figure 110: Layout and design of the test facility

behind the heating surface of the heat exchanger to obtain a grid measurement. Additional NiCr-Ni thermocouples measure the air temperature at the Venturi nozzle and behind the fan as well as the gas temperature behind the burner. Compensation for reference points is achieved by software.

The mass flow of water is measured using a hot water meter with an electronic sensor. The mass flow of air is measured by determining the pressure difference at the Venturi nozzle in front of the inlet collector. This pressure difference as well as others are detected using Honeywell series 160 differential pressure micro switch sensors.

All measured values are transmitted in the form of electrical signals to the process computer and processed there. This is done by means of a PC with measurement value periphery by National Instruments and the LabView program system. The test facility is operated only through the screen displays; no other instruments are available. At the outset of testing, an HP process computer was used for data acquisition and later replaced by the present system in 2004. The test facility thus continues to be used for measurements on finned tubes as well as on other types of heat exchangers.

## Literature

- [1] *Schmidt, E. Th.:*  
Der Waermeuebergang an Rippenrohre und die Berechnung von Rohrbuendelwaermeaustauschern.  
Kaeltetechnik 15 (1963), H.4, p. 88
- [2] *Heat Exchanger Design Handbook(HEDH):*  
Rev. 1987.  
Hemisphere Publ. Corp. Washington New York London
- [3] *Stasiulevicius, J. u. Skrinska, A.:*  
Heat Transfer of Finned Tube Bundles in Crossflow.  
Hemisphere Publ. Corp. Washington New York London, 1988
- [4] *VDI – Waermeatlas:*  
4th Edition 1984.  
VDI Verlag GmbH Duesseldorf
- [5] *Mirkovics, Z.:*  
Heat Transfer and Flow Resistance Correlation for Helically Finned and Staggered Tube Banks in Crossflow.  
in: Heat Exchangers: Afgan N. u. Schluender E. U., 1974  
Mc Graw Hill New York
- [6] *Frass, F. u. Linzer, W.:*  
Waermeuebergangsprobleme an querangestromten Rippenrohrbuendeln.  
BWK 44(1992), H.7/8, p. 333
- [7] *Biery, J. C.:*  
Prediction of Heat Transfer Coefficients in Gas Flow Normal to Finned and Smooth Tube Banks.  
ASME, J. Heat Transfer 1981, Vol.103, p.705
- [8] *Weierman, C.:*  
Correlations ease the selection of finned Tubes.  
Oil and Gas Journal 1976, Sept. 6, p. 94
- [9] *Brandt, F.:*  
Waermeuebertragung in Dampferzeugern und Waermeaustauschern.  
FDBR Fachbuchreihe Bd.2  
Vulkan Verlag Essen 1985

- [10] *FDBR Handbuch Waerme – und Stroemungstechnik.:*  
Fachverband Dampfkessel-, Behaelter- und Rohrleitungsbau.  
Essen, Juli 1980
- [11] *Rohsenow, W. M., Hartnett, J. P., Ganic, E. N.:*  
Handbook of Heat Transfer Fundamentals.  
2nd Edition, 1985 McGraw Hill, New York
- [12] *ESCOA Engineering Manual Solidfin HF.:*  
ESCOA, Pryor, Oklahoma 1979.
- [13] *Scholand, E.:*  
Waermeuebergang an von heissen Abgasen umstroemten berippten Rohren.  
Diss. Univ. Trier Kaiserslautern, 1974.
- [14] *Vampola, J.:*  
Waermeuebergang und Druckverlust beim Stroemen von Gasen durch ein  
Rippenrohrbuendel.  
Translation from Czech.  
Strojirenstvi (Mech. engineering) 16 (1966), Number 7, p. 501
- [15] *VDI – Waermeatlas:*  
7th Edition 1994  
VDI Verlag Duesseldorf
- [16] *Scholz, F.:*  
Einfluss der Rohrreihenzahl auf den Druckverlust und Waermeuebergang von  
Rohrbuendeln bei hohen Reynoldszahlen.  
Chemie Ing. Techn., 40 (1968), No. 20, p. 983
- [17] *ESCOA Turb – X HF Rating Instructions:*  
ESCOA, Pryor, Oklahoma 1979
- [18] *Nir, A. :*  
Heat Transfer and Friction Factor Correlations for Crossflow  
over Staggered Finned Tube Banks.  
Heat Transf. Eng., Vol. 12(1991), No. 1, p. 43
- [19] *Kaminski, S. u. Gross, U. :*  
Luftseitiger Waermeuebergang und Druckverlust in Lamellenrohr Waer-  
meuebertragern.  
KI Luft- und Kaeltetechnik 2000, No. 1, p. 13

- [20] *Haaf, S.:*  
Waermeuebertragung in Luftkuehlern.  
in: Handbuch der Kaeltetechnik, Vol. 6B: Waermeaustauscher, 1988  
Springer Verlag Berlin Heidelberg New York
- [21] *Kays, W. M. u. London, A. L.:*  
Compact Heat Exchangers.  
3rd Edition 1984  
McGraw Hill, New York
- [22] *Kearney, S. P. u. Jacobi, A. M.:*  
Local Convective Behavior and Fin Efficiency in Shallow Banks of In-Line  
and Staggered Annularly Finned Tubes.  
ASME, J. Heat Transf., Vol. 118(1996), p. 317
- [23] *Gnielinski, V.:*  
Waermeuebergang an einzelne Rohre, Draehte und Zylinder unter Quer-  
anstroemung. Forsch. Ing. Wes. 41(1975), No. 5, p. 145
- [24] *Rohsenow, W. M., Hartnett, J. P., Ganic, E. N.:*  
Handbook of Heat Transfer Applications.  
2nd Edition 1985 McGraw Hill, New York
- [25] *Reid, D. R. u. Taborek, J. :*  
Selection Criteria for Plain and Segmented Finned Tubes for Heat Recovery  
Systems.  
ASME J.of Eng. f. Gas Turbines and Power. Vol. 116(1994), p. 406
- [26] *VDI – Waermeatlas:*  
6. Edition 1991  
VDI Verlag Duesseldorf
- [27] *Sparrow, E. M. u. Hossfeld, L. M.:*  
Effect of rounding of protruding edges on heat transfer and pressure drop in  
a duct.  
Int. J.Heat Mass Transfer. Vol. 27 (1984), No. 10, pp. 1715-1723.
- [28] *Kaminski, S. u. Gross, U.:*  
Luftseitige Transportprozesse in Lamellenrohrbuendeln-numerische Unter-  
suchung.  
KI Luft- und Kaeltetechnik 2003, No. 5, P. 220
- [29] *Mirth, D. R. u. Ramadhyani, S.:*  
Correlations for predicting the air side Nusselt numbers and friction factors  
in chilled water cooling coils.  
Exp. Heat Transfer, No. 7 (1994), pp. 143-162.

- [30] *Geiser, P.:*  
Numerische Berechnung und Messung der Transportvorgaenge sowie integraler Kenngroessen in querangestromten Rippenrohrwaermeuebertragern.  
Progress Report VDI, Series 19, No. 141 (2003)
- [31] *Stephan, K. u. Mitrovic, J.:*  
Massnahmen zur Intensivierung des Waermeuebergangs.  
Chem. Ing. Tech. 36 (1984), p. 427
- [32] *VDI – Waermeatlas:*  
8th Edition 1996  
VDI Verlag Duesseldorf
- [33] *VDI – Waermeatlas:*  
9th Edition 1997  
Springer Verlag Berlin Heidelberg New York
- [34] *Baehr, H. D. u. Stephan, K.:*  
Waerme- und Stoffuebertragung  
Springer Verlag Berlin Heidelberg 1994
- [35] *Ebeling, N. u. Schmidt, G.:*  
Waermeleistung von Rippenrohr-Waermeaustauschern.  
BWK, Vol. 50 (1998), No. 5/6 , p. 64
- [36] *Kunttysh, V. B. u. Stenin, N. N.:*  
Heat Transfer and Pressure Drop in Cross Flow through Mixed In-Line-Staggered Finned-Tube Bundles.  
Thermal Engineering, Vol. 40(1993), No. 2, p. 126
- [37] *Ward, D. J. u. Young, E. H.*  
Heat transfer and pressure drop of air in forced convection across triangular pitch bank of finned tubes.  
Chem. Eng. Prog. Symp. Ser. 55(1958), No. 29, p. 37
- [38] *Brockmann, M.:*  
Druckverlust bei Stroemungen quer zu Rippenrohrbuendeln.  
Progress Report VDI, Series 6, No. 431 (2000)
- [39] *Rohsenow, W. M., Hartnett, J. P., Cho, Y. I.:*  
Handbook of Heat Transfer.  
3rd Edition 1988 McGraw-Hill
- [40] *Wehle, F.:*  
Theoretische und experimentelle Untersuchungen der Waermeuebertragung bei Rippenrohrbuendeln und Einfluss der Temperaturabhaengigkeit der Stoffwerte auf den Waermeuebergang.  
Diss., Darmstadt, 1982. Progress Report VDI, Series 6, No. 121 (1983)







Professor Friedrich Frass is a retired scientist who worked for more than 40 years at the Department for Power Systems and Applied Thermodynamics at the Vienna University of Technology in Austria.

He was born in Vienna in 1940 and he graduated from the Vienna University of Technology (Austria) in 1964 with a Master degree in Mechanical Engineering and in 1967 with the Ph. D. Degree in Mechanical Engineering.

Friedrich Frass started to work as an assistant at the Department of Applied Thermodynamics, Steam Boilers and Nuclear Reactors. During the first 2 years, he was sent as a trainee for several months to a firm for steam boiler design and to Siemens at Erlangen for the design of nuclear power reactors. In cooperation, F. Frass designed and built a test rig for the examination of two phase flow of water and steam mixtures at high pressure in horizontal and in inclined tubes. The phase distribution of water and steam was measured by a gamma ray emitting isotope.

From 1989 to 2005 F. Frass designed, built, and operated a test installation to measure heat transfer and pressure loss of finned tubes in cross flow at temperatures up to 400 °C. The result of this attempt is a book about this topic, beside of many other papers in national and International Journals. As scientist F. Frass held lectures on nuclear power reactors and on cleaning of flue gases of steam boilers in respect of pollutants as  $\text{SO}_2$ ,  $\text{NO}_x$  and others for many years. In 2005, F. Frass retired but kept in continuing collaboration with the department.

